

Metal complexes with tris(1,2,3-triazolyl) phosphine oxides and derivatives

Inaugural-Dissertation
to obtain the academic degree
Doctor rerum naturalium (Dr. rer. nat.)

Submitted to the Department of Biology, Chemistry, Pharmacy
of Freie Universität Berlin

Bo Li

Berlin, 2020

1. Supervisor: Prof. Dr. Ulrich Abram

2. Supervisor: Prof. Dr. Dieter Lentz

date of defense: 27.10.2020

Acknowledgement

I would like to express my great gratitude to my supervisor Prof. Dr. Ulrich Abram for providing me with this chance to study as a doctoral student, also for his kind supervision, guidance and support throughout these years. With his valuable suggestions and patience, this study and the dissertation were able to be accomplished. His attitude to pursuing perfection in experiments and thesis deeply influenced me, which is greatly helpful to my future career. The time I spent in his research group has benefited me quite a lot, and those days will benefit me also in the future.

I gratefully thank Prof. Dr. Dieter Lentz for being my second supervisor.

I would like to extend my appreciation to Dr. Adelheid Hagenbach for her scientific help and constructive discussions in the area of X-ray crystallography, especially in these pandemic days. Beyond her work, her intensive support during my time in Germany is highly appreciated.

Very special thanks go to my friends Abdullah Abdulkader, Pham Chien Thang, Max Roca Jungfer, Felipe Dornelles and Carlos Rojas for valuable discussions on chemistry as well as interesting intercultural communications. I am also indebted to Jacqueline Grewe, Detlef Wille and all my current and former colleagues of this research group. My experience of studying in such a professional and friendly environment is going to be my priceless life-long treasure.

I would like to sincerely thank the Institute of Chemistry and Biochemistry of the Freie Universität Berlin, particularly for the analytical services.

I appreciate the financial support from the China Scholarship Council for the research discussed in this dissertation.

Finally, this dissertation is dedicated to my parents and my friends. It is with their strong support and encouragement that I can reach this far today. There are no words that could express my gratitude for them.

Content

Acknowledgement	iii
1. Introduction.....	9
1.1 Tris(azolyl)borates, tris(azolyl)methanes, tris(azolyl)phosphines and tris(azolyl)phosphine oxides	9
The goal of the present thesis.....	12
2. Results and Discussions.....	15
2.1 Synthesis of the ligands	15
2.2 Tricarbonylrhenium(I) complexes with tris(1,2,3-triazolyl) phosphine oxides	17
2.3 Tricarbonyltechnetium(I) complexes with tris(1,2,3-triazolyl) phosphine oxides	28
2.4 Reactions of $[Re(CO)_5Br]$ with tris(1-benzyl-1H-1,2,3-triazol-4-yl) phosphine (L^2').....	32
2.5 Reactions of $(NBu_4)[ReOCl_4]$ with tris(1,2,3-triazolyl)phosphine oxides	37
2.5.1 Reactions of $(NBu_4)[ReOCl_4]$ with L^1	38
2.5.2 Reactions of $(NBu_4)[ReOCl_4]$ with L^2	42
2.6 Other metal complexes - Reactions of Cu(II) and Ni(II) ions with tris(1,2,3-triazolyl)phosphine oxides	50
2.6.1 Reactions of Cu(II) ions with L^2	51
2.6.2 Reactions of Ni(II) ions with L^2	54
3. Experimental Section	57
3.1 Starting materials	57
3.2 X-ray crystallography	57
3.3 Spectroscopical and analytical methods	57
3.4 Syntheses.....	58
4. Summary	68

5. References.....	72
6. Appendix	76
6.1 Crystallographic data	76
6.2 Spectroscopic data	130
6.2.1 Spectroscopic data of L ¹	130
6.2.2 Spectroscopic data of L ²	132
6.2.4 Spectroscopic data of [Re(CO) ₃ Br(κ ² N-L ¹)] (1)	134
6.2.5 Spectroscopic data of [Re(CO) ₃ (κ ³ N-L ¹)] (2)	136
6.2.5 Spectroscopic data of [Re(CO) ₃ Br(κ ² N-L ²)] and [Re(CO) ₃ Cl(κ ² N-L ²)] (3a and 3b).....	137
6.2.6 Spectroscopic data of [Re(CO) ₃ (κ ³ N-L ²)]Br (4)	139
6.2.7 Spectroscopic data of [{Re(CO) ₃ (μ-1κ ³ N, 2κ ^P -L ² ')} ₂ {Re(CO) ₂ Br ₂ }]Br (7).....	141
6.2.8 Spectroscopic data of (NBu ₄)[Cl ₃ (O)Re{O ₂ P(^{1,2,3} Tz ^{1-Ph}) ₃ }Re(O)Cl ₂] (8)	
143	
6.2.9 Spectroscopic data of (NBu ₄)[ReOCl ₃ {O ₂ P(^{1,2,3} Tz ^{1-Ph}) ₂ }] (9)	145
6.2.10 Spectroscopic data of (NBu ₄)[Cl ₃ (O)Re{O ₂ P(^{1,2,3} Tz ^{1-benz}) ₃ }Re(O)Cl ₂] (10).....	147
6.2.11 Spectroscopic data of (NBu ₄)[Cl ₃ (O)Re{O ₂ P(^{1,2,3} Tz ^{1-benz}) ₂ }Re(O)Cl ₃] (11).....	149
6.2.13 Spectroscopic data of [Cu(κ ³ N-L ²) ₂](NO ₃) ₂ (12)	151
6.2.12 Spectroscopic data of [Ni(κ ³ N-L ²) ₂](NO ₃) ₂ (13)	153

1. Introduction

1.1 Tris(azolyl)borates, tris(azolyl)methanes, tris(azolyl)phosphines and tris(azolyl)phosphine oxides

Tris(azolyl) ligands, such as tris(azolyl)borates, tris(azolyl)methanes or tris(azolyl)-phosphines and their derivatives are tripodal ligands, which form stable complexes with a variety of metal ions. The fundamental features of all tris(azolyl) ligand complexes are the six-membered rings at the coordination center, which contain central boron, carbon or phosphorus atoms, the metal ion and four atoms of two azolyl rings. Many metal ions form stable complexes with tris(azolyl) ligands [1, 2], and potential and actual applications in catalysis, biomimetic reactions and pharmaceutics of tris(azolyl) complexes have been reported in the literature. For example, Pombeiro reports that several tris(pyrazolyl)methane and tris(pyrazolyl)borate ligands form stable complexes with the $\{\text{VO}_2\}^+$ core. The resulting vanadium complexes show catalytic activity to carboxylation and peroxidative oxidation reactions [3]. Many examples of applications of tris(azolyl) ligand complexes have been given in other reviews [4, 5]. The review of Charles G. Young reports several molybdenum tris(pyrazolyl)borates [2]. These molybdenum complexes act as biomimetic models for processes in living creatures, including OAT (oxygen atom transfer) reactions, CEPT (coupled electron-proton transfer) reactions and molybdenum hydroxylases catalysis. Some Zn(II) complexes of tris(imidazolyl)phosphines are designed as active site models of carbonic anhydrase [6, 7]. Similar structures with Fe ions are created as active site models of non-heme iron proteins [8]. A comprehensive review of tris(azolyl) ligand complexes in catalysis has been published [9]. In the following paragraphs, different tris(azolyl) ligands will be introduced separately based on their apical atoms (Figure 1).

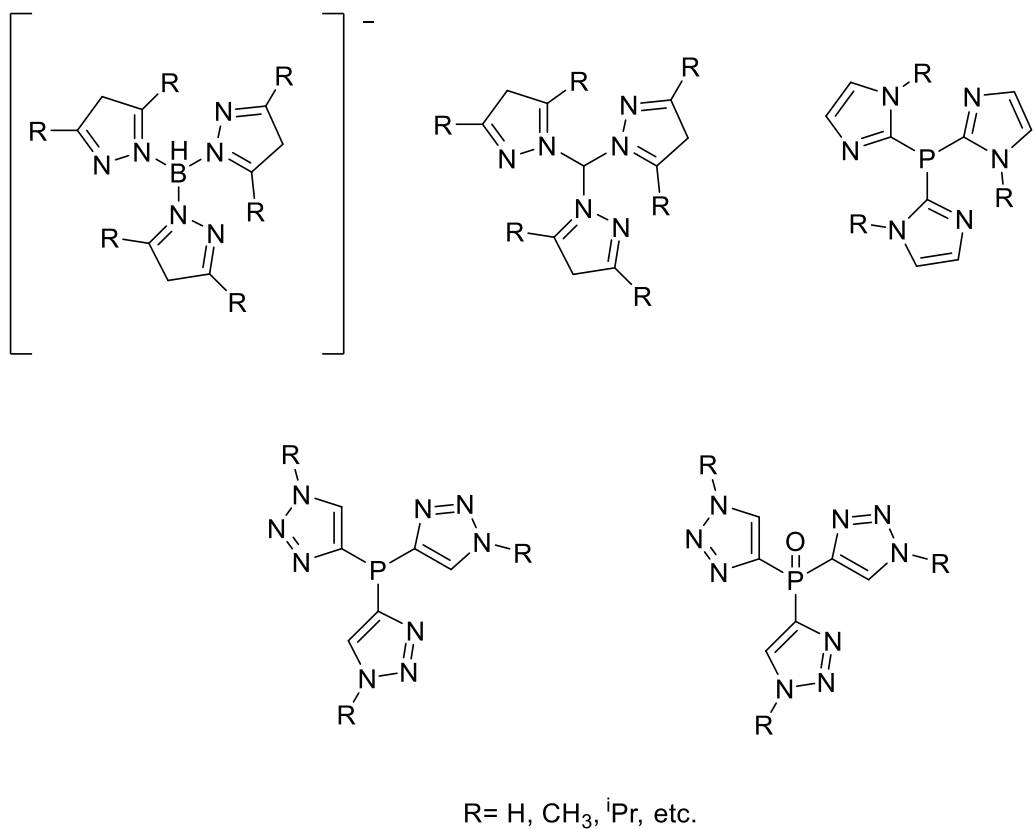


Figure 1. Different kinds of tris(azolyl) ligands.

Tris(azolyl)borates were developed as the first family of tris(azolyl) substituted tridentate ligands by S. Trofimenko in 1966 [10, 11]. They were synthesized by reactions of pyrazole or its derivatives with KBH_4 . The ligands carry a negative charge, which allows the formation of neutral complexes with positively charged metal ions. These tridentate ligands have been proved to bind metal ions of all size from beryllium to uranium with a variety of coordination numbers from 4 to 9 [10]. Gerard Parkin reported iron(II) and cobalt(II) complexes with tris(3-tert.-butylpyrazolyl)hydroborate. The bulky tert.butyl substituents on the pyrazolyl rings provide strong steric hindrance towards the metal ions. As a result, low-coordination-number complexes are formed [12]. Similar four-coordinate complexes are also found with magnesium or beryllium ions [13, 14].

On the other hand, small substituents allow higher coordination numbers and form frequently six-coordinate complexes. For example, Herdtweck et al. reported a Re(VII)

complex with tris(pyrazolyl)borate, $[\{HB(pz)_3\}ReO_3]$, without substituents on the pyrazolyl rings [15]. Also the heterocyclic ring of the ligand can be varied. Rare examples of derivatives with a pyridine moiety or other *N*-atom containing aromatic moieties were reported, some of them gave metal complexes as well. Phenyl-tris(1,2,4-diazaphospholyl)borate formed tridentate complexes with several transition metal ions [16]. Phenyltris(2-pyridyl)borates were designed to bind iron(II) and ruthenium(II) ions. The phenyl moieties on the ligands could be modified for bioconjugation [17]. Tris(azolyl)borates are also good ligands to bind lanthanide ions [9].

Tris(azolyl)methanes are analogs to the borate ligands, but the apical atom is carbon. The approach to such compounds is diversified, based on different moieties on the carbon atom. The common way to synthesize neutral tris(azolyl)methanes, is the reactions of pyrazole or its derivatives with chloroform under alkaline conditions. $(NBu_4)Br$ is used in such reactions for phase transfer. Tris(pyrazol-1-yl)methane was the first and the simplest tris(azolyl)methane [5]. The hydrogen atom on the carbon atom can be replaced by other functional groups (SO_3H or CH_2OH), which modifies the water-solubility of the tris(azolyl)methanes [13]. Like their boron counterparts, tris(azolyl)methanes are suitable ligands to bind many kinds of metal ions. For example, tris(pyrazol-1-yl)methane forms tridentate complexes with Mg^{2+} , Ca^{2+} , Sc^{3+} , Y^{3+} , Ln^{3+} , Ti^{3+} , V^{5+} , Cr^{3+} and Zn^{2+} ions [5]. Water-soluble tris(azolyl)methanes such as lithium tris(pyrazol-1-yl)methanesulfonate or 2,2,2-tris(pyrazol-1-yl)ethanol are able to bind rhenium ions [18].

Similar to tris(pyrazolyl)borates, tris(azolyl)phosphines or tris(azolyl)phosphine oxides contain three azoles, which are linked by a central atom. In contrast to the borate ligands, tris(azolyl)phosphines or tris(azolyl)phosphine oxides are neutral ligands and their *P* atoms act as convenient NMR probes. In the corresponding phosphine ligands, sometimes the *P* atom is also a coordination site [19, 20]. There are many kinds of tris(azolyl)phosphines or tris(azolyl)phosphine oxides, such as tris(imidazolyl)-phosphines, tris(pyrazolyl)phosphines, tris(thiazolyl)phosphines or tris(triazolyl)-

phosphines and their oxides. With these ligands, also some metal complexes have been obtained [20]. The coordination chemistry of tris(azolyl)phosphines and their oxides has been dominated for a long time by the corresponding imidazolyl and pyrazolyl derivatives, which have been used as mimics in models of bioinorganic chemistry. A comprehensive review covering all these aspects has been published recently [20]. Relatively little is known about corresponding pyrazolyl and triazolyl derivatives. Some tris(1,2,4-triazolyl)phosphine derivatives are used for triazolylation and phosphorylation reactions. Particularly, the corresponding phosphine oxides have been found to be useful synthons for the synthesis of nucleosides [21-26]. The common approach for the synthesis of tris(azolyl)phosphines and their oxides is the use of PCl_3 in reactions with azole compounds and a Lewis base. The exploration of the chemistry of tris(1,2,3-triazolyl)phosphines started in 2008, when Lammertsma et al. synthesized tris(1-phenyl-1H-1,2,3-triazol-4-yl)phosphine oxide, $\text{OP}^{(1,2,3\text{-Tz}^{\text{1-Ph}})}_3$, by a Cu(I)-catalyzed Huisgen cycloaddition [19]. One benefit of this kind of synthesis is that the reaction proceeds in the air at ambient temperature, which makes the last step of the synthesis easy. Using different organic azides, tris(1,2,3-triazolyl)phosphine oxides with a variety of functional groups can be synthesized. The compounds can act as tripodal ligands via three nitrogen donor atoms, as has been shown with the synthesis of a corresponding Rh(III) complex, but also, other coordination modes have been found [27-29]. Reduction of $\text{OP}^{(1,2,3\text{-Tz}^{\text{1-Ph}})}_3$ with PhSiH_3 , or an alternative one-pot synthesis starting with a [2 + 3] cycloaddition of an alkynyl Grignard reagent, gives the related phosphine $\text{P}^{(1,2,3\text{-Tz}^{\text{1-Ph}})}_3$, which has also been demonstrated to be a versatile ligand with variable denticity in Zn(II) complexes and heterobimetallic units [19, 30].

The goal of the present thesis

The chemistry of tris(azolyl)phosphines and tris(azolyl)phosphine oxides with rhenium (and technetium) is hitherto unexplored and shall be the matter of the present

thesis. For this, representatives of this class of ligands have been used in reactions with rhenium(I), technetium(I) and rhenium(V) starting materials.

In this thesis, two tris(1,2,3-triazolyl)phosphine oxides, L¹ and L² (see Figure 2), have been used. The approach to L¹ has already been developed by K. Lammertsma et al. [19]. This synthesis is also applicable for the preparation of L². L² was reduced to corresponding tris(1,2,3-triazolyl)phosphine (L^{2·}). The spectroscopic properties of these ligands and their complexes are discussed in the following Chapters.

L¹ and L² were used for reactions with [Re(CO)₅Br]. The two ligands were also applied for reactions with (NBu₄)[Tc₂(μ-Cl)₃(CO)₆], which is a technetium(I) compound. The synthesis of which was improved by Dr. S. Hildebrandt [31]. The reduced ligand L^{2·} has been used for a reaction with [Re(CO)₅Br].

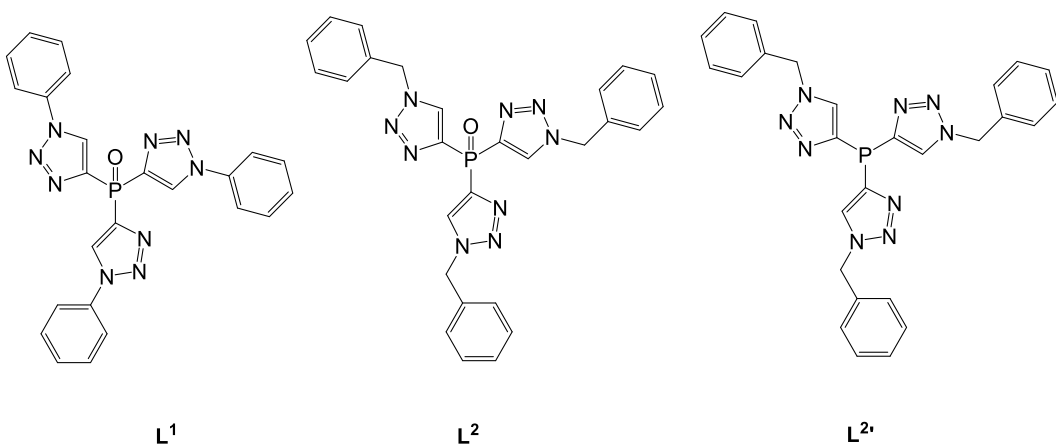


Figure 2. Ligands used in the thesis.

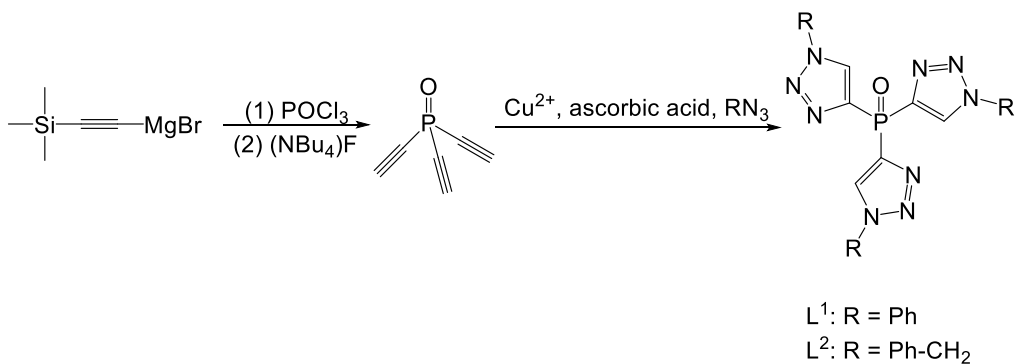
Reactions of oxidorhenium(V) complexes with L¹ and L² resulted in unexpected and unprecedented products such as dioxyphosphorane ligands. The mechanism of the formation of the dioxyphosphorane moiety in the complexes has been investigated by an isotope-labeling experiment and will be discussed.

The reactions of L² with Ni(NO₃)₂ · 6 H₂O and Cu(NO₃)₂ · 5 H₂O result in bis-chelates. Their structural and spectroscopic features are given.

2. Results and Discussions

2.1 Synthesis of the ligands

The syntheses of the ligands L¹ and L² are shown in Scheme 1. A freshly prepared magnesium Grignard reagent with a trimethylsilyl acetylenyl moiety was used in the reaction with phosphoryl chloride at 273 K in an argon atmosphere. The resulting intermediate is partially hydrolyzed by treating it with (NBu₄)F on silica gel to form the desired tris(ethylenyl)phosphine oxide. The tris(ethylenyl)phosphine oxide was used in the reactions with organic azides, such as phenyl azide or benzyl azide under formation of L¹ and L², respectively. The performed copper-catalyzed Huisgen cycloadditions follow the synthetic procedure given by K. Lammertsma et al. [19].



Scheme 1. Syntheses of L¹ and L².

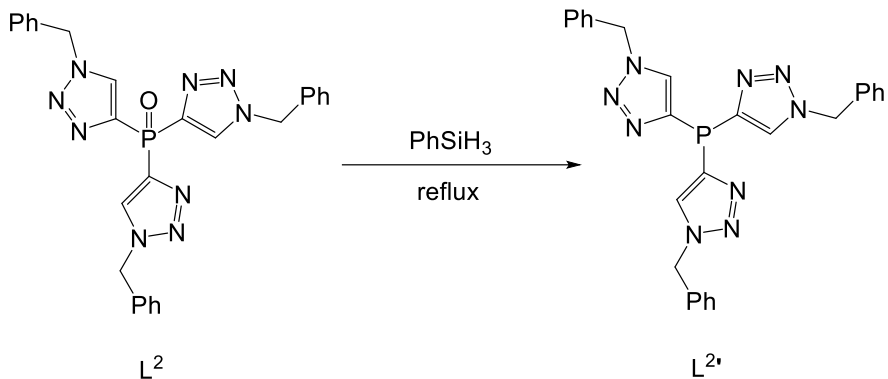
Attempts were made to replace (NBu₄)F on silica gel by KF or (NBu₄)F in THF solution. But for KF, the product yield of tris(ethylenyl) phosphine oxide was the same as that for the (NBu₄)F-on-silica-gel reaction (45%). And for (NBu₄)F in THF solution, the product yield was much lower (15%). The “Click Reactions” gave L¹ and L² with high product yields of 95%.

The IR spectra of L¹ and L² are quite similar. This is not unexpected, since the only structural difference between L¹ and L² is, that there is an additional methylene group in the L² molecule. Consequently, the vibrational bands of the same functional groups in L¹ and L² are at the same wavenumbers. Both bands of the P=O vibrations are at

1260 cm⁻¹ and the characteristic vibrations of the rings are around 1450-1500 cm⁻¹.

The other bands of L¹ and L² are generally the same.

The ¹H NMR spectra of L¹ and L² are similar, except that there is an extra signal at 5.54 ppm for L², which refers to the protons of the -CH₂- groups. Also the protons of the tris(triazolyl) rings give different chemical shifts. For L¹, the resonance is at 8.86 ppm, while for L² the resonance is at 8.14 ppm. The ³¹P NMR spectra of the ligands show single peaks at chemical shifts of -6.4 ppm (L¹) and -5.8 ppm (L²). However, in the following chapters we will see that the ³¹P resonances will differ depending on the individual complexes formed.

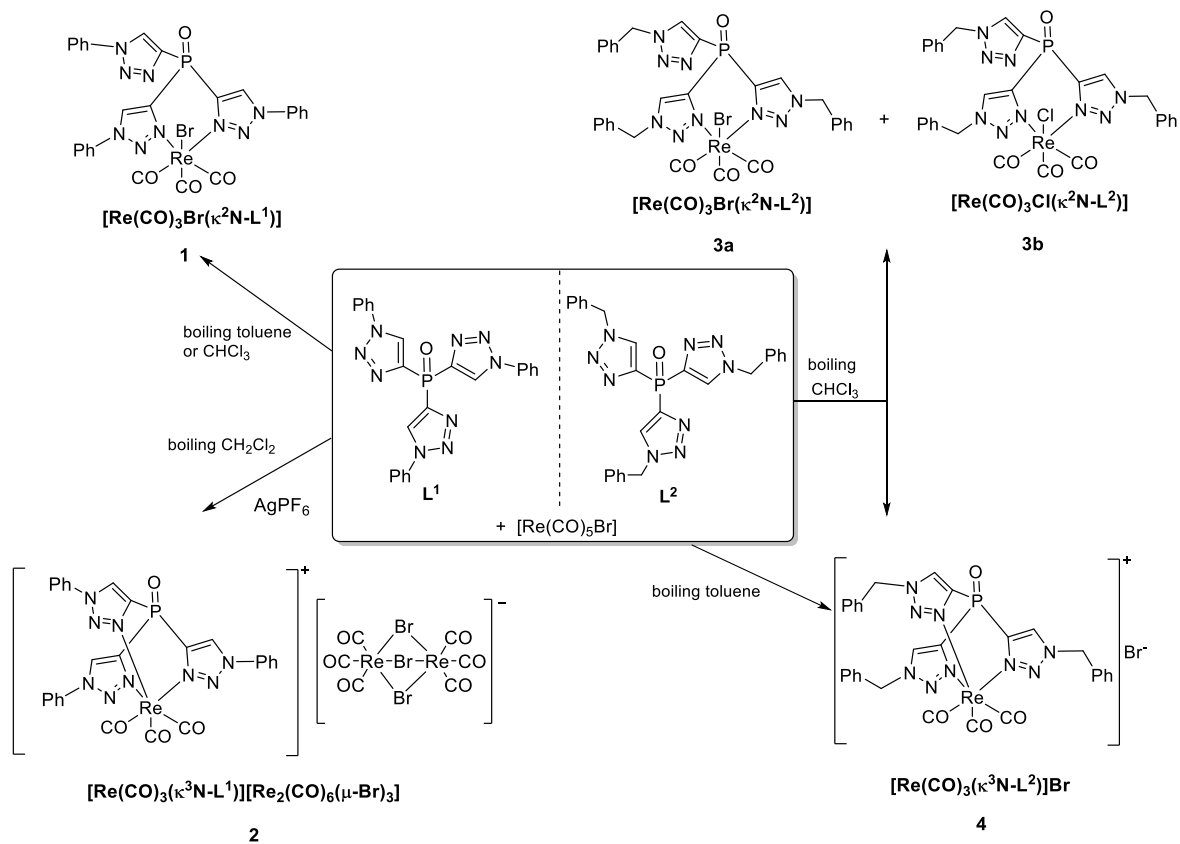


Scheme 2. Synthesis of L^{2'}.

The reaction of L² with neat phenylsilane gives the phosphine L^{2'}. The synthetic route follows the literature [19]. The course of the reaction is presented in Scheme 2. The resulting product is air-sensitive and must be stored under argon atmosphere at -20°C, so as to prevent that L^{2'} is re-oxidized to L². The ³¹P NMR spectrum of the ligand L^{2'} gives a single resonance at -63.7 ppm, which is far away from the resonance of ligand L². Such a great difference results from the reduction of the phosphine oxide and can be used to check the purity of the phosphine L^{2'}.

2.2 Tricarbonylrhenium(I) complexes with tris(1,2,3-triazolyl) phosphine oxides

The tricarbonylrhenium(I) unit is an important core for rhenium(I) complexes. It resembles the radioactive $\{\text{Tc}(\text{CO})_3\}^+$ core, which is very helpful to understand the chemistry of technetium carbonyl compounds. Complexes with the $\{\text{Re}(\text{CO})_3\}^+$ units are under considerations for nuclear medical diagnostic procedures [32, 33]. Additionally, complexes with the $\{\text{Re}(\text{CO})_3\}^+$ core are considered as potential β^- emitters for radiopharmaceutical therapy with the nuclides ^{186}Re or ^{188}Re [34]. Records on Re(I) complexes, mostly $[\text{Re}(\text{CO})_3]^+$ core, with several tris(azolyl) ligands are available [32-35].



Scheme 3. Reactions of L^1 and L^2 with $[\text{Re}(\text{CO})_5\text{Br}]$.

The tris(1,2,3-triazolyl)phosphine oxides L^1 and L^2 were used in reactions with pentacarbonylrhenium(I) bromide, $[\text{Re}(\text{CO})_5\text{Br}]$. It became evident that the course of the

reactions with the only slightly different ligands were not fully consistent. Scheme 3 summarizes the performed reactions and obtained products.

When L¹ was heated on reflux with [Re(CO)₅Br] in toluene or CHCl₃ for 24 hours, a colorless precipitate was formed. The ³¹P NMR spectrum of the reaction mixture indicates that the signal of L¹ disappeared and only one new species was formed. The ³¹P NMR signal of the new species appears at -10.3 ppm. Thus, a unique product was formed from the reaction of [Re(CO)₅Br] with L¹ independent of the reaction temperature applied. By treating the reaction mixtures with n-hexane, a crude product of compound **1** ([Re(CO)₃Br(κ^2 N-L¹)]) was precipitated, which was further recrystallized from dichloromethane/CCl₄ to give colorless crystals suitable for X-ray analysis.

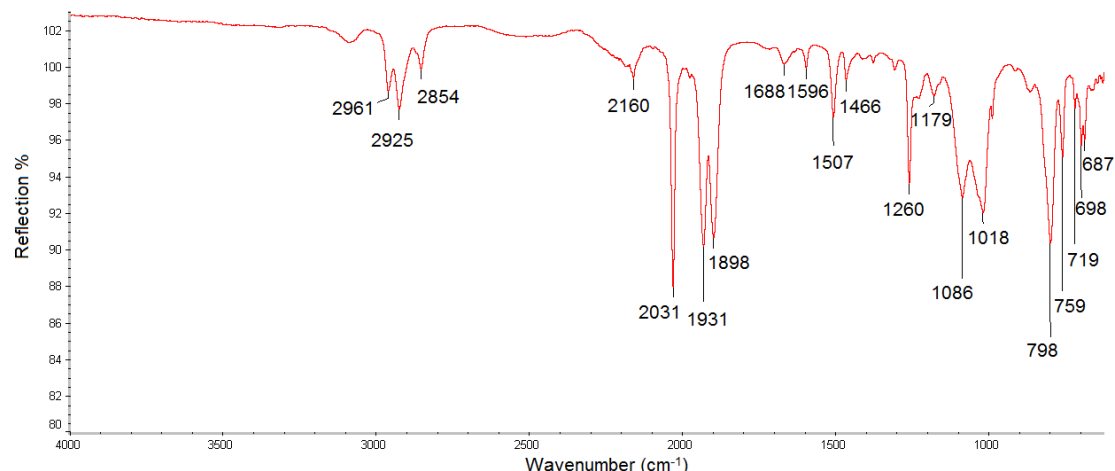


Figure 3. The IR spectrum of [Re(CO)₃Br(κ^2 N-L¹)] (**1**).

The IR spectrum of compound **1** (Figure 3) shows three bands at 1898, 1931 and 2031 cm⁻¹, which is the typical facial tricarbonyl absorption pattern for an asymmetric coordination environment. For a {Re(CO)₃}⁺ core with an isotropic environment, only two vibration bands of CO should be observed in the IR spectrum. However, if the symmetry in the molecule is broken, one band of these may split. This result implies that a complex with a bi-coordinated ligand was generated in the reaction, which was finally verified by X-Ray diffraction.

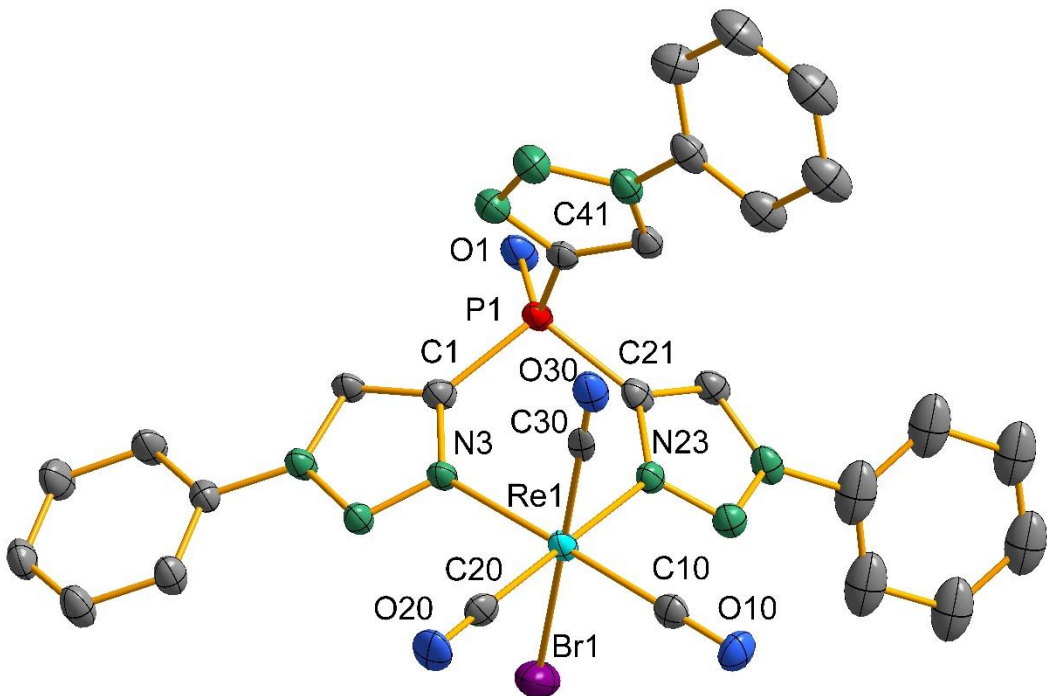


Figure 4. Ellipsoid representation of the molecular structure of compound **1**. Hydrogen atoms are omitted for clarity.

Figure 4 depicts an ellipsoid representation of the molecular structure of compound **1**. It clearly shows that only two triazole rings coordinate to the $\{\text{Re}(\text{CO})_3\}^+$ core. The third triazole ring of the ligand L^1 is not involved in the coordination, and a bromine atom completes the octahedral coordination sphere of rhenium. The structure implies that even under drastic reaction conditions (boiling toluene) no tripodal coordination of L^1 on a $\{\text{Re}(\text{CO})_3\}^+$ core is obtained.

Selected bond lengths and angles of $[\text{Re}(\text{CO})_3\text{Br}(\kappa^2\text{N-L}^1)]$ (**1**) are listed in Table 1. The Re1-C30 bond length ($1.959(7)$ Å) is slightly longer than the other two Re-C bonds. Such a difference may be due to the high electronegativity of the Br1 atom which is *trans* to the C30 atom and rules the structural *trans* influence of the carbonyl ligands. Another important feature of the structure is that the N11-Re1-N21 ,

N1-Re1-Br1 and N31-Re1-Br1 angles are smaller than 90°. This distortion may attribute to the shape of the ligand L¹, the rigid structure of which does not allow the formation of a regular octahedral coordination sphere around the rhenium ion.

Table 1. Selected bond lengths (Å) and angles (°) in compound **1**.

Re1-C10	1.909(6)	C30-Re1-N3	95.0(2)
Re1-C20	1.918(6)	C10-Re1-N23	92.1(2)
Re1-C30	1.959(7)	C20-Re1-N23	175.9(2)
Re1-Br1	2.5837(8)	C30-Re1-N23	95.6(2)
Re1-N3	2.186(5)	N3-Re1-N23	85.1(2)
Re1-N23	2.199(5)	C10-Re1-Br1	91.4(2)
P1-C1	1.779(6)	C20-Re1-Br1	91.7(2)
P1-C21	1.789(6)	C30-Re1-Br1	179.6(2)
P1-C41	1.777(6)	N3-Re1-Br1	84.7(2)
P1-O1	1.471(4)	N23-Re1-Br1	84.7(2)
C1-P1-C21	104.0(3)	C10-Re1-C20	89.9(2)
C21-P1-C41	103.4(3)	C10-Re1-C30	88.9(2)
C1-P1-C41	106.6(3)	C20-Re1-C30	88.0(2)
O1-P1-C41	114.6(3)	C10-Re1-N3	175.4(2)
O1-P1-C1	112.4(2)	C20-Re1-N3	92.7(2)
O1-P1-C21	114.9(3)		

Compound **1** is soluble in most organic solvents such as chloroform, dichloromethane, acetone, methanol, etc., but decomposes in such solutions gradually over weeks.

Although the reaction of [Re(CO)₅Br] with L¹ was undertaken at a high temperature in boiling toluene, the formation of a tripodal coordination of the organic ligand could not be achieved, even at prolonged reaction times. For this reason, AgPF₆ were introduced in the reactions of [Re(CO)₅Br] and L¹. No pure substance could be isolated from the reactions. However, there were some IR and MS spectroscopical evidence for the formation of a tripodal coordination of L¹ in the products. The IR spectra taken from the colorless solids isolated from such reaction mixtures show only two bands for the CO vibration, which is the typical facial absorption pattern for a symmetric

coordination environment. Mass spectra show peaks at $m/z = 748$ and 750 , which exactly match the calculation for the $[\text{Re}(\text{CO})_3(\kappa^3\text{N-L}^1)]^+$ ion. These results may indicate the formation of a complex with a tridentate coordinated ligand L^1 on the $\{\text{Re}(\text{CO})_3\}^+$ core. Finally, a small amount of single crystals could be obtained from the reaction of $[\text{Re}(\text{CO})_5\text{Br}]$, L^1 and AgPF_6 , which were characterized by X-ray diffraction. The compound was $[\text{Re}(\text{CO})_3(\kappa^3\text{N-L}^1)][\text{Re}_2(\text{CO})_6(\mu\text{-Br})_3]$ (**2**).

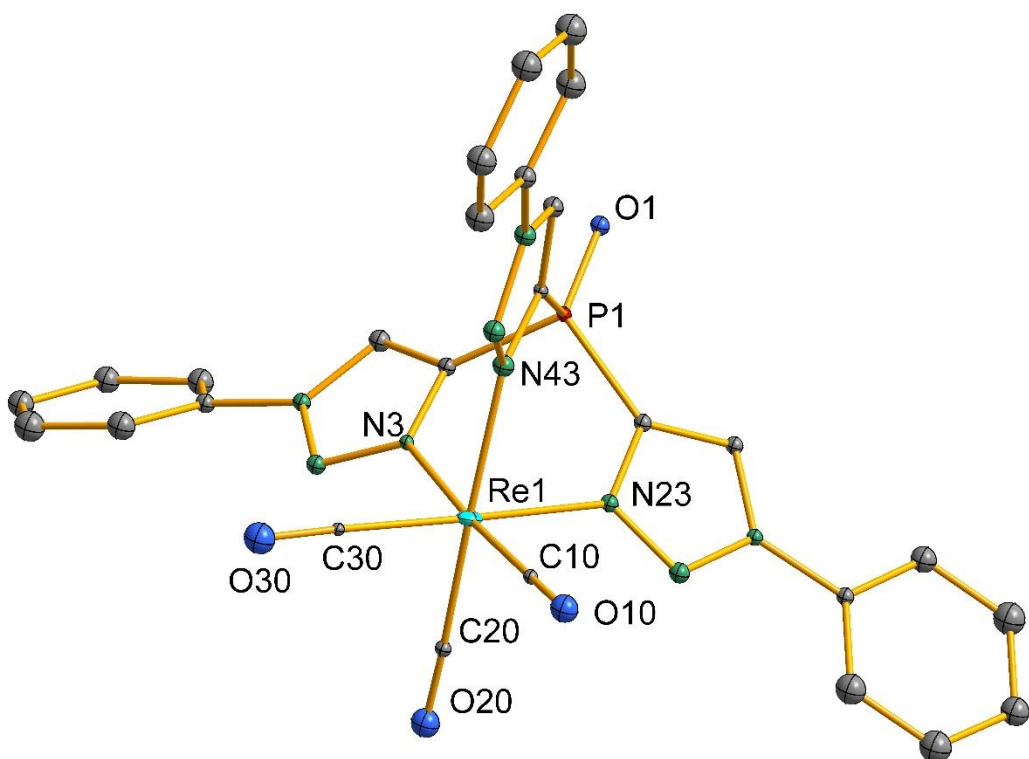


Figure 5. Ellipsoid representation of the complex cation of compound **2**. Hydrogen atoms are omitted for clarity.

Figure 5 presents the structure of the $[\text{Re}(\text{CO})_3(\kappa^3\text{N-L}^1)]^+$ cation. The result indicates that the formation of a tricarbonyl rhenium(I) complex with a tripodal coordination is possible, when the bromido ligand of $[\text{Re}(\text{CO})_3\text{Br}(\kappa^2\text{N-L}^1)]$ is removed by the addition of Ag^+ ions. As can be seen from the formed counterion $[\text{Re}_2(\text{CO})_6(\mu\text{-Br})_3]^-$, a strict control of the reaction conditions is required. When such a control of the precip-

itation of AgBr is not done, a series of side-reactions become evident. The formed anion $[\text{Re}_2(\text{CO})_6(\mu\text{-Br})_3]^-$ can be regarded as a side-product, which finally binds the released bromido ligands. Despite several attempts, no reliable protocol for the synthesis of a pure compound of the composition $[\text{Re}(\text{CO})_3(\kappa^3\text{N-L}^1)](\text{PF}_6)$ could be developed.

Although the quality of the obtained single-crystals of compound **2** was limited and the refinement converged at an R_1 value of only 9.4%, all important structural features of the complex cation could be derived. The selected bond lengths and angles in Table 2, however, are given for reference only and shall not be discussed in detail.

Table 2. Selected bond lengths (\AA) and angles ($^\circ$) in compound **2**.

Re1-C10	1.94(2)	C30-Re1-N3	91.3(5)
Re1-C20	1.94(2)	C10-Re1-N23	93.9(5)
Re1-C30	1.94(2)	C20-Re1-N23	175.6(5)
Re1-N3	2.16(2)	C30-Re1-N23	97.8(5)
Re1-N23	2.17(2)	N3-Re1-N23	84.4(5)
Re1-N43	2.19(2)	C10-Re1-N43	93.0(5)
P1-C1	1.80(2)	C20-Re1-N43	92.4(5)
P1-C21	1.80(2)	C30-Re1-N43	173.3(5)
P1-C41	1.80(2)	N3-Re1-N43	82.8(5)
P1-O1	1.48(2)	N23-Re1-N43	82.9(5)
C1-P1-C21	102.1(7)	C10-Re1-C20	92.1(6)
C21-P1-C41	101.0(7)	C10-Re1-C30	90.4(6)
C1-P1-C41	102.0(7)	C20-Re1-C30	86.6(6)
O1-P1-C41	113.7(6)	C10-Re1-N3	175.6(5)
O1-P1-C1	116.5(7)	C20-Re1-N3	92.1(5)
O1-P1-C21	118.9(7)		

On the other side, the clear formation of a tricarbonyl rhenium(I) complex with a tripodal coordination of a tris(1,2,3-triazolyl)phosphine oxide was observed during the reaction of L^2 with $[\text{Re}(\text{CO})_5\text{Br}]$. Prolonged heating of a mixture of L^2 and $[\text{Re}(\text{CO})_5\text{Br}]$ in boiling toluene resulted in the formation of a colorless precipitate.

The ^{31}P NMR spectra of the reaction mixture as well as of the isolated solid give only one signal at -11.2 ppm. The product was isolated by the addition of n-hexane to the reaction mixture. The colorless single crystals of $[\text{Re}(\text{CO})_3(\kappa^3\text{N-L}^2)]\text{Br}$ (**4**) were obtained by recrystallization of the crude product from dichloromethane/n-hexane. The IR spectrum of compound **4** shows two bands which are related to the CO vibrations. This indicates the formation of a symmetric structure with the $\{\text{Re}(\text{CO})_3\}^+$ core. This conclusion was confirmed by an X-ray structure determination of compound **4**.

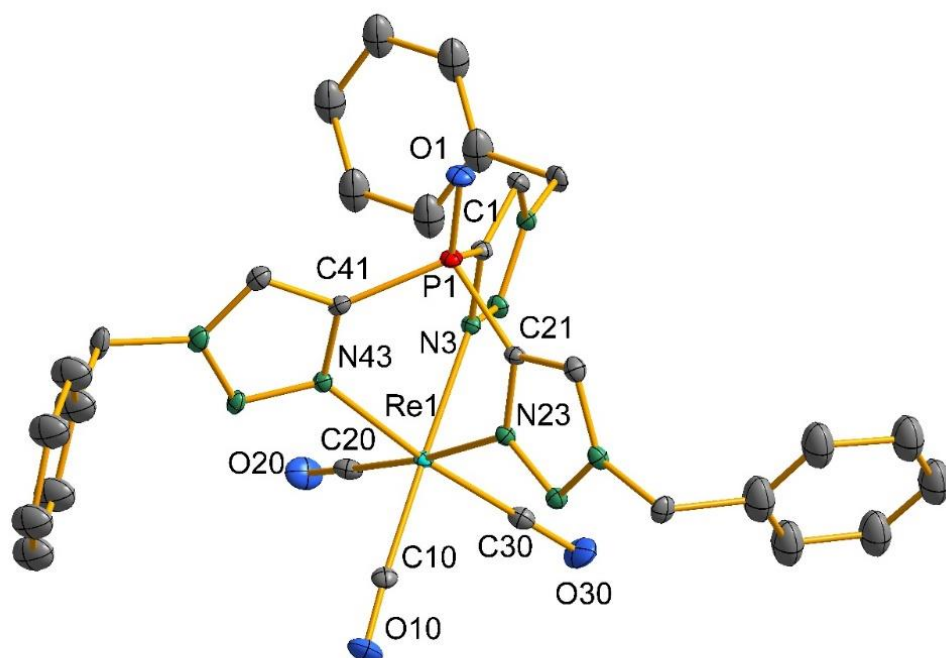


Figure 6. Ellipsoid representation of the cation of compound **4**. Hydrogen atoms and the Br^- counterion are omitted for clarity.

Figure 6 shows an ellipsoid representation of the cation of compound **4**. The $\{\text{Re}(\text{CO})_3\}^+$ core is coordinated by ligand L^2 under formation of an N,N,N -chelate. The rhenium atom has a slightly distorted octahedral coordination sphere. Like the corresponding complex of L^1 , main distortions of the coordination sphere are due to the steric restrictions given by the ligand L^2 . Selected bond lengths and angles are given in the Table 3.

Under more mild conditions, the reaction of L² with [Re(CO)₅Br] in boiling dichloromethane proceeded stepwise. Subsequently, the signal of L² in the ³¹P NMR spectrum of the reaction mixture disappeared, but two new resonances at -8.7 ppm and -11.2 ppm appeared. After a chromatographic separation on a silica gel column, the two components could be isolated. One of them is the known [Re(CO)₃(κ³N-L²)]Br (**4**) with a ³¹P NMR resonance at -11.2 ppm. The NMR signal observed at -8.7 ppm belongs to a mixture of the two compounds: [Re(CO)₃Br(κ²N-L²)] (**3a**) and [Re(CO)₃Cl(κ²N-L²)] (**3b**) as could be concluded from an X-ray crystallographic study on the isolated single crystals. Obviously, a partial exchange of the bromido ligand against Cl⁻ from the solvent CH₂Cl₂ occurred.

Table 3. Selected bond lengths (Å) and angles (°) in compound **4**.

Re1-C10	1.928(4)	C10-Re1-N3	177.4(2)
Re1-C20	1.927(4)	C20-Re1-N23	175.0(2)
Re1-C30	1.929(4)	C30-Re1-N43	174.0(2)
Re1-N3	2.180(3)	C10-Re1-N43	96.8(2)
Re1-N23	2.187(3)	N3-Re1-N43	83.0(2)
Re1-N43	2.186(3)	C20-Re1-N43	93.6(2)
P1-C1	1.784(3)	C30-Re1-N23	92.9(2)
P1-C21	1.775(4)	C10-Re1-N23	93.9(2)
P1-C41	1.790(4)	N3-Re1-N23	83.6(2)
P1-O1	1.475(3)	N43-Re1-N23	82.9(2)
C1-P1-C21	104.4(2)	C20-Re1-C30	90.3(2)
C21-P1-C41	103.2(2)	C20-Re1-C10	90.1(2)
C1-P1-C41	105.4(2)	C30-Re1-C10	87.7(2)
O1-P1-C41	114.5(2)	C20-Re1-N3	92.4(2)
O1-P1-C1	111.6(2)	C30-Re1-N3	92.4(2)
O1-P1-C21	116.7(2)		

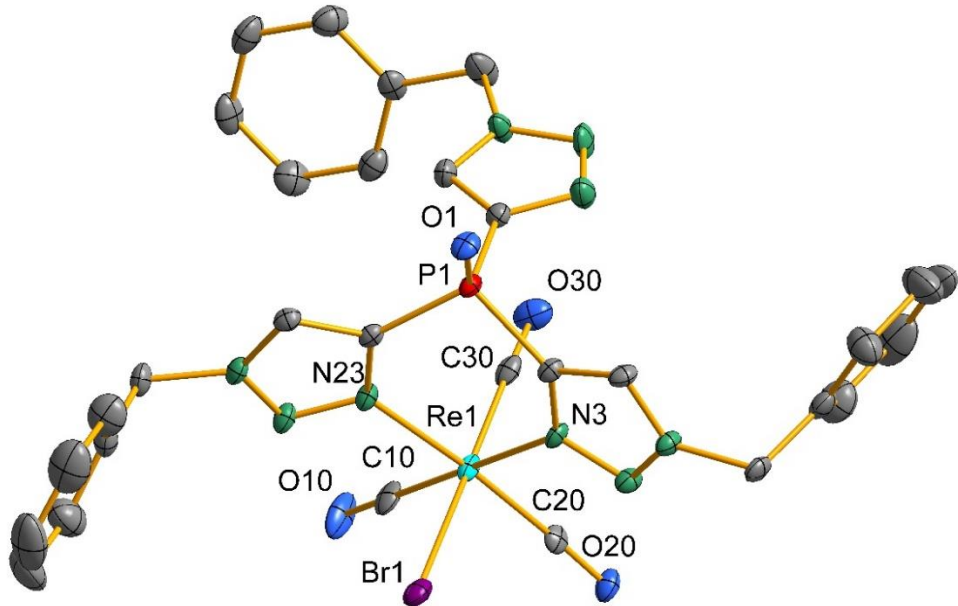


Figure 7. Ellipsoid representation of the molecular structure of compound **3a**. Hydrogen atoms are omitted for clarity.

Table 4. Selected bond lengths (\AA) and angles ($^\circ$) in compound **3a**.

Re1-C10	1.917(4)	C20-Re1-Br1	92.6(3)
Re1-C20	1.912(4)	C10-Re1-Br1	177.5(3)
Re1-C30	1.929(4)	C30-Re1-Br1	91.5(3)
Re1-N3	2.186(3)	N3-Re1-Br1	86.6(3)
Re1-N23	2.197(3)	N23-Re1-Br1	81.4(3)
Re1-Br1	2.59(2)	C20-Re1-C10	89.6(2)
P1-C1	1.784(3)	C20-Re1-C30	90.3(2)
P1-C21	1.775(4)	C10-Re1-C30	89.6(2)
P1-C41	1.790(4)	C20-Re1-N3	91.4(2)
P1-O1	1.475(3)	C10-Re1-N3	92.3(2)
C1-P1-C21	104.4(2)	C30-Re1-N3	177.6(2)
C21-P1-C41	103.2(2)	C20-Re1-N23	173.9(2)
C1-P1-C41	105.4(2)	C10-Re1-N23	96.4(2)
O1-P1-C41	114.5(2)	C30-Re1-N23	91.2(2)
O1-P1-C1	111.6(2)	N3-Re1-N23	87.0(2)
O1-P1-C21	116.7(2)		

Figure 7 presents an ellipsoid plot of the molecular structure of compound **3a**. The structure of this complex is very similar to that of compound **1**. Two of the nitrogen atoms of L² bind to rhenium, the coordination sphere of which is completed by a halide. Selected bond lengths and angles of compound **3a** are given in Table 4. Bond lengths and angles inside the organic ligand are very similar to the values derived for compound **1**. Details about the coordination sphere of rhenium cannot reliably be discussed because of the co-crystallization of the bromine and chlorine derivatives.

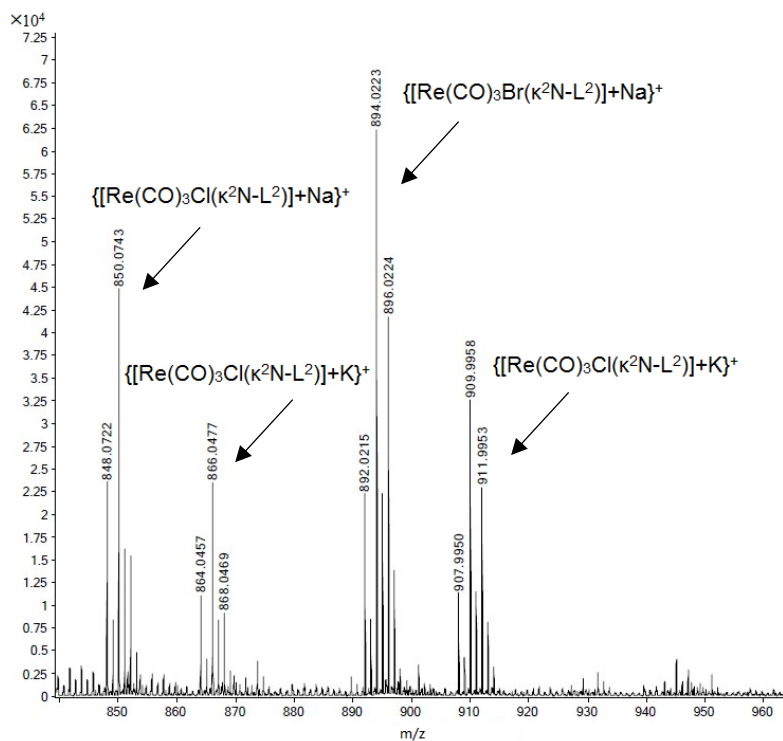


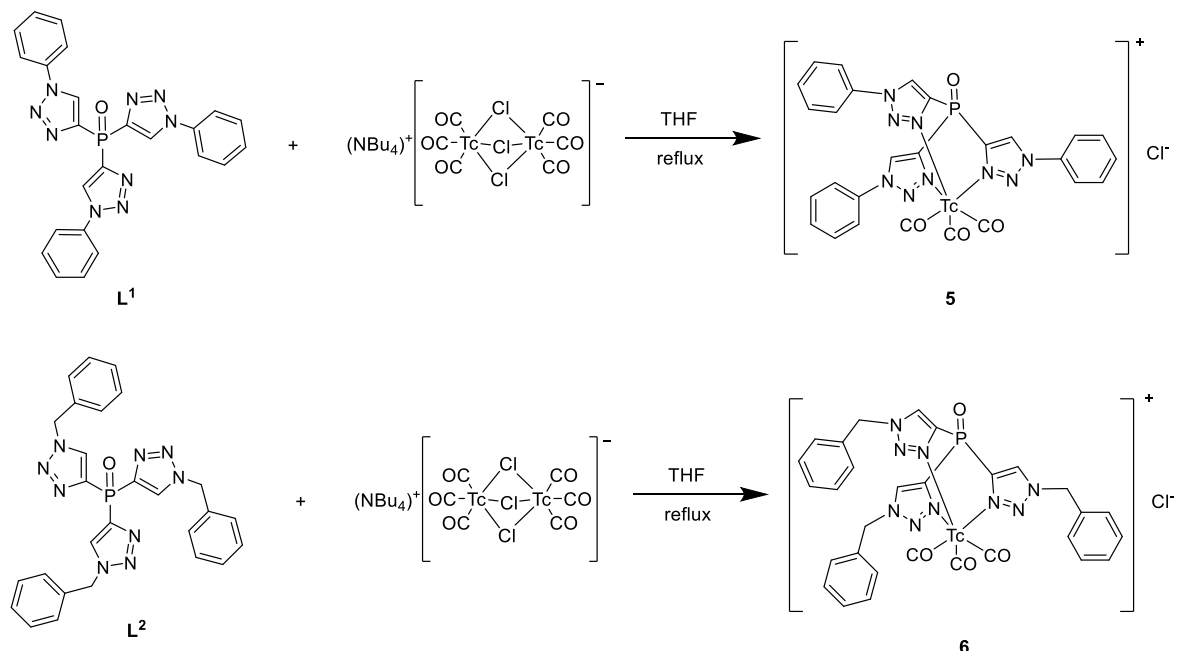
Figure 8. Molecular ion region of the ESI+ mass spectrum of the mixture obtained containing $[\text{Re}(\text{CO})_3\text{Br}(\kappa^2\text{N}-\text{L}^2)]$ (**3a**) and $[\text{Re}(\text{CO})_3\text{Cl}(\kappa^2\text{N}-\text{L}^2)]$ (**3b**).

The co-crystallization of compounds **3a** and **3b** is not an accidental incident for the measured single-crystal, but is representative for the bulk of the isolated solid. The proton NMR spectrum of the precipitate of the reaction between $[\text{Re}(\text{CO})_5\text{Br}]$ and L² shows two sets of signals. Also the recorded mass spectra of the product confirm the formation of a mixture of $[\text{Re}(\text{CO})_3\text{Br}(\kappa^2\text{N}-\text{L}^2)]$ and $[\text{Re}(\text{CO})_3\text{Cl}(\kappa^2\text{N}-\text{L}^2)]$. Figure 8 shows the molecular ion region of the mass spectrum. It gives clearly evidence for the

presence of a Br/Cl mixture. The peaks at $m/z = 894$ and 909 can be assigned to $\{[\text{Re}(\text{CO})_3\text{Br}(\kappa^2\text{N-L}^2)]+\text{Na}\}^+$ and $\{[\text{Re}(\text{CO})_3\text{Br}(\kappa^2\text{N-L}^2)]+\text{K}\}^+$, while the two signals at $m/z = 850$ and 866 belong to the corresponding Cl-containing ions. The presence of two compounds (**3a** and **3b**) in the product could not be resolved in the IR spectrum, which gives three CO bands as has been discussed for compound **1**.

2.3 Tricarbonyltechnetium(I) complexes with tris(1,2,3-triazolyl)-phosphine oxides

Reactions of L¹ and L² with (NBu₄)⁺[Tc₂(μ-Cl)₃(CO)₆] gave exclusively complexes of the composition [Tc(CO)₃(κ³N-L¹)]Cl (**5**) and [Tc(CO)₃(κ³N-L²)]Cl (**6**) (Scheme 4). Compounds with only bidentate coordination of the phosphine oxide ligands could not be isolated or detected spectroscopically in the reaction mixtures [31].



Scheme 4. Reactions of L¹ and L² with (NBu₄)⁺[Tc₂(μ-Cl)₃(CO)₆].

The ³¹P NMR spectra of compound **5** and **6** give single resonances in each spectrum, the chemical shifts of which are -5.4 ppm and -9.5 ppm [31]. The values are also close to those of L¹ and L². Such situations are very similar to the corresponding rhenium(I) reactions. This indicates that in these rhenium(I) and technetium(I) reactions, before and after coordination there is no significant change of the electron density at the phosphorus atoms.

The ⁹⁹Tc NMR spectra of compound **5** and **6** show single resonances at -1050 ppm and -1023 ppm in CDCl₃. The spectrum of the technetium(I) starting material (NBu₄)⁺[Tc₂(μ-Cl)₃(CO)₆]⁻ gives a single resonance at -947 ppm in CD₂Cl₂ [31]. In

comparison to the corresponding rhenium(I) reactions, it is easier to detect the formation of new compounds in technetium(I) reactions due to the usage of ^{99}Tc NMR spectroscopy.

Both the IR spectra of compound **5** and **6** show typical CO bands with a facial absorption pattern for a symmetric coordination environment (compound **5**: 2041 cm^{-1} and 1944 cm^{-1} , compound **6**: 2050 cm^{-1} and 1954 cm^{-1}), which suggests the formation of structures with tridentate coordinated ligands. The X-ray diffraction study on single crystals of compounds **5** and **6** match these observations (see Figure 9).

This finding is in agreement with the fact that the kinetics of Tc complexes as a metal of the second transition metal row is generally faster than reactions on their rhenium counterparts [36]. Thus, also reactions on the $\{\text{Tc}(\text{CO})_3\}^+$ centers are fast and intermediates could not be detected, while reactions of the $\{\text{Re}(\text{CO})_3\}^+$ species are slower, and intermediately formed compounds with bidentate coordinated L^1 and L^2 ligands could be isolated when the reactions are performed under mild conditions. In the reactions of the rhenium complex with L^1 , the removal of the Br^- ligand even requires the addition of silver salts to convert the bipodal coordinated complex of the $\{\text{Re}(\text{CO})_3\}^+$ core into the tripodal coordinated one.

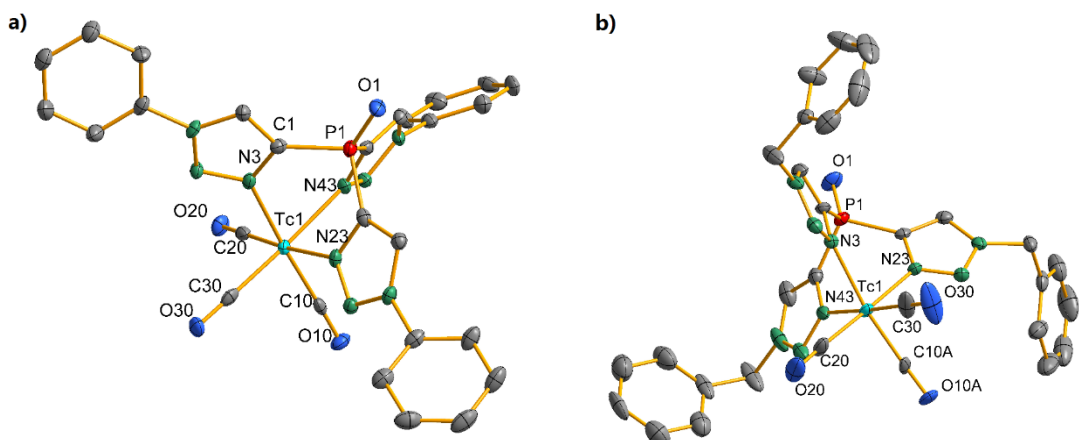


Figure 9. Ellipsoid representations of the cations of compound **5** (a) and compound **6** (b). Hydrogen atoms are omitted for clarity.

Figure 9 presents ellipsoid representations of the structures of the complex cations of compounds **5** and **6**. The structures of the two compounds share great resemblance. Both contain tridentate coordinated ligands and in both compounds the Tc(I) ions have slightly distorted octahedral coordination spheres. Selected bond lengths and angles of compound **5** and **6** are listed in Table 5. The related parameters of the two cations are quite similar except those on the atoms C10 and C10A, which is due to the disorder in the single crystal of compound **6**.

Table 5. Selected bond lengths (\AA) and angles ($^\circ$) in compound **5** and compound **6**.

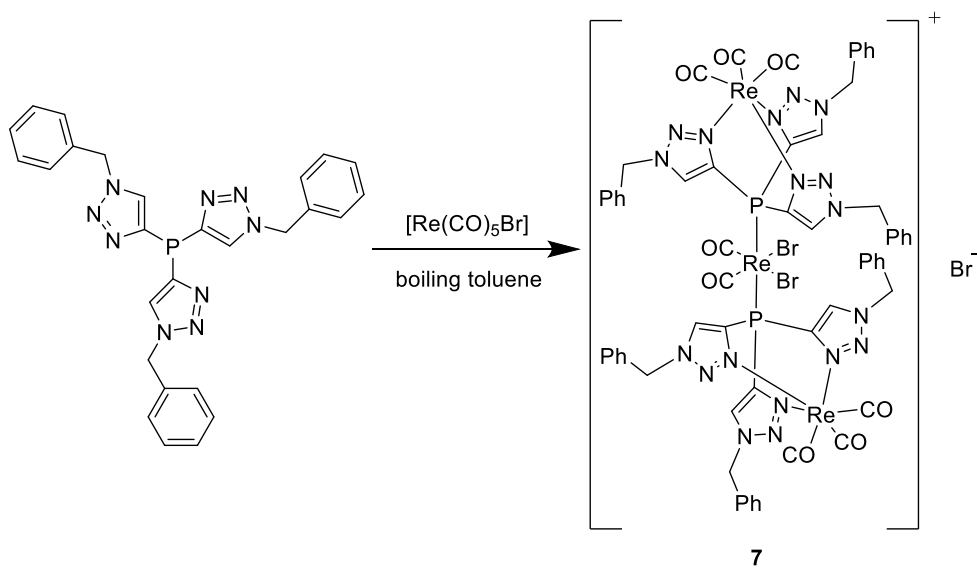
	Compound 5	Compound 6
Tc1-C10(A)	1.929(7)	1.898(9)
Tc1-C20	1.928(8)	1.937(4)
Tc1-C30	1.904(7)	1.920(5)
Tc1-N3	2.180(5)	2.186(3)
Tc1-N23	2.189(5)	2.170(3)
Tc1-N43	2.192(5)	2.175(3)
N3-Tc1-N23	83.4(2)	83.6(1)
N3-Tc1-N43	84.3(2)	83.7(1)
N23-Tc1-N43	84.6(2)	84.2(1)
C10(A)-Tc1-N3	174.7(2)	172.2(5)
C10(A)-Tc1-N23	91.3(2)	91.0(6)
C10(A)-Tc1-N43	94.3(2)	101.4(3)
C20-Tc1-N3	96.2(2)	95.4(2)
C20-Tc1-N23	175.4(2)	177.5(2)
C20-Tc1-N43	90.7(2)	93.3(2)
C20-Tc1-C10(A)	88.9(3)	90.2(7)
C30-Tc1-N3	92.4(2)	94.9(2)
C30-Tc1-N23	94.8(2)	92.7(2)
C30-Tc1-N43	176.7(2)	176.7(2)
C30-Tc1-C10(A)	88.9(3)	79.8(4)
C30-Tc1-C20	89.8(3)	89.7(2)

When comparing these parameters to those in their corresponding rhenium compounds (compound **2** and **4**), it is evident that all the four cationic structures share typical bonding features: the N-M-N angles are generally smaller than the C-M-C angles (M = Re or Tc) in these structures. This attributes to the rigid restrictions of the L¹ and L² ligands. The bond lengths of Tc-N and Tc-C bonds are similar to those of Re-N and Re-C bonds in there complexes with tridentate coordinated ligands.

To summarize, the reactions of L¹ and L² with (NBu₄)[Tc₂(μ-Cl)₃(CO)₆] reveal a faster kinetics when compared with the reactions of L¹ or L² with [Re(CO)₅Br]. Unlike the rhenium(I) reactions, which proceed stepwise, the technetium(I) reactions directly result in the formation of compounds with tridentate coordinated ligands. No stable compound with bidentate coordinated ligand can be isolated from the reactions as intermediates. The spectroscopic and structural features of the resulting compound **5** and **6** show resemblance to their corresponding rhenium(I) compounds **2** and **4** in their ³¹P NMR spectra, bond lengths and angles.

2.4 Reactions of [Re(CO)₅Br] with tris(1-benzyl-1H-1,2,3-triazol-4-yl)phosphine ($L^{2'}$)

Reduction of $OP(^{1,2,3}Tz^{1-Ph})_3$ with PhSiH₃, or an alternative one-pot synthesis starting with a [2 + 3] cycloaddition of an alkynyl Grignard reagent, give the related phosphine $P(^{1,2,3}Tz^{1-Ph})_3$, which has also been demonstrated to be a versatile ligand with variable denticity in Zn(II) complexes and heterobimetallic units [19, 27]. In the current thesis, the former method was used for the synthesis of $L^{2'}$.



Scheme 5. The reaction of $L^{2'}$ with $[Re(CO)_5Br]$.

The reaction of $L^{2'}$ with $[Re(CO)_5Br]$ was performed in dry toluene under argon atmosphere (see Scheme 5). The suspension firstly turned clear, but got turbid again within 90 minutes. The measurement of subsequent ^{31}P NMR spectra of the reaction mixture indicates that multiple phosphorus-containing species were formed within the first 30 minutes. However, most of these species disappeared gradually and only one new ^{31}P resonance remained in the NMR spectrum at -63.7 ppm. The reaction mixture was treated with hexane to precipitate all solids from the suspension. The colorless precipitate was filtered off and recrystallized from dichloromethane/acetone. Slow evaporation gave colorless single crystals, which were suitable for XRD analysis.

The IR spectrum of the compound **7** indicates three CO vibrations at 1851, 1919 and 2035 cm⁻¹. Frequently, such findings indicate a bi-coordinated structure, and the two bands at 1851 and 1919 cm⁻¹ should have a similar amplitude. However, the amplitudes of the two bands of compound **7** are quite different. Successless attempts to separate the components of a potential mixture by thin layer chromatography on a silica gel plate with acetone as eluent revealed that the compound is pure. Basing on these features, a single crystal XRD analysis of the compound has been undertaken.

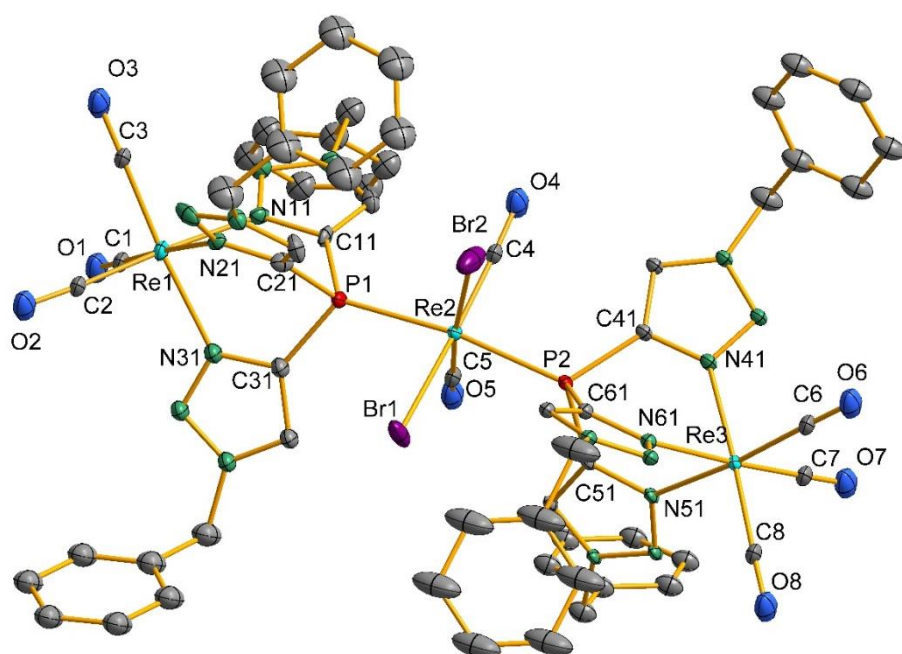


Figure 10 Ellipsoid representation of the cation of compound **7**. Hydrogen atoms are omitted for clarity.

Figure 10 shows an ellipsoid representation of the structure of the cation of compound **7**. Two different Re(I) cores are found. There are two $\{\text{Re}(\text{CO})_3\}^+$ units and one $\{\text{ReBr}_2(\text{CO})_2\}^-$ unit. The three rhenium atoms are linked by two $\text{L}^{2'}$ molecules, forming a sandwich-type structure. Both the *P* and *N* atoms on $\text{L}^{2'}$ are involved in the coordination.

Selected bond lengths and angles of compound **7** are given in the Table 6. The rhenium atoms Re1 and Re3 share an almost regular octahedral configuration. The coordination environment of Re2 is strongly distorted. The reason behind this is still unknown. Beside this, all Re-C bonds lengths are similar. The bond lengths and angles of the $\{\text{Re}(\text{CO})_3\}^+$ core in compound **7** show resemblance to those in compound **4**. The N-Re-N angles in compound **7** are smaller than the C-Re-C angles due to the rigid restriction of the ligands. This is also the case in compound **4**. In the octahedral coordination sphere of Re2, all the atoms, which are *trans* to each other give angles, which are significantly smaller than 180 degrees. This might be due to the strong hindrance effect from the two ligands on the complex.

No previous report of structures with the $\{\text{Re}(\text{CO})_3\}^+$ and $\{\text{ReBr}_2(\text{CO})_2\}^-$ cores in one molecule has been found in the CCDC database [37]. A plenty of structures with the $\{\text{Re}(\text{CO})_3\}^+$ core have been reported in the past [38]. Though a number of records with isomeric *cis*- $\{\text{ReX}_2\text{Br}_2(\text{CO})_2\}^-$ units can be found in literatures [39, 40], the structures with *trans*- $\{\text{ReX}_2\text{Cl}_2(\text{CO})_2\}^-$ or *trans*- $\{\text{ReX}_2\text{Br}_2(\text{CO})_2\}^-$ unit, in which the four ligands (Br and CO ligands) are on the same plane, are less common to find, still the number of records is limited and few of them are provided with crystal structures [41, 42]. In the ref. 41, the bond lengths and angles of structure with $\{\text{ReCl}_2(\text{CO})_2\}^-$ unit are provided. Just like in compound **7**, the two Cl-Re-C angles of the structure are smaller than 180 degrees ($174.6(4)^\circ$). And the C-Re-C angle of the $\{\text{ReCl}_2(\text{CO})_2\}^-$ unit is smaller than 90 degrees ($84.6(4)^\circ$), which is similar to that of compound **7**.

Table 6. Selected bond lengths (\AA) and angles ($^\circ$) in compound **7**.

Re1-C1	1.94(2)	C2-Re1-N21	94.6(5)
Re1-C2	1.90(1)	C3-Re1-N21	94.3(5)
Re1-C3	1.93(1)	C1-Re1-N21	174.2(4)
Re1-N11	2.15(1)	N11-Re1-N21	82.6(4)
Re1-N21	2.19(1)	C2-Re1-N31	94.1(4)
Re1-N31	2.20(1)	C3-Re1-N31	175.4(4)
Re2-C4	1.89(1)	C1-Re1-N31	93.7(4)
Re2-C5	1.99(2)	N11-Re1-N31	82.8(4)
Re2-Br1	2.630(2)	N21-Re1-N31	82.4(4)
Re2-Br2	2.655(2)	C4-Re2-C5	87.3(5)
Re2-P1	2.367(3)	C4-Re2-P1	93.6(4)
Re2-P2	2.398(3)	C5-Re2-P1	84.1(3)
Re3-C6	1.95(2)	C4-Re2-P2	94.1(4)
Re3-C7	1.91(2)	C5-Re2-P2	93.5(3)
Re3-C8	1.95(2)	P1-Re2-P2	171.78(9)
Re3-N41	2.143(9)	C4-Re2-Br1	173.3(4)
Re3-N51	2.169(9)	C5-Re2-Br1	99.4(4)
Re3-N61	2.172(9)	P1-Re2-Br1	86.28(8)
C2-Re1-C3	89.4(5)	P2-Re2-Br1	86.34(8)
C2-Re1-C1	89.4(5)	C4-Re2-Br2	84.7(4)
C3-Re1-C1	89.3(5)	C5-Re2-Br2	171.6(4)
C2-Re1-N11	176.3(5)	P1-Re2-Br2	98.90(8)
C3-Re1-N11	93.6(4)	P2-Re2-Br2	84.53(8)
C1-Re1-N11	92.7(5)	Br1-Re2-Br2	88.67(6)
C2-Re1-N21	95.2(5)	C7-Re3-C6	88.1(5)
C3-Re1-N21	94.0(6)	C7-Re3-C8	92.0(5)
C1-Re1-N21	174.2(5)	C6-Re3-C8	87.9(5)
N11-Re1-N21	82.5(4)	C7-Re3-N41	91.6(4)
C2-Re1-N31	94.0(5)	C6-Re3-N41	92.6(4)
C3-Re1-N31	175.4(6)	C8-Re3-N41	176.4(5)
C1-Re1-N31	93.5(5)	C7-Re3-N61	92.7(5)
N11-Re1-N31	82.8(4)	C6-Re3-N61	174.9(4)
N21-Re1-N31	82.6(4)	C8-Re3-N61	97.2(4)
C2-Re1-C3	89.3(6)	N41-Re3-N61	82.3(3)
C2-Re1-C1	89.9(6)	C7-Re3-N51	173.2(5)
C3-Re1-C1	89.7(6)	C6-Re3-N51	96.0(4)
C2-Re1-N11	175.9(5)	C8-Re3-N51	93.5(4)
C3-Re1-N11	93.8(6)	N41-Re3-N51	82.8(4)
C1-Re1-N11	92.7(5)	N61-Re3-N51	82.7(3)

Since the chemical environment of the two L^2' molecules inside the structure is identical, it is reasonable to observe just one single resonance in the ^{31}P NMR spectrum. Compound 7 is chiral with a center of chirality at atom Re2. When viewed along the Re1-Re3 direction (Figure 11a), it is clear that there are no symmetric relationships between the two L^2' ligands. Consequently, the atoms P1 and P2 are not identical when they are considered in the coordination sphere of the atom Re2. As a result, the mirror image of the octahedral coordination sphere of the atom Re2 does not superimpose with the original one (see Figure 11b).

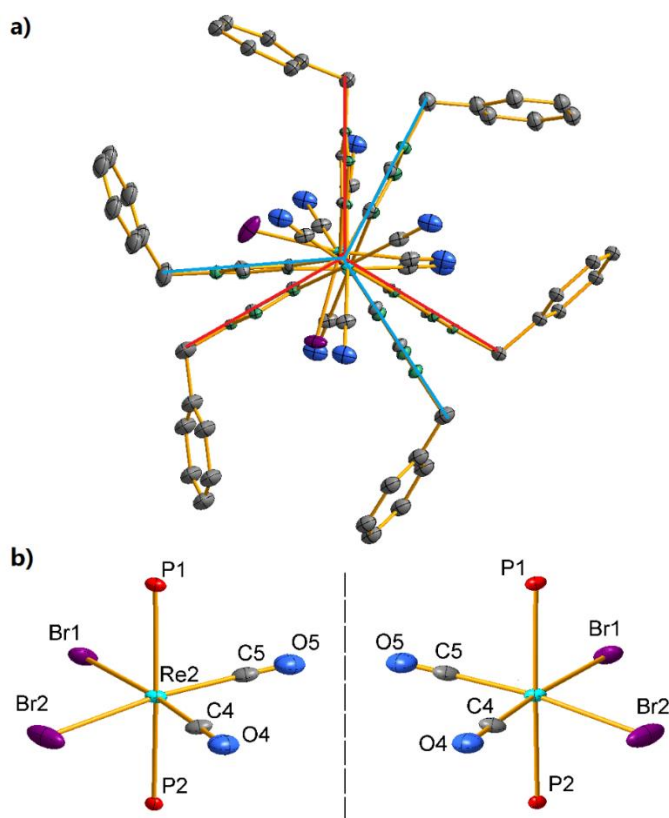
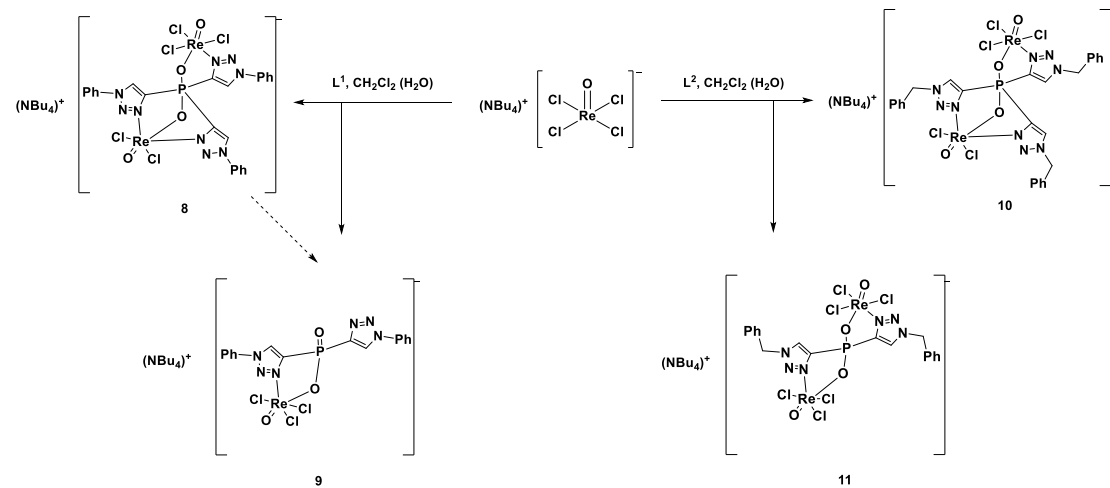


Figure 11. **a)** Ellipsoid representation of the cation of compound 7, viewed along the Re1-Re2-Re3 axis. **b)** Coordination sphere of Re2 atom and its mirror image.

Compound 7 only sparingly dissolves in most organic solvents and is only soluble in dichloromethane or chloroform. The stability of the compound is low in solution and a slow decomposition was observed during the recrystallization.

2.5 Reactions of $(\text{NBu}_4)[\text{ReOCl}_4]$ with tris(1,2,3-triazolyl)phosphine oxides

In this Chapter, reactions of rhenium(V) complexes with the ligands L^1 and L^2 will be discussed. Although there is no previous report on tris(1,2,3-triazolyl)phosphine oxides and oxidorhenium complexes, such complexes with other tripodal ligands have been studied. For instance, a number of Re(VII) complexes with the $\{\text{ReO}_3\}^+$ core and tris(pyrazolyl)hydridoborate or tris(pyrazolyl)methane have been reported [43, 44]. The reduction of a Re(VII) tris(pyrazolyl)hydridoborate complex gives a Re(V) compound with a $\{\text{ReOCl}_2\}^+$ core [43]. Other studies about Re(V) or Re(III) complexes with tris(azolyl) ligands are rare [45].



Scheme 6. The reactions of L^1 and L^2 with $(\text{NBu}_4)[\text{ReOCl}_4]$.

Tetrabutylammonium tetrachlorooxorhenate(V), $(\text{NBu}_4)[\text{ReOCl}_4]$, is a common Re(V) starting material. It is used in the reactions with the tris(1,2,3-triazolyl)phosphine oxides (Scheme 6).

2.5.1. Reactions of (NBu₄)[ReOCl₄] with L¹

The reaction of (NBu₄)[ReOCl₄] with L¹ in dichloromethane gave a green solution within one minute. The ³¹P NMR signal of the ligand at -6.4 ppm disappeared and a new signal was detected at -61.7 ppm. Such a value is not in the common range for organic phosphine oxides. The tremendous difference in the observed chemical shifts before and after the reaction indicates that the structure of the phosphorus compound has been changed. The reaction mixture was treated with a large amount of diethyl ether to get a crude precipitate. A ³¹P NMR monitoring of the reaction shows that one single phosphorus-containing species is obtained as main product. During the crystallization process, however, new components were formed, as can be detected from multiple signals observed. The green precipitate was dissolved in dichloromethane and treated with hexane. Green single crystals of compound **8**, which were suitable for X-ray diffraction, were obtained by recrystallization. After the separation of crystals of compound **8**, the solution was further evaporated, which gave a sticky green resin. Repeated dissolution of this material and evaporation of the solvent gave bright green single crystals of compound **9**.

Compound **8** was identified as a binuclear, anionic rhenium(V) complex containing a dihydroxylphosphorane ligand. An ellipsoid representation of the structure of the complex anion is shown in Figure 12. The counterion is tetrabutylammonium. The two rhenium atoms have different coordination spheres. One is a {ReOCl₂}⁺ unit, which is bonded to one triazolyl nitrogen atom and the oxygen atom of the ligand L¹. The second rhenium atom binds to the oxido ligand, two chlorido ligands, two nitrogen atoms of the former L¹, and the second oxygen atom of the dihydroxylphosphorane ligand. The source of this oxygen atom will be discussed later.

Table 7 gives selected bond lengths and angles for compound **8**. The two rhenium atoms have distorted octahedral configurations. One important feature here is the length of phosphorus-oxygen bonds. The bond lengths are shorter than common P-O

single bonds, but longer than P=O double bonds. The O-P-O angle is almost 180 degrees.

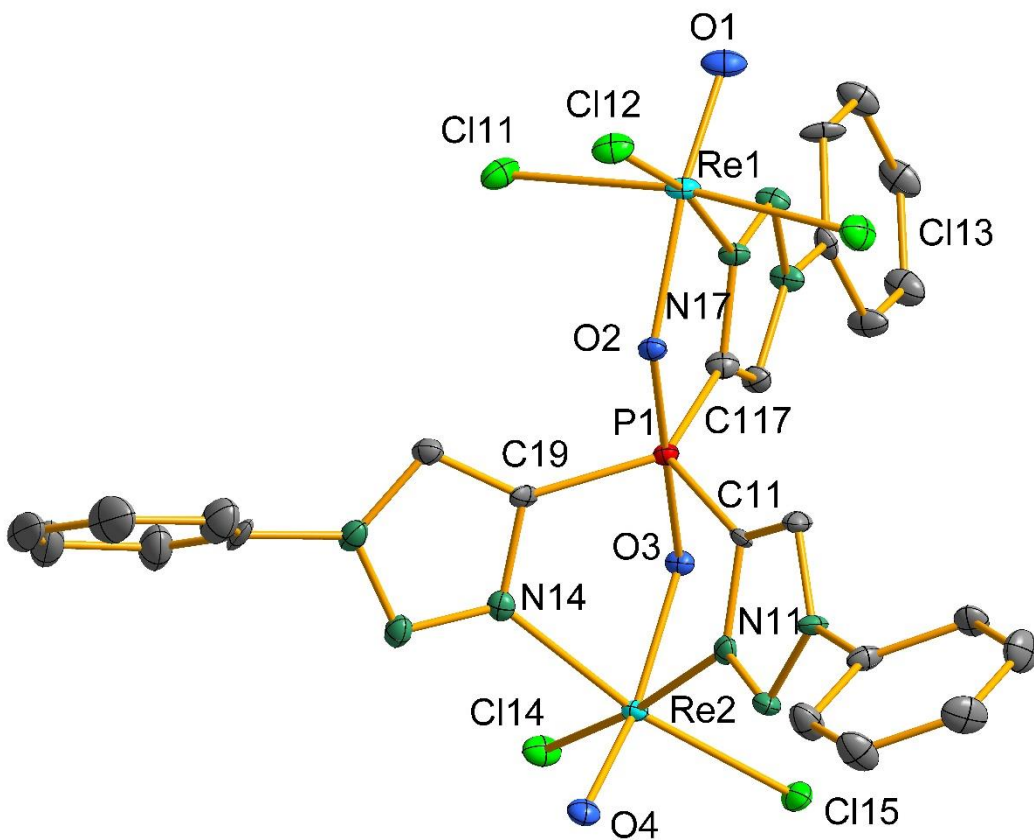


Figure 12. Ellipsoid representation of the complex anion of compound **8**. Hydrogen atoms are omitted for clarity.

Such kind of dioxophosphorane compounds can be found in organic chemistry as well. Organic dioxophosphoranes have been discovered decades ago [46, 47]. However, it is the first time to observe a metal complex with such kind of moiety. Just like its organic counterpart, compound **8** is unstable in solution. When dissolved in dichloromethane, compound **8** slowly decomposes within weeks. When dispersed in polar solvents such as methanol, ethanol or acetone, a rapid decomposition of compound **8** is observed. This resembles the chemical properties of organic dioxophosphoranes [46, 47].

Table 7. Selected bond lengths (\AA) and angles ($^\circ$) in compound **8**.

Re1-O1	1.684(3)	N11-Re2-Cl14	171.5(2)
Re1-O2	1.977(3)	O4-Re2-Cl15	100.7(2)
Re1-N17	2.121(4)	O3-Re2-Cl15	95.38(9)
Re1-Cl11	2.403(2)	N14-Re2-Cl15	169.7(2)
Re1-Cl12	2.362(2)	N11-Re2-Cl15	89.6(1)
Re1-Cl13	2.396(2)	Cl14-Re2-Cl15	91.29(4)
Re2-O3	1.922(3)	O1-Re1-O2	163.1(2)
Re2-O4	1.699(3)	O1-Re1-N17	87.8(2)
Re2-N14	2.142(4)	O2-Re1-N17	75.4(2)
Re2-N11	2.151(4)	O1-Re1-Cl12	102.8(2)
Re2-Cl14	2.344(2)	O2-Re1-Cl12	94.10(9)
Re2-Cl15	2.351(2)	N17-Re1-Cl12	169.4(2)
P1-O2	1.632(3)	O1-Re1-Cl13	94.4(2)
P1-O3	1.712(3)	O2-Re1-Cl13	85.20(9)
O4-Re2-O3	155.9(2)	N17-Re1-Cl13	91.3(2)
O4-Re2-N14	89.2(2)	Cl12-Re1-Cl13	89.03(4)
O3-Re2-N14	74.3(2)	O1-Re1-Cl11	94.5(2)
O4-Re2-N11	87.9(2)	O2-Re1-Cl11	85.92(9)
O3-Re2-N11	74.2(2)	N17-Re1-Cl11	87.8(2)
N14-Re2-N11	87.9(2)	Cl12-Re1-Cl11	90.25(4)
O4-Re2-Cl14	100.2(2)	Cl13-Re1-Cl11	171.01(4)
O3-Re2-Cl14	97.23(9)	O2-P1-O3	178.6(2)
N14-Re2-Cl14	89.8(1)		

The ^{31}P NMR spectrum of compound **8** shows a single signal at -61.7 ppm. This value is similar to those of organic dioxophosphoranes (e.g. -55 ppm for diethoxytriphenylphosphorane) [46]. The IR spectrum of complex **8** shows characteristic bands of the P=O and Re=O vibrations at 1260 cm^{-1} and 987 cm^{-1} . The mass spectrum of compound **8** gives a series of peaks between $m/z = 1071$ and $m/z = 1085$. Due to the existence of $^{35}\text{Cl}/^{37}\text{Cl}$ and other isotopes, the typical peak set of ^{185}Re and ^{187}Re was not properly resolved in the spectrum. However, the mass distribution in the spectrum matches the result of corresponding simulations [48].

Metal complexes that share similar structures as compound **9** have been previously reported and can be considered as phosphinic acid complexes. Figure 13 depicts an ellipsoid representation of the anion of compound **9**. Unlike compound **8**, the product is a mononuclear rhenium complex. One P-C bond of the ligand has been cleaved under formation of a diarylphosphinic acid. Such a result may be due to the hydrolysis of the ligand during the recrystallization. Similar mechanisms of the formation of other hypophosphorous acid metal complexes have been proposed [49, 50]. Just like compound **8**, compound **9** is unstable and decomposes gradually. The octahedral coordination sphere of the metal center is slightly distorted and the P1-O3 bond length is slightly larger than the P1-O1 double bond (see Table 8). A resonance at 1.8 ppm is observed in the ^{31}P NMR spectrum of the complex. In the infrared spectrum, the Re=O vibration at 950 cm^{-1} and the P=O band at 1257 cm^{-1} are observed.

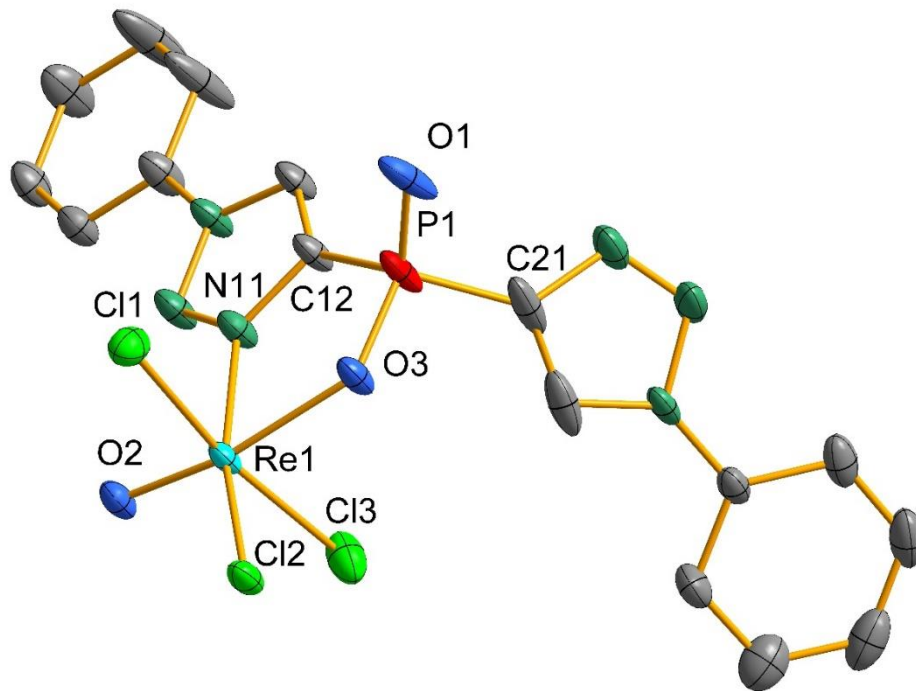


Figure 13. Ellipsoid representation of the anion of compound **9**. Hydrogen atoms are omitted for clarity.

Table 8. Selected bond lengths (\AA) and angles ($^\circ$) in compound **9**.

Re1-N11	2.132(2)	O2-Re1-Cl3	94.82(7)
Re1-O2	1.671(2)	O3-Re1-Cl2	89.50(5)
Re1-O3	2.069(2)	O3-Re1-Cl3	86.07(6)
Re1-Cl1	2.3754(7)	O3-Re1-Cl1	84.67(6)
Re1-Cl2	2.3302(6)	O3-Re1-N11	76.58(7)
Re1-Cl3	2.3858(8)	N11-Re1-Cl1	88.96(7)
P1-O1	1.476(2)	N11-Re1-Cl3	90.41(7)
P1-O3	1.536(2)	N11-Re1-Cl2	166.05(6)
O2-Re1-O3	166.08(8)	Cl1-Re1-Cl3	170.61(2)
O2-Re1-N11	89.52(8)	Cl2-Re1-Cl1	88.86(2)
O2-Re1-Cl2	104.38(6)	Cl2-Re1-Cl3	89.50(3)
O2-Re1-Cl1	94.54(7)		

Table 8 presents selected bond lengths and angles in compound **9**. The octahedral coordination sphere of the Re ion is not regular. Due to the rigid structure of the ligand, the O3-Re1-N11 angle is significantly smaller than 90° . The O2-Re1-Cl1 and O2-Re1-Cl3 angles are larger than 90° , which might be influenced by the atom O2.

2.5.2 Reactions of $(\text{NBu}_4)[\text{ReOCl}_4]$ with L^2

For the reaction of L^2 with $(\text{NBu}_4)[\text{ReOCl}_4]$, similar observations have been made like for the corresponding reaction of L^1 : within less than one minute the color of the reaction mixture changed to blue-green. The ^{31}P NMR signal of ligand L^2 disappeared at -5.7 ppm and a new single signal appeared at -62.0 ppm.

Also in the case of L^2 , a gradual decomposition of the ligand was observed during recrystallization. The solution was treated with diethyl ether, which resulted in the precipitation of a blue solid. The precipitate was dissolved in dichloromethane and treated with hexane. Light green crystals of compound **11** could be isolated from this solution. Subsequently, blue-green single crystals of compound **10** separated from the reaction mixture. The light-green single crystals of compound **11** were recrystallized from acetone/chloroform. Compound **11** can be obtained in better yield and without

the parallel formation of compound **10**, when the reaction is performed under dry and inert condition. A corresponding reaction in a Schlenk tube using dry THF as solvent and an argon atmosphere gave compound **11** with a yield of 50%. Single crystals were grown by diffusing n-hexane into a THF solution of the compound. The crystals were suitable for XRD analysis and the structure of compound **11** was determined by X-ray diffraction.

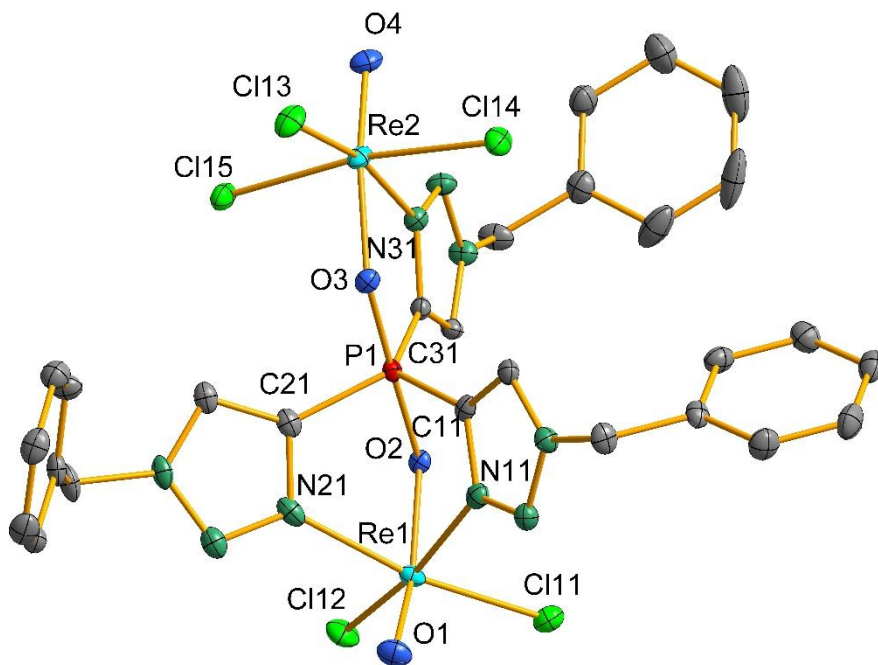


Figure 14. Ellipsoid representation of the anion of compound **10**. Hydrogen atoms are omitted for clarity.

Figure 14 shows an ellipsoid representation of the structure of the anion of compound **10**. A number of similarities are shared by compound **8** and compound **10**. As it is presented, the structure contains two rhenium ions. The two rhenium cores are not identical. One is a $\{\text{ReOCl}_2\}^+$ unit, which is bonded to one triazolyl nitrogen atom and the oxygen atom of the ligand L^2 , just like in the case of compound **8**. The coordination sphere of the second rhenium atom is the same as that of the corresponding rhenium atom in compound **8**. Also here is an extra oxygen atom in the structure which

does not come from the ligand L². Both coordination spheres of the rhenium ions are distorted.

Table 9. Selected bond lengths (Å) and angles (°) in compound **10**.

Re1-N11	2.149(4)	N11-Re1-Cl12	166.5(2)
Re1-N21	2.154(4)	N21-Re1-Cl12	88.5(2)
Re1-O1	1.686(3)	O1-Re1-Cl11	101.1(2)
Re1-O2	1.927(3)	O2-Re1-Cl11	94.5(1)
Re1-Cl11	2.347(2)	N11-Re1-Cl11	89.6(2)
Re1-Cl12	2.340(2)	N21-Re1-Cl11	168.9(2)
Re2-O3	1.967(3)	Cl12-Re1-Cl11	90.83(5)
Re2-O4	1.682(4)	O4-Re2-O3	164.3(2)
Re2-Cl13	2.401(2)	O4-Re2-N31	88.8(2)
Re2-Cl14	2.349(2)	O3-Re2-N31	75.5(2)
Re2-Cl15	2.404(2)	O4-Re2-Cl14	103.6(2)
Re2-N31	2.123(4)	O3-Re2-Cl14	92.2(1)
P1-O2	1.708(3)	N31-Re2-Cl14	167.4(2)
P1-O3	1.621(3)	O4-Re2-Cl13	93.8(2)
O3-P1-O2	177.3(2)	O3-Re2-Cl13	85.0(1)
O1-Re1-O2	157.8(2)	N31-Re2-Cl13	84.5(2)
O1-Re1-N11	89.5(2)	Cl14-Re2-Cl13	92.19(4)
O2-Re1-N11	74.8(2)	O4-Re2-Cl15	95.0(2)
O1-Re1-N21	89.8(2)	O4-Re2-Cl15	86.0(1)
O2-Re1-N21	74.5(2)	N31-Re2-Cl15	93.3(2)
N11-Re1-N21	88.5(2)	Cl14-Re2-Cl15	88.01(4)
O1-Re1-Cl12	103.7(2)	Cl13-Re2-Cl15	170.91(4)
O2-Re1-Cl12	91.7(2)		

The selected bond lengths and angles of compound **10** given in Table 9 are similar to those in compound **8**. The bond lengths of P1-O2 and P1-O3 are not identical, and both of them are longer than a P=O bond length. Most of the angles at the rhenium atoms are not 90° or 180°. The distortion of the rhenium coordination spheres might be due to the rigid structure of the ligand. There is hitherto no record on metal complexes with dihydroxylphosphorane ligands or similar structures other than compound **8** and compound **10**.

The ^{31}P NMR spectrum of compound **10** shows a single resonance at -62.0 ppm. This value is similar to that of compound **8** and similar resonances have been observed for organic dioxophosphoranes [46, 47]. The IR spectrum confirms the presence of the Re=O double bonds with medium bands at 976 and 990 cm^{-1} .

In contrast to the corresponding reaction with ligand L^1 , another side-product was isolated from that with L^2 : compound **11**. The proton NMR spectroscopy shows that the protons on the pyrazolyl rings share the same chemical environment (a single resonance at 8.76 ppm). The ^{31}P NMR spectrum of compound **11** gives a singlet at 14.1 ppm, which is totally different to that of L^2 . The spectroscopic data above suggests that the ligand in compound **11** might no longer be a dihydroxylphosphoranate. These findings coincide with the X-ray diffraction study.

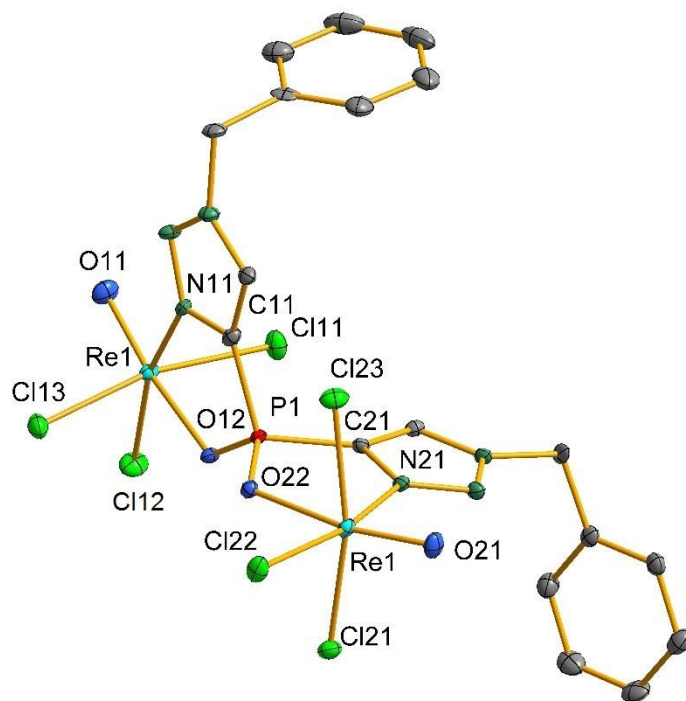


Figure 15. Ellipsoid representation of the anion of compound **11**. Hydrogen atoms are omitted for clarity.

Figure 15 shows an ellipsoid representation of the anion of compound **11**. It is a binuclear Re(V) complex with a hydrolysis product of L^2 . The two rhenium centers are

identical. Just like in compound **9**, an additional oxygen atom O22 is found in the structure. Because of hydrolysis, one triazolyl group of L² is missing in the anion of compound **11**.

Table 10. Selected bond lengths (Å) and angles (°) in compound **11**.

Re1-Cl11	2.3647(9)	O12-Re1-Cl11	83.47(6)
Re1-Cl12	2.3295(9)	Cl12-Re1-Cl11	88.76(3)
Re1-Cl13	2.3657(9)	O11-Re1-Cl13	96.72(9)
Re1-N11	2.132(3)	N11-Re1-Cl13	93.01(7)
Re1-O11	1.660(2)	O12-Re1-Cl13	82.60(6)
Re1-O12	2.140(2)	Cl12-Re1-Cl13	88.77(3)
Re2-Cl21	2.3542(8)	Cl11-Re1-Cl13	165.79(3)
Re2-Cl22	2.3185(8)	O21-Re2-N21	90.6(1)
Re2-Cl23	2.3730(8)	O21-Re2-O22	165.9(2)
Re2-O21	1.663(2)	N21-Re2-O22	75.68(9)
Re2-N21	2.128(3)	O21-Re2-Cl22	104.11(8)
Re2-O22	2.171(2)	N21-Re2-Cl22	165.27(8)
P1-O12	1.509(2)	O22-Re2-Cl22	89.63(6)
P1-O22	1.507(2)	O21-Re2-Cl21	98.22(8)
O22-P1-O12	117.9(1)	N21-Re2-Cl21	89.28(7)
O11-Re1-N11	88.9(1)	O22-Re2-Cl21	84.99(6)
O11-Re1-O12	164.3(2)	Cl22-Re2-Cl21	88.49(3)
N11-Re1-O12	75.43(9)	O21-Re2-Cl23	95.33(8)
O11-Re1-Cl12	104.39(9)	N21-Re2-Cl23	90.21(7)
N11-Re1-Cl12	166.26(7)	O22-Re2-Cl23	81.76(6)
O12-Re1-Cl12	91.32(6)	Cl22-Re2-Cl23	88.58(3)
O11-Re1-Cl11	97.45(9)	Cl21-Re2-Cl23	166.45(3)
N11-Re1-Cl11	86.19(7)		

Table 10 contains selected bond lengths and angles of compound **11**. The coordination spheres of the atoms Re1 and Re2 are distorted. The P1-O11 and P1-O22 bonds are identical and their bond lengths are larger than a P=O double bond, but shorter than normal P-O single bond values. The O-P-O angle of compound **11** is 117.9(1)^o, which is in contrast to the values obtained for the dihydroxylphosphorante compound **10**.

As the two rhenium centers of the compound **11** are identical, only one medium band for the Re=O vibration at 999 cm^{-1} is found in the IR spectrum. The ESI mass spectrum of compound **11** meets the calculated values.

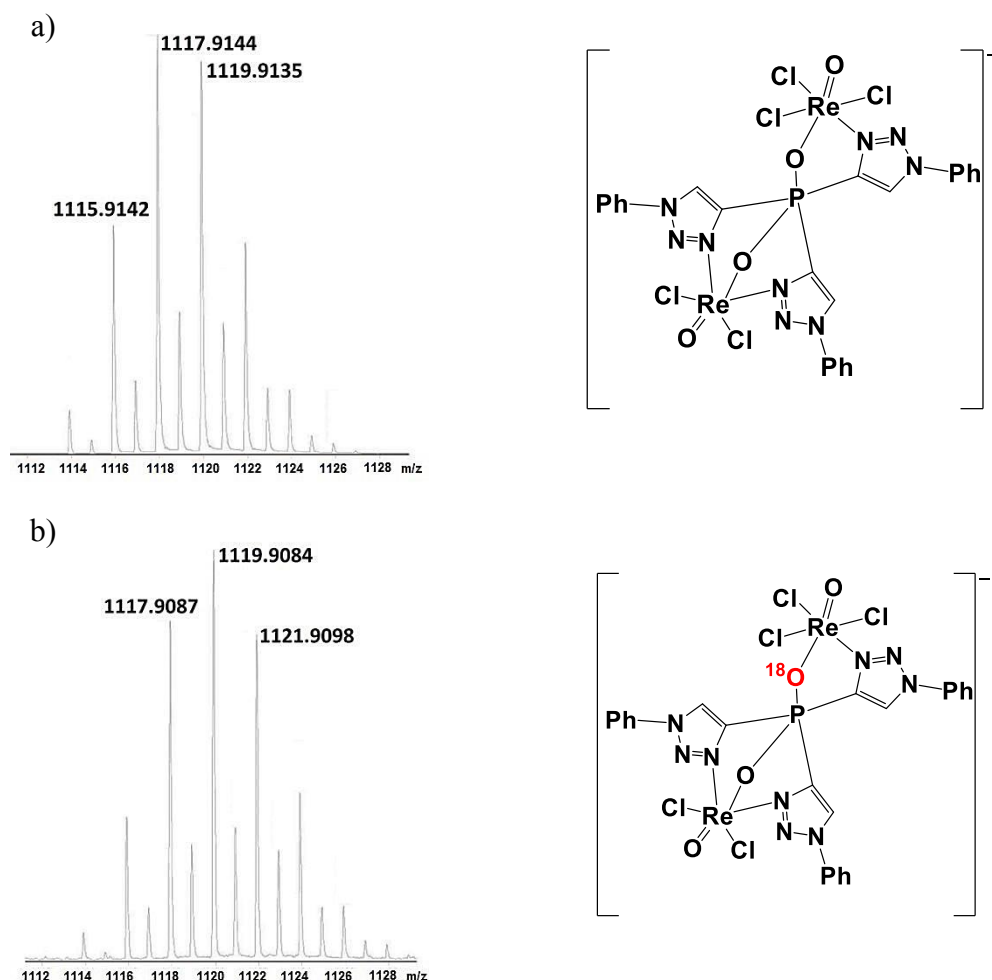


Figure 16. Molecular region of the ESI- mass spectra of compound **8** without (a) and with (b) ^{18}O labelling.

The organic ligands in all the four isolated rhenium(V) compounds above underwent a hydrolytic reaction. Their phosphorus atoms are bonded to two oxygen atoms in the complexes. The first oxygen atom naturally comes from the phosphine oxide ligands. The source of the second oxygen atom, however, is more difficult to explain. An assumption has been made that the extra oxygen atom comes from the water in the air. To validate the assumption that hydrolysis plays a role, a special experiment has been

performed. Carefully dried dichloromethane was saturated with ^{18}O water. The synthesis of compound **8** was done in this ^{18}O -enriched wet dichloromethane in a Schlenk flask. The resulting product was analyzed by ESI mass spectrometry. Figure 16 illustrates the molecular ion region of the two isolated products. It can clearly be seen that the isotopic pattern of the peaks of natural isotopic abundance is shifted by two units when ^{18}O labelled water was used. This corresponds to the replacement of one oxygen atom (^{16}O to ^{18}O) and supports the assumption of hydrolytic reactions during the regarded reactions of L^1 and L^2 with $(\text{NBu}_4)[\text{ReOCl}_4]$. It is interesting to note that the hydrolysis only is observed in the presence of the transition metal complex, while solutions of pure L^1 and L^2 in the same solvent show no decomposition.

As already mentioned above, no similar complexes have been found in the past, only the organic counterparts of compound **8** and **10**, the dioxophosphoranes exist. Taking diethoxytriphenylphosphorane as an example, its ^{31}P NMR spectrum shows a single signal at -55.0 ppm. Such a value is close to those observed for compounds **8** and **10**. This also indicates the similarities of their chemical behavior. Organic dioxylphosphoranes are also unstable substances. They slowly decompose in solvents having a low polarity, but quickly decompose in high-polarity solvents. Since there is no metal ion in the structure, the organic dioxylphosphoranes decompose under formation of phosphine oxides.

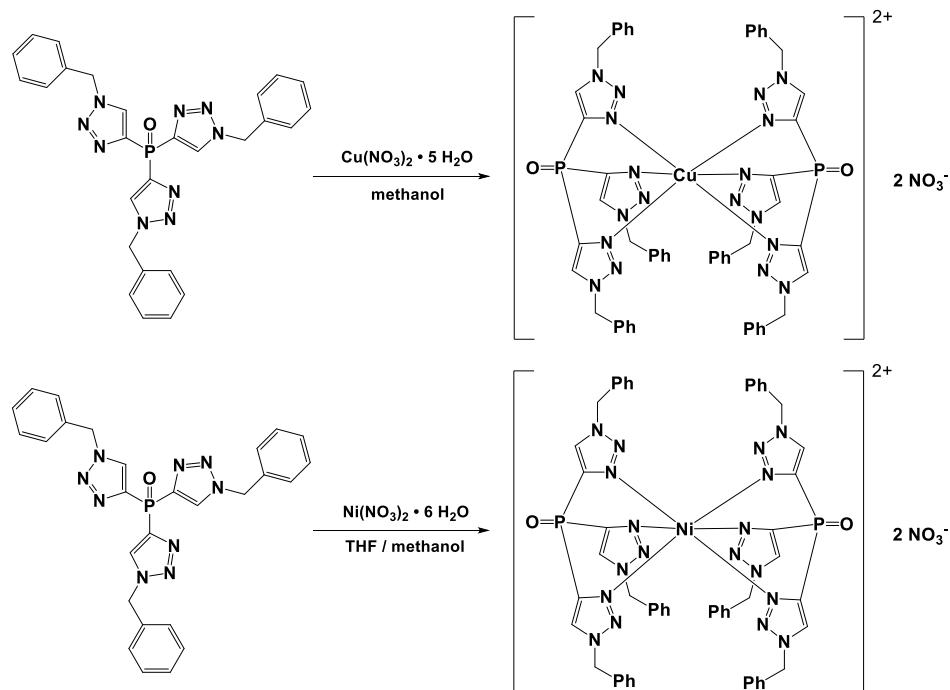
Compounds **9** and **11** are unstable substances. They decompose gradually in solution. In polar solvent this process proceeds faster. This is similar to their potential precursors, compounds **8** and **10**. Time resolved ^{31}P NMR spectra of the reaction of $(\text{NBu}_4)[\text{ReOCl}_4]$ with L^1 and L^2 suggest that the complexes **8** and **10** are formed first and partially converted into **9** and **11**. The formation of other unknown species was detected in low-polarity solvents such as dichloromethane or chloroform. Keeping the compounds in solution for weeks, the result will be the conversion of the rhenium complexes into perrhenate. The observed decomposition is faster in methanol or acetone: in less than 1 minute, the green colors of compound **8** and **10** disappears. In the

resulting brown solution, tetrabutylammonium perrhenate and released ligands were detected.

2.6 Other metal complexes - Reactions of Cu(II) and Ni(II) ions with tris(1,2,3-triazolyl)phosphine oxides

Tris(1,2,3-triazolyl)phosphine oxides form stable complexes with Rh(III), Pt(II)/Pt(IV) and Cu(I) ions [18, 26, 28]. For the case of Pt(IV), L¹ forms κ³ / κ² complexes [27]. The corresponding study reveals that the conversion between κ³ / κ² isomers is possible [29]. It is also reported that L¹ forms several complexes with Cu(I) ions [27].

As an addition of the reactions with rhenium and technetium species, also reactions of L¹ and L² with metal ions including Ga³⁺, In³⁺, Pr³⁺, Cu²⁺ and Ni²⁺ ions have been performed. However, only Cu(II) and Ni(II) ions gave stable complexes from the reactions with L². Both the Cu(II) and Ni(II) ions form stable complexes with tris(azolyl) tripodal ligands. There are sandwich-type structures (two ligand molecules with one metal ion) [51, 52] and mono-chelate structures (one ligand molecule with one metal ion) [51, 53]. The number is limited, when it is compared with that of complexes with terpyridine-type ligands [54].



Scheme 7. Reactions of L² with Cu(NO₃)₂ · 5 H₂O or Ni(NO₃)₂ · 6 H₂O.

The reactions of L^2 with Cu(II) or Ni(II) ions result in sandwich-type structures. Compound **12** refers to $[Cu(\kappa^3N-L^2)_2](NO_3)_2$. Compound **13** refers to $[Ni(\kappa^3N-L^2)_2](NO_3)_2$. A reaction scheme is presented in Scheme 7.

2.6.1 Reactions of Cu(II) ions with L^2

To obtain compound **12**, an excess amount of $Cu(NO_3)_2 \cdot 5 H_2O$ was used in the reaction with L^2 in methanol. The resulting mixture was filtered and all the volatiles were evaporated to give a blue residue. The blue residue was treated with CH_2Cl_2 to obtain a light blue solution, which excluded the remaining $Cu(NO_3)_2 \cdot 5 H_2O$. Few drops of hexane were added to the solution. Light blue single crystals of compound **12** were formed by evaporation of the solvents.

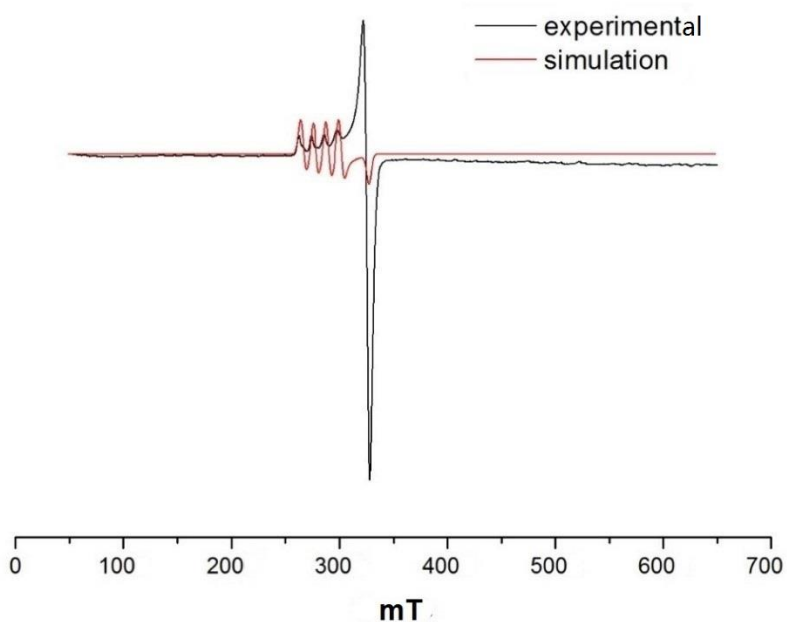


Figure 17. The EPR spectrum of compound **12** in frozen solution (methanol).

The EPR spectrum of compound **12** in frozen solution is presented in Figure 17. It gives the typical line splitting for cooper(II) compound, in which four lines are ex-

pected. One special phenomenon was observed in the mass spectrum of compound **12**. The cation of the compound **12**, $[\text{Cu}(\kappa^3\text{N-L}^2)_2]^{2+}$, carries two positive charges. Based on calculations, a peak at $m/z = 552.6484$ should be observed in the mass spectrum. However, in the measurement no such peak is detected. Instead, a set of peaks are found, with a main peak at $m/z = 1105.3030$. The isotope distribution of the peak matches the calculation result for a $[\text{Cu}(\kappa^3\text{N-L}^2)_2]^+$ ion, which refers to a monocationic copper complex.

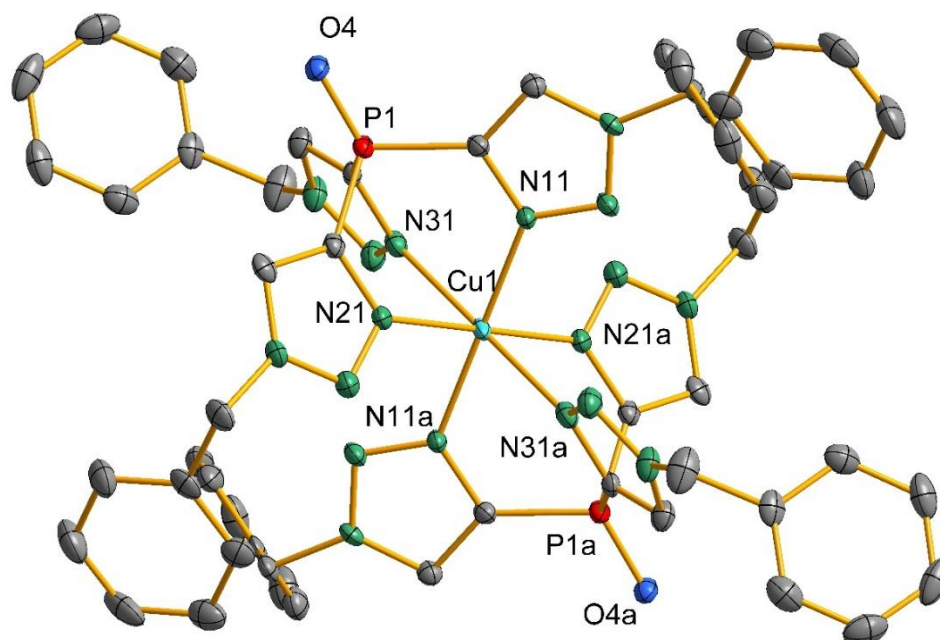


Figure 18. Ellipsoid representation of the complex cation of compound **12**. Hydrogen atoms are omitted for clarity (equivalent atoms are generated using the symmetry operation $-x, -y, -z$).

Figure 18 presents an ellipsoid representation of the cation of compound **12**. As it is shown here, the complex has a bis-chelate structure. Though an excess amount of $\text{Cu}(\text{NO}_3)_2 \cdot 5 \text{ H}_2\text{O}$ was added in the reaction, the ligand L^2 still prefers to wrap the copper(II) ion in a 2:1 complex.

Table 11. Selected bond lengths (\AA) and angles ($^\circ$) in compound **12**.

Cu1-N11	1.997(2)	N11-Cu1-N21	87.16(8)
Cu1-N21	2.043(2)	N11-Cu1-N31	86.21(8)
Cu1-N31	2.382(2)	N21-Cu1-N31	86.29(8)
P1-O4	1.467(2)		

Table 11 gives the bond lengths and angles of compound **12**. It shall be noted that the Cu1-N31 bond (2.382(2) \AA) is much longer than those of the other Cu-N bonds (1.997(2) - 2.043(2) \AA). This is an example for the Jahn-Teller effect. The electron configuration of the Cu(II) ion is d^9 . Consequently, in this octahedral coordination sphere there will be three fully occupied t_{2g} orbitals, one fully occupied e_g orbital and one half-filled e_g orbital. To lower the energy further, the octahedral coordination sphere is elongated. As a result, the fully filled e_g orbital has lower energy than the half-filled one. The overall energy of the whole system is lowered.

All N-Cu-N angles are smaller than 90° (ranging from 86° to 88°) due to the rigid restriction of the ligand structure and the resulting steric hindrance. Although no previous reports on Cu(II) complexes with L^1 and L^2 have been found, a Cu(I) complex with L^1 has been described [26]. The structure contains a four-coordinate Cu(I) ion with a tri-coordinate L^1 and one carbonyl ligand. Due to the low coordination number (or lower steric hindrance), the N-Cu-N angles in the structure are slightly larger than 90° , ranging from 90° to 91° . The second example of a Cu(I) complex with L^1 comes from the same reference. It has a dimeric structure with two units of L^1 and two four-coordinate Cu(I) ions. Still in this compound, the N-Cu-N angles are slightly larger than 90° .

2.6.2 Reactions of Ni(II) ions with L²

To obtain compound **13**, an excess amount of $\text{Ni}(\text{NO}_3)_2 \cdot 6 \text{ H}_2\text{O}$ was dissolved in methanol and L^2 was dispersed in THF. By mixing the two parts, the reaction started. L^2 dissolved in the solvent mixture and light pink single crystals precipitated from the solution spontaneously within 30 minutes.

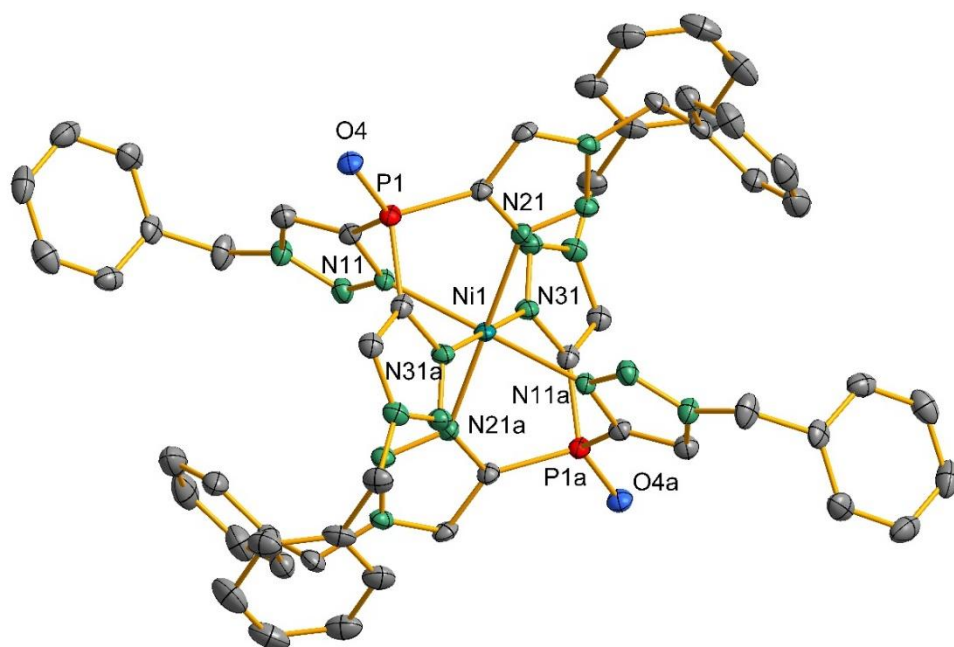


Figure 19. Ellipsoid representation of the complex cation of compound **13**. Hydrogen atoms are omitted for clarity (equivalent atoms are generated using the symmetry operation $-x$, $-y$, $-z$).

The molecular structure of the complex cation of compound **13** is shown in Figure 19. Just like compound **12**, the compound **13** has bis-chelate structure. This means the ratio of ligand to the metal ion is independent of the ratio of the starting materials. In the mass spectra of compound **13**, neither the peak of $[\text{Ni}(\kappa^3\text{N-L}^2)_2]^{2+}$ nor $[\text{Ni}(\kappa^3\text{N-L}^2)_2]^+$ was detected. However, a peak at $m/z = 1162.2983$ was observed along with other peaks nearby. The distribution of the peaks matches the calculation result

for $\{[\text{Ni}(\kappa^3\text{N-L}^2)_2](\text{NO}_3)\}^+$. Such a result indicates that there are interactions between the complex cation $[\text{Ni}(\kappa^3\text{N-L}^2)_2]^{2+}$ and one nitrate anion in the gas phase. The two ions act as one unit in the mass spectrometry measurement.

Table 12 gives the bond lengths and angles of compound **13**. Just like compound **12**, all N-Ni-N bond angles are slightly smaller than 90° , and, thus, very similar to those in compound **12**. The N-M bond lengths of compound **13** are larger than those in compound **12**.

Table 12. Selected bond lengths (\AA) and angles ($^\circ$) in compound **13**.

Ni1-N21	2.062(3)	N21-Ni1-N31	87.1(2)
Ni1-N31	2.105(3)	N21-Ni1-N11	88.1(2)
Ni1-N11	2.115(4)	N31-Ni1-N11	87.1(2)
P1-O4	1.467(3)		

According to the literature [50-52], the formation of mono-chelate structures of bis-chelate structures is influenced by molar ratio and solvents used. The compound **12** and **13** are bis-chelate complexes. The molar ratio of reactants have no influence on the resulting products. When the solvents are changed in the reactions, for example, methanol to other solvents for the synthesis of compound **12**, the reactions fail. The same is observed for the synthesis of compound **13**. Consequently, the interplay between the solvents and resulting structures of Cu(II)/Ni(II) reactions still remain unclear. The obtained two compounds represent the two more examples of metal complexes with tris(1,2,3-triazolyl) phosphine oxide ligands.

3. Experimental Section

3.1 Starting materials

All solvents were used as received (pure for synthesis) unless otherwise mentioned. All chemicals were reagent grade and used without further purification. The syntheses of following materials have been prepared by literature procedures: (NBu₄)[ReOCl₄] [55], [Re(CO)₅Br] [56], tris(ethynyl)phosphine oxide [19], L¹ [19] and benzylazide [57].

3.2 X-ray crystallography

The intensities for the X-ray determinations were recorded on a Bruker Smart CCD 100 M instrument with Mo/K α radiation ($\lambda = 0.71073 \text{ \AA}$) except compound **13**, which is measured by Cu/K α radiation ($\lambda = 1.5406 \text{ \AA}$). The space groups were determined using WinGX [58]. The structure solution and refinement were performed with the SHELXS and SHELXL [59] programs. Absorption corrections were carried out by SADABS [60]. Hydrogen atoms were calculated for the idealized positions and treated with the ‘riding model’ option of SHELXL. Details are given in the Appendix. The representation of molecular structures was done by the program DIAMOND 4 [61].

3.3 Spectroscopical and analytical methods

All IR spectra except those of Tc compounds were obtained on a Nicolet iS10 FT-IR spectrometer. The IR spectra of Tc compounds were obtained on a Shimadzu – FTIR 8300 spectrometer.

The ¹H and ³¹P NMR spectra were recorded at 298 K on a JEOL 400 MHz spectrometer.

The EPR spectra were measured on a Magnetech Miniscope MS400 spectrometer with the rectangular resonator TE102. The sample of compound **12** was measured in methanol.

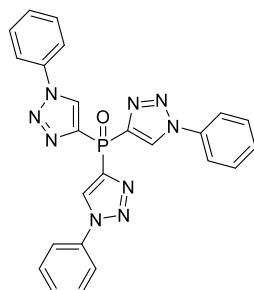
ESI-MS data were measured on an Agilent 6210 ESI-TOF mass spectrometer (Agilent Technologies, Santa Clara, CA, USA). Spray voltage was set to 4 kV. The solvent flow rate was adjusted to 4 μ L/min. The drying gas flow rate was set to 15 psi (1 bar). All other parameters were adjusted for a maximum abundance of the relative ions. All MS results are given in the form: m/z, assignment.

Elemental analyses (CHN) were performed on a Heraeus Vario EL elemental analyzer from Elementar Analysensysteme GmbH. For technetium compounds, elemental analyses were performed on a HIDEX 300 SL scintillation counter.

3.4 Syntheses

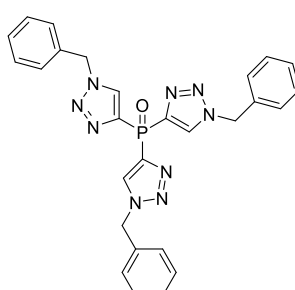
Tris(1-phenyl-1H-1,2,3-triazol-4-yl)phosphine oxide (L¹**)**

The synthesis followed the method by K. Lammertsma et al. [19]. Yield: 95%. Elemental analysis: calcd for C₂₄H₁₈N₉OP: N, 26.3; C, 60.1; H, 3.8%; found: N, 26.3; C, 60.2; H, 4.3%. ¹H NMR (CDCl₃, ppm): 8.86 (s, 3H, C=C-H), 7.76–7.78 (m, 6H, Ph-H), 7.48–7.58 (m, 9H, Ph-H). ³¹P NMR (CDCl₃): -6.4 ppm. IR (cm⁻¹): 1232 (P=O). MS (ESI+): [M + Na]⁺ m/z = 544.1744 (calcd for C₂₄H₁₈N₉OPNa⁺: 544.1739).



Tris(1-benzyl-1H-1,2,3-triazol-4-yl)phosphine oxide (L²**)**

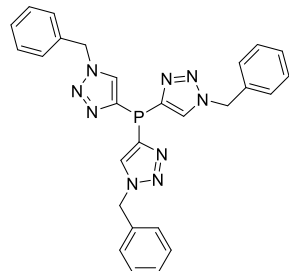
Benzylazide (3.33 g, 25 mmol), tris(ethynyl)phosphine oxide (1 g, 8.33 mmol) and CuSO₄·5 H₂O (100 mg, 0.4 mmol) were dissolved in a mixture of acetonitrile (2 mL) and water (0.5 mL). Sodium ascorbate (150 mg, 0.8 mmol) was added in small portions. The mixture was stirred for 24 h at room temperature, and then extraction was performed with CHCl₃ (3 × 20 mL). The combined organic extracts were



dried over MgSO₄ and all solids were removed by filtration over Celite. The Celite plug was washed with CHCl₃ (3 × 10 mL), and all volatiles were evaporated. The product was purified by recrystallization from hexane. Yield: 4.1 g (95%). Elemental analysis: calcd for C₂₇H₂₄N₉OP · 1/2 CHCl₃: C, 56.8; H, 4.3; N, 21.7%; found: C, 56.8; H, 4.9; N, 21.1%. ¹H NMR (CD₂Cl₂, ppm): 8.14 (s, 3H, C=C-H), 7.26–7.35 (m, 15H, Ph-H), 5.54 (m, 6H, Ph-CH₂-). ³¹P NMR (CDCl₃): -5.8 ppm. IR (cm⁻¹): 1259 (P=O). MS (ESI+): [M + Na]⁺: m/z = 544.1744 (calcd for C₂₇H₂₄N₉OPNa⁺: 544.1739); [M + K]⁺ m/z = 560.1488 (calcd for C₂₇H₂₄N₉OPK⁺: 560.1478).

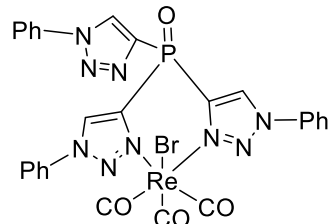
Tris(1-benzyl-1H-1,2,3-triazol-4-yl)phosphine (L^{2'}).

The synthesis followed the method by K. Lammertsma et al. [19]. Yield: 96%. ¹H NMR (CDCl₃, ppm): 7.76 (s, 3H, C=C-H), 7.33–7.44 (m, 9H, Ph-H), 7.20–7.22 (m, 6H, Ph-H), 5.47 (m, 6H, Ph-CH₂-). ³¹P NMR (): -63.7 ppm.



[Re(CO)₃Br(κ^2 N-L¹)] (1).

[Re(CO)₅Br] (40 mg, 0.1 mmol) and L¹ (48 mg, 0.1 mmol) were dispersed in chloroform and heated under reflux for 24 hours, during which the suspension turned clear. Hexane was added to the resulting mixture to give a colorless precipitate. The precipitate was filtered off and re-dissolved in dichloromethane. The solution was treated with CCl₄ and recrystallized several times by evaporating the solvent in a refrigerator to give colorless single crystals of compound **1**. Unsuccessful attempt to use methanol to recrystallize compound **1** introduced methanol into the unit cell. Yield: 21 mg (21%). Elemental analysis calcd for C₂₇H₁₈N₉O₄PReBr·CH₂Cl₂·C₆H₁₄: N: 12.6, C: 40.8, H: 3.4%. Found N: 12.9, C: 39.1, H: 3.0%. ¹H NMR (CD₂Cl₂, ppm): 8.98 (s, 2H, C=C-H), 8.27 (s, 1H, C=C-H), 7.51–7.87 (m, 15H, Ph-H). ³¹P NMR (CDCl₃):



-8.2 ppm. IR (cm^{-1}): 2031 (CO), 1931 (CO), 1898 (CO), 1260 (P=O). MS (ESI+): [M - Br]⁺ m/z = 750.0680 (calcd for $[\text{C}_{27}\text{H}_{18}\text{N}_9\text{O}_4\text{PRe}]^+$ 750.0771).

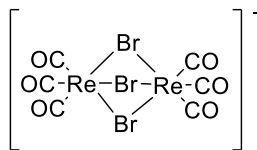
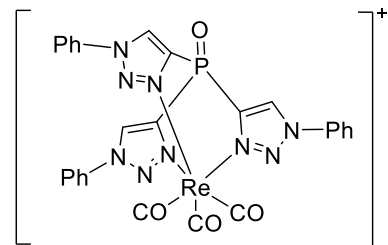
[Re(CO)₃(κ^3 N-L¹)][Re₂(CO)₆Br₃] (2).

[Re(CO)₅Br] (20 mg, 0.05 mmol), L¹ (24 mg, 0.05 mmol) and an excess amount of AgPF₆ were dispersed in dichloromethane and heated under reflux for 90 mins.

During this time, the suspension turned clear. Hexane was added to the resulting mixture to give a colorless precipitate. The precipitate was filtered off

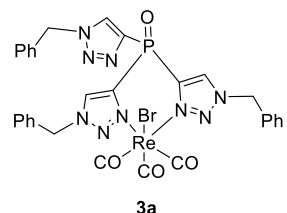
and recrystallized from dichloromethane/hexane. Due to side reactions in the mixture, few single crystals were obtained for X-ray diffraction. Unsuccessful prior attempt to use chloroform to recrystallize compound **2** introduced chloroform into the unit cell.

MS (ESI+): $[\text{C}_{30}\text{H}_{24}\text{N}_9\text{O}_4\text{PRe}]^+$ m/z = 750.0752 (calcd for $[\text{C}_{30}\text{H}_{24}\text{N}_9\text{O}_4\text{PRe}]^+$: 750.0771).

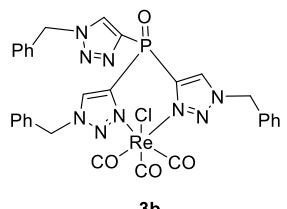


[Re(CO)₃Br(κ^2 N-L²)] (3a) and [Re(CO)₃Cl(κ^2 N-L²)]

(3b). [Re(CO)₅Br] (20 mg, 0.05 mmol) and L² (26 mg, 0.05 mmol) were dispersed in chloroform and heated under reflux for 24 hours. During this time, the suspension turned clear. Hexane was added to the resulting mixture to give a colorless precipitate. The precipitate was filtered off and the mixture was separated by silica gel column chromatography with CH₂Cl₂, acetone and methanol as eluents.



3a

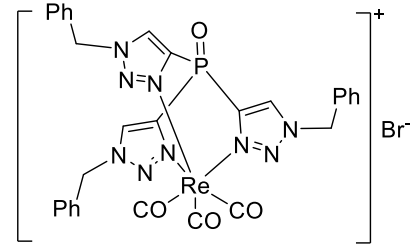


3b

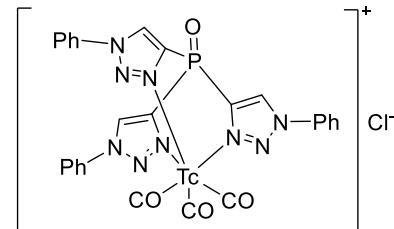
The component flushed by acetone is compound **4** (see below), while that flushed by methanol consists of compound **3a** and **3b**. Colorless crystals of compound **4** were further purified by recrystallization from dichloromethane/hexane. Yield: 18 mg (40%). Elemental analysis: calcd for C₃₀H₂₄Br_{0.3}Cl_{0.7}N₉O₄PRe: N: 15.0, C: 42.9, H:

2.9%. Found: N: 13.8% C: 43.0% H: 2.4%. ^1H NMR (CD_2Cl_2 , ppm): 8.21 (s, 2H, C=C-H), 7.57 - 7.60 (s, 1H, C=C-H), 7.22 - 7.42 (m, 15H, Ph-H), 5.59 - 5.80 (m, 4H, - CH_2 -), 5.46 (s, 2H, - CH_2 -). ^{31}P NMR (CD_2Cl_2): -8.7 ppm. IR (cm^{-1}): 2026 (CO), 1925 (CO), 1893 (CO), 1216 (P=O). MS (ESI+): $[\text{M}(3\text{a}) + \text{Na}]^+$ m/z = 894.0223 (calcd for $\text{C}_{30}\text{H}_{24}\text{BrN}_9\text{O}_4\text{PReNa}^+$: 894.0327); $[\text{M}(3\text{b}) + \text{Na}]^+$ m/z = 850.0743 (calcd for $\text{C}_{30}\text{H}_{24}\text{ClN}_9\text{O}_4\text{PReNa}^+$: 850.0833)

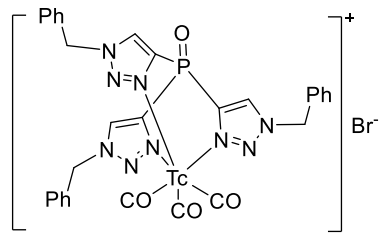
[Re(CO)₃($\kappa^3\text{N-L}^2$)]Br (4). [Re(CO)₅Br] (20 mg, 0.05 mmol) and L² (26 mg, 0.05 mmol) were dispersed in toluene and heated under reflux for 90 mins. During this time, the suspension turned clear. Hexane was added to the resulting mixture to give a colorless precipitate. The precipitate was filtered off and recrystallized from dichloromethane/hexane to give colorless crystals. Yield: 22 mg (50%). Elemental analysis calcd for $\text{C}_{30}\text{H}_{24}\text{BrN}_9\text{O}_4\text{PRe}$: N: 14.5, C: 41.3, H: 2.8%; found: N: 14.1, C: 41.9, H: 3.4%. ^1H NMR (CDCl_3 , ppm): 9.17 (s, 3H, C=C-H), 7.30 - 7.56 (m, 15H, Ph-H), 5.88 (m, 6H, - CH_2 -). ^{31}P NMR (CD_2Cl_2): -11.2 ppm. IR (cm^{-1}): 2042 (CO), 1933 (CO), 1259 (P=O). MS (ESI+): $[\text{C}_{30}\text{H}_{24}\text{N}_9\text{O}_4\text{PRe}]^+$ m/z = 792.1230 (calcd for $[\text{C}_{30}\text{H}_{24}\text{N}_9\text{O}_4\text{PRe}]^+$: 792.1246).



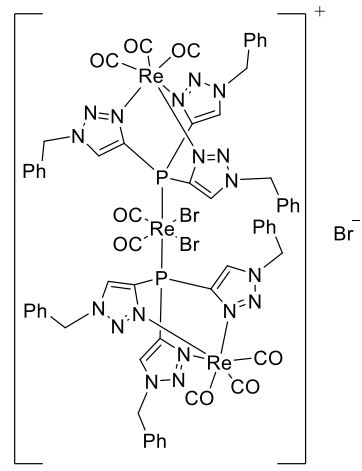
[Tc(CO)₃($\kappa^3\text{N-L}^1$)]Cl (5). The synthesis has been done by a reported procedure [31]. Yield: 69 %. Elemental analysis: calcd for $\text{C}_{27}\text{H}_{18}\text{ClN}_9\text{O}_4\text{PTc}$: Tc 14.2 %; found: Tc 14.4 %. ^1H NMR (CDCl_3 , ppm): 8.89 (s, 3H, C=C-H), 7.77 - 7.25 (m, 15H, Ph-H). $^{13}\text{C}-\{{}^1\text{H}\}$ NMR (CDCl_3 , ppm): 136.4, 130.6, 130.1, 130.0, 129.7, 121.3. ^{31}P NMR (CDCl_3): -5.4 ppm. ^{99}Tc NMR (CDCl_3): -1050 ppm, $\nu_{1/2} = 1680$ Hz.



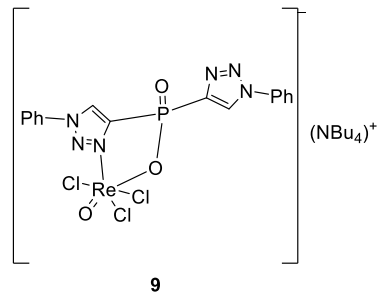
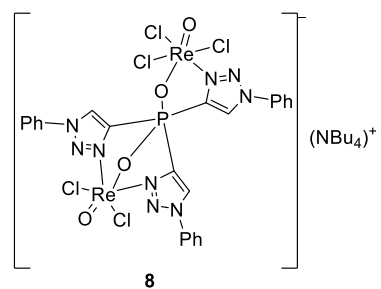
[Tc(CO)₃(κ³N-L²)]Cl (6). The synthesis has been done by a reported procedure [31]. Yield: 64 %. Elemental analysis: calcd for C₂₇H₁₈ClN₉O₄PTc: Tc 13.4 %; found: Tc 13.8 %. ¹H NMR (CDCl₃, ppm): 8.20 (s, 3H, C=C-H), 7.77 - 7.29 (m, 15H, Ph-H), 5.56 (s, 6H, -CH₂-). ¹³C-{¹H}-NMR (CDCl₃, ppm): 133.6, 129.5, 129.3, 129.2, 128.8, 128.7. ³¹P NMR (CDCl₃): -9.5 ppm. ⁹⁹Tc NMR (CDCl₃): -1023 ppm, $\nu_{1/2}$ = 520 Hz.



[{Re(CO)₃(μ-1κ³N,2κ^P-L^{2'})}₂{Re(CO)₂Br₂}]Br (7). [Re(CO)₅Br] (81 mg, 0.2 mmol) and L^{2'} (100 mg, 0.2 mmol) were dispersed in dry toluene under an argon atmosphere and heated under reflux for 90 mins. The suspension first became clear then turned turbid. The mixture was treated with hexane to obtain a colorless precipitate. The precipitate was filtered off and recrystallized from CH₂Cl₂/acetone several times to form colorless crystals. Yield: 42 mg (20%). Elemental analysis calcd for C₆₂H₄₈Br₃N₁₈O₈P₂Re₃: N: 12.4, C: 36.6, H: 2.4%; found: N: 12.5, C: 36.7, H: 2.7%. ¹H NMR (CD₂Cl₂, ppm): 9.57 (s, 3H, C=C-H), 7.34 - 7.49 (m, 15H, Ph-H), 5.73 (s, 6H, -CH₂-). ³¹P NMR (CD₂Cl₂): -63.7 ppm. IR (cm⁻¹): 2035 (CO), 1919 (CO), 1851 (CO). MS (ESI+): [C₆₂H₄₈Br₂N₁₈O₈P₂Re₃]⁺ m/z = 1953.0255 (calcd for [C₆₂H₄₈Br₂N₁₈O₈P₂Re₃]⁺: 1953.0417)



(NBu₄)[Cl₃(O)Re{O₂P(^{1,2,3}Tz^{1-Ph})₃}Re(O)Cl₂] (8) and **(NBu₄)[ReOCl₃{O₂P(^{1,2,3}Tz^{1-Ph})₂}]** (9). L¹ (48 mg, 0.1 mmol) was dissolved in 2 mL of CH₂Cl₂, and (NBu₄)[ReOCl₄] (116 mg, 0.2 mmol) was added. The mixture was stirred for 5 min at room temperature, during when its color turned green. Diethyl ether (20 mL) was added, which resulted in the formation of a green precipitate. This solid was filtered off and dried in vacuum. It was dissolved in 2 mL of dichloromethane, and n-hexane (0.5 mL) was added. Green



crystals of compound **8** deposited during slow evaporation of the solvent to a volume of about 1 mL. They were filtered off and the residual solution was brought to dryness, which resulted in the formation of a sticky, blue-green resin. Repeated dissolution of this material in CH₂Cl₂ and treatment with n-hexane finally gave the light green crystals of compound **9**. Yields: 36 mg (24%) for compound **8** and 22 mg (24%) for compound **9**.

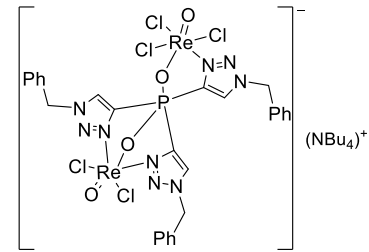
Compound 8. Elemental analysis: calcd for C₄₀H₅₄Cl₅N₁₀O₄PRE₂: C, 36.4; H, 4.1; N, 10.6%; found: C, 36.9; H, 4.4; N, 10.5%. ¹H NMR (CDCl₃, ppm): 8.94 (s, 2H, C=C-H), 8.66 (s, 1H, C=C-H), 7.70–7.75 (m, 6H, Ph-H), 7.43–7.58 (m, 8H, Ph-H), 3.20–3.24 (m, 8H, N-CH₂-), 1.63 (m, 8H, -CH₂-), 1.45–1.48 (m, 8H, -CH₂-), 0.98–1.01 (m, 12H, -CH₃). ³¹P NMR (CDCl₃): -61.7 ppm. IR (cm⁻¹): 987 (Re=O), 973 (Re=O). MS (ESI-): [C₂₄H₁₈Cl₅N₉O₄PRE₂]⁻ m/z = 1075.8801(calcd for [C₂₄H₁₈Cl₅N₉O₄PRE₂]⁻ 1075.8777).

Compound 9. Elemental analysis: calcd for C₃₂H₄₈Cl₃N₇O₃PRE: C, 42.6; H, 5.4; N, 10.6%; found: C, 43.6; H, 5.4; N, 10.8%. ¹H NMR (CDCl₃, ppm): 8.66 (s, 1H, C=C-H), 8.56 (s, 1H, C=C-H), 7.43–7.73 (m, 10H, Ph-H), 3.12–3.16 (m, 8H, N-CH₂-), 1.60–1.65 (m, 8H, -CH₂-), 1.34–1.43 (m, 8H, -CH₂-), 0.94–0.99(t, 9H,

-CH₃). ³¹P NMR (CDCl₃): 1.8 ppm. IR (cm⁻¹): 1257 (P=O), 989 (Re=O). MS (ESI-): [C₁₆H₁₂Cl₃N₆O₃PRe]⁻ m/z = 658.9271(calcd for [C₁₆H₁₂Cl₃N₆O₃PRe]⁻ : 658.9332).

(NBu₄)[Cl₃(O)Re{O₂P(^{1,2,3}Tz^{1-benz})₃}Re(O)Cl₂] (10).

L² (52 mg, 0.1 mmol) was dissolved in 2 mL of CH₂Cl₂. (NBu₄)[ReOCl₄] (116 mg, 0.2 mmol) was added, and the mixture was stirred for 5 mins. The solution turned green. Diethyl ether (20 mL) was

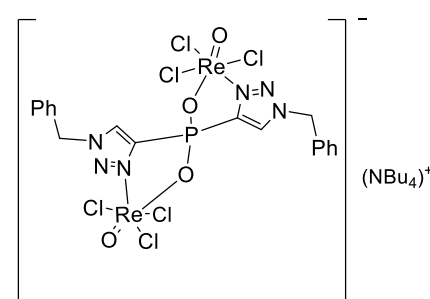


added, which resulted in the dissolution of unreacted L² and the formation of a blue-green precipitate. The solid was filtered off and dried in vacuo. Single crystals were obtained by recrystallization from CH₂Cl₂/n-hexane. Yield: 27 mg (20%).

Elemental analysis: calcd for C₄₃H₆₀Cl₅N₁₀O₄PR₂: C, 37.9; H, 4.5; N, 10.3%; found: C, 38.0; H, 4.5; N, 10.3%. ¹H NMR (CDCl₃, ppm): 8.36 (s, 2H, C=C-H), 8.01 (s, 1H, C=C-H), 7.30 - 7.37 (m, 18H, Ph-H), 5.71 (s, 2H, Ph-CH₂-), 5.63 (s, 4H, Ph-CH₂-), 3.06 - 3.10 (m, 8H, N-CH₂-), 1.54 - 1.61 (m, 8H, -CH₂-), 1.37 - 1.43 (m, 8H, -CH₂-), 0.97 - 1.24 (m, 12H, -CH₃). ³¹P NMR (CDCl₃): -62.0 ppm. IR (cm⁻¹): 990 (Re=O), 976 (Re=O). MS (ESI-): [C₂₇H₂₄Cl₅N₉O₄PR₂]⁻ m/z = 1117.9144 (calcd for [C₂₇H₂₄Cl₅N₉O₄PR₂]⁻ : 1117.9252.)

(NBu₄)[Cl₃(O)Re{O₂P(^{1,2,3}Tz^{1-benz})₂}Re(O)Cl₃]

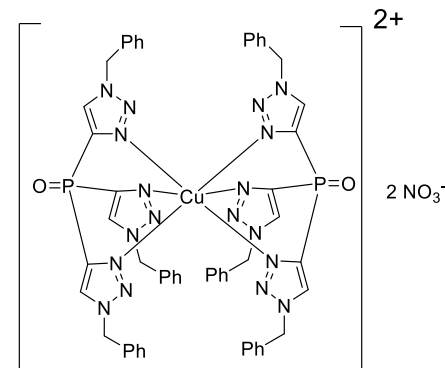
(11). L² (52 mg, 0.1 mmol) and (NBu₄)[ReOCl₄] (116 mg, 0.2 mmol) were placed in a Schlenk tube. CH₂Cl₂ (5 mL) was added, which gave a green solution. This solution was over-layered with 5 mL



of n-hexane. A light green resin and some green crystals were formed upon standing for 5 days. Single crystals for X-ray diffraction were obtained by recrystallization from acetone/CHCl₃ on air. Yield: 65 mg (50%). Elemental analysis: calcd for C₃₄H₅₂Cl₆N₇O₄PR₂: C, 33.0; H, 4.2; N, 7.91%; found: C, 34.0; H, 4.4; N, 8.23%. ¹H

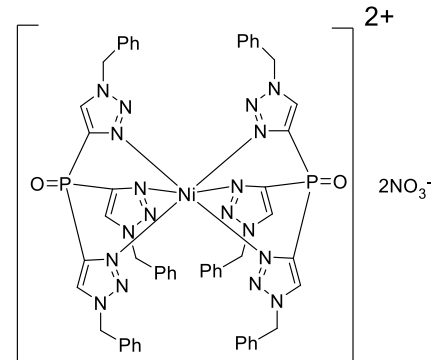
NMR (acetone-d₆, ppm): 8.76 (s, 2H, C=C-H), 7.55 - 7.57 (m, 4H, Ph-H), 7.41 - 7.45 (m, 6H, Ph-H), 6.19 (s, 4H, Ph-CH₂-), 3.39 - 3.41 (m, 8H, N-CH₂-), 1.77 - 1.80 (m, 8H, -CH₂-), 1.37 - 1.41 (m, 8H, -CH₂-), 0.93 - 0.95 (m, 12H, -CH₃). ³¹P NMR (CDCl₃): 14.1 ppm. IR (cm⁻¹): 999 (Re=O). MS (ESI-): [C₁₈H₁₆Cl₆N₆O₄PRE₂]⁻ m/z = 996.8107 (calcd for [C₁₈H₁₆Cl₆N₆O₄PRE₂]⁻: 996.8187).

[Cu(κ³N-L²)₂](NO₃)₂ (**12**). Cu(NO₃)₂ · 5 H₂O (26 mg, 0.11 mmol) was dissolved in methanol and L² (26 mg, 0.05 mmol) was added to the solution. The suspension was stirred for 24 hours. During this time, L² gradually dissolved. All volatiles were evaporated and the residue was ex-



tracted with CH₂Cl₂. The resulting light blue solution was filtered and few drops of hexane were added to the solution. Blue crystals were obtained by evaporation of the solvent. Yield: 21 mg (28%). Elemental analysis: calcd for C₅₄H₄₈N₂₀O₈P₂Cu·3.5 CH₂Cl₂: C, 44.32; N, 19.93; H, 3.61%; found: C, 45.20; N, 18.34; H, 3.63%. IR (cm⁻¹): 1635 (N=O), 1381 (NO₃⁻), 1304 (NO₃⁻), 1232 (P=O), 825 (NO₃⁻). MS (ESI+): [C₅₄H₄₈N₂₀O₈P₂Cu]⁺ m/z = 1105.3030 (calcd for [C₅₄H₄₈N₂₀O₈P₂Cu]⁺: 1105.2979). EPR (77 k, methanol): A_{||} = 117 · 10⁻⁴ cm⁻¹, A_⊥ = 0.1 · 10⁻⁴ cm⁻¹, g_{||} = 2.38, g_⊥ = 2.07.

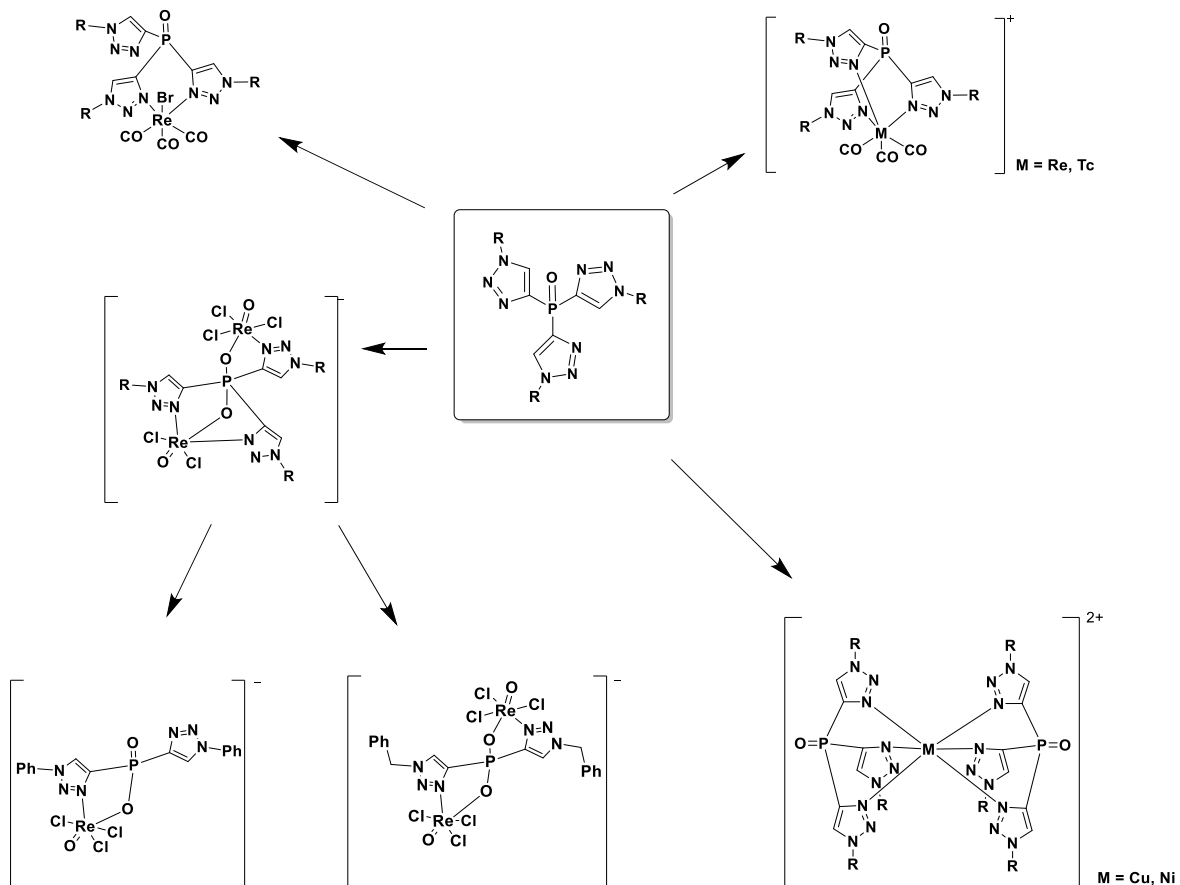
[Ni(κ³N-L²)₂](NO₃)₂ (**13**). In a glass vial, Ni(NO₃)₂ · 6 H₂O (31 mg, 0.11 mmol) was dissolved in 2 mL methanol. L² (26 mg, 0.05 mmol) was dispersed in 2 mL THF in another glass vial. Few drops of dichloromethane was added to improve the solubility. The two systems were mixed and light pink single crystals precipitated from the solution spontaneously within 30 mins. The crystals were filtered off and directly used for analysis. Yield: 76 mg



(62%). Elemental analysis: calcd for $C_{54}H_{48}N_{20}O_8P_2Ni$: C, 48.2; N, 20.1; H, 3.8%; found: C, 48.7; N, 20.5; H, 4.4%. IR (cm^{-1}): 1628 (N=O), 1381 (NO_3^-), 1331 (NO_3^-), 1234 (P=O), 828 (NO_3^-). MS (ESI+): $[\text{C}_{54}\text{H}_{48}\text{N}_{18}\text{O}_2\text{P}_2\text{Ni}\cdot\text{NO}_3]^+$ $m/z = 1162.2983$ (calcd for $[\text{C}_{54}\text{H}_{48}\text{N}_{18}\text{O}_2\text{P}_2\text{Ni}\cdot\text{NO}_3]^+$: 1162.2920).

4. Summary

Two tris(1,2,3-triazolyl) phosphine oxides, L^1 and L^2 , have been synthesized. The ligands were used in reactions with a variety of metal ions, such as Re(I) ions, Tc(I) ions, Re(V) ions, Cu(II) ions and Ni(II) ions. They give relatively stable complexes in reactions with L^1 and L^2 .



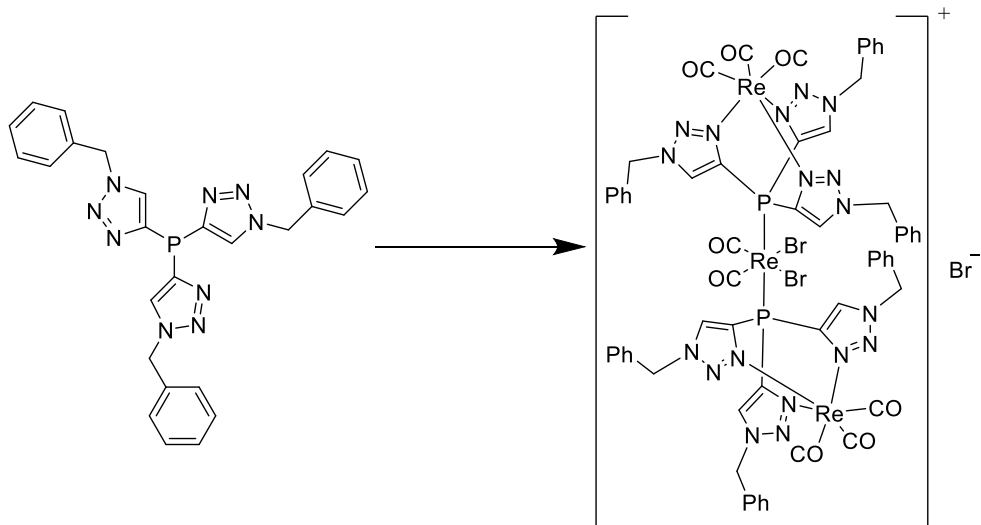
Scheme 8. Summary of the reactions of L^1 and L^2 with different metal ions ($R = \text{Ph}$ or $\text{CH}_2\text{-Ph}$).

Scheme 8 summarizes the reactions of L^1 and L^2 with difference metal ions. In the case of Re(I) and Tc(I) ions, the resulting products are either complexes with bi-coordinated ligands or tri-coordinated ligands. Reaction temperature and the kinetics play important roles in the formation of κ^3 / κ^2 isomers. The increase of reaction

temperatures in rhenium(I) reactions converts κ^2 isomers into κ^3 isomers. No κ^2 isomers have been detected or isolated in the reactions with technetium(I) ions.

The reactions of L^1 and L^2 with Re(V) ions result in the hydrolysis of the ligands, which produce dihydroxylphosphoranato ligands as derivatives of L^1 and L^2 . It is the first time to observe metal complexes with such kind of ligands. The two dihydroxylphosphoranato Re(V) compounds are unstable. During the decomposition, the compounds convert to novel phosphinato Re(V) complexes. An isotope labelling experiment reveals that water molecules are essential for the formation of the dihydroxylphosphoranate moiety. The extra oxygen atoms in these structures come from water molecules. However, L^1 and L^2 themselves do not undergo hydrolysis when dispersed in water. Thus, the formation of the dihydroxylphosphoranato Re(V) complexes is a metal-driven hydrolysis process.

Reactions of L^1 and L^2 with Cu(II) ions and Ni(II) ions result in two bis-chelate structures.

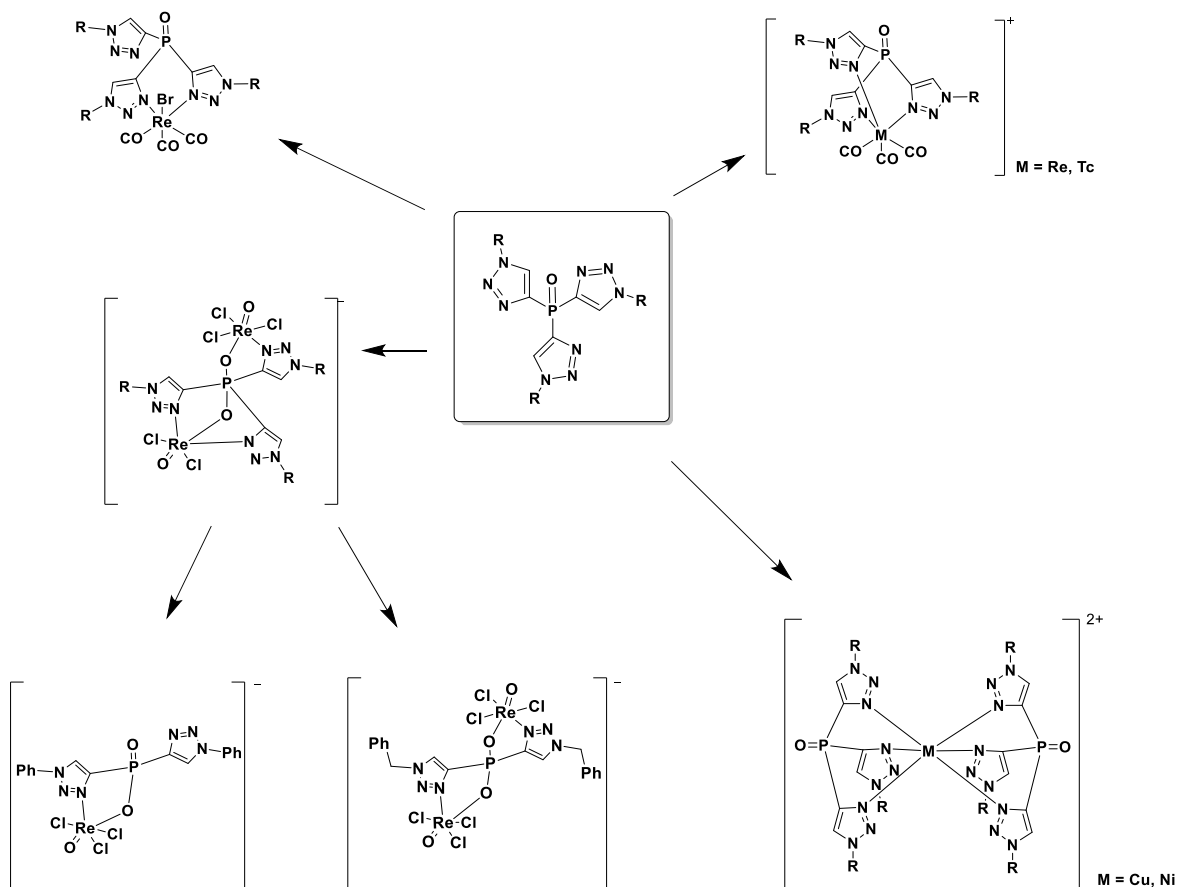


Scheme 9. Formation of $\left[\{\text{Re}(\text{CO})_3(\mu-\text{1}\kappa^3\text{N},2\kappa^{\text{P}}\text{-}\text{L}^2)\}_2\{\text{Re}(\text{CO})_2\text{Br}_2\}\right]\text{Br}$.

L^2 has been reduced to $L^{2'}$. The resulting phosphine ligand was used for a reaction with $[\text{Re}(\text{CO})_5\text{Br}]$. The reaction product is a trimeric cation with two $L^{2'}$ ligands (see Scheme 9).

Zusammenfassung

Die Tris(1,2,3-triazolyl)phosphhanoxide L^1 und L^2 wurden dargestellt. Diese Liganden bildeten mit Re(I)-, Tc(I)-, Re(V)-, Cu(II)- und Ni(II)-Ionen relativ stabile Metallkomplexe.

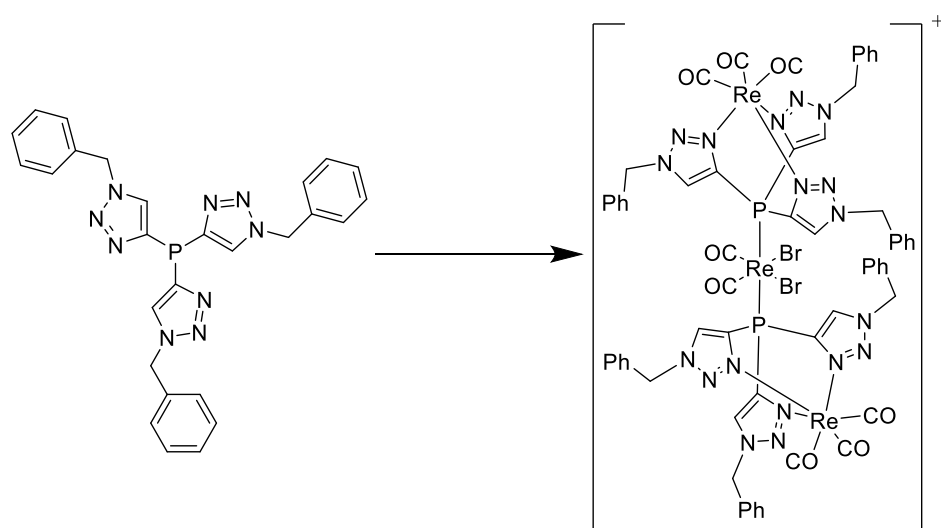


Schema 8^{a)}. Eine Zusammenfassung der Reaktionen von L^1 und L^2 mit unterschiedlichen Metallionen ($R = \text{Ph}$ oder $\text{CH}_2\text{-Ph}$).

Schema 8^{a)} zeigt die Reaktionen der Liganden L^1 und L^2 mit unterschiedlichen Metallionen. Im Fall der Re(I)- und Tc(I)-Ionen wurden sowohl Komplexe mit zweifach koordinierenden als auch mit dreifach koordinierenden Liganden isoliert. Die Reaktions temperatur und die Reaktionskinetik spielen eine wichtige Rolle bei der Bildung der κ^3 / κ^2 Isomere. Höhere Temperaturen führen in den Rhenium(I) Reaktionen zu einer Umwandlung der κ^2 Isomere in die κ^3 Isomere. In den Reaktionen mit Technetium(I)-Ionen wurden hingegen keine κ^2 Isomere beobachtet oder isoliert.

L^1 und L^2 reagierten mit Re(V)-Ionen unter Hydrolyse der Liganden. Als Konsequenz daraus wurden erstmals Metallkomplexe mit den aus L^1 und L^2 abgeleiteten Dihydroxylphosphoranato-Liganden isoliert. Die beiden Dihydroxylphosphoranato Re(V) Verbindungen sind instabil. Sie zersetzen sich weiter zu neuen Re(V) Komplexen mit Phosphinato-Liganden. Ein Isotopenmarkierungsexperiment zeigte, dass Wassermoleküle essenziell für die Bildung der Dihydroxylphosphoranat-Einheit sind. Das zusätzliche Sauerstoffatom in diesen Strukturen kommt aus einem Wassermolekül. Die unkoordinierten Phosphanoxide L^1 und L^2 sind hingegen stabil gegen Hydrolyse, selbst wenn sie für einige Zeit in Wasser gerührt werden. Die Bildung der Dihydroxylphosphoranato Re(V) Komplexe ist daher eine metall-basierte Hydrolyse.

Mit Cu(II)- und Ni(II)-Ionen bilden L^1 und L^2 jeweils sandwichartige Strukturen.



Schema 9^{a)}. Bildung des Komplexes $[\{Re(CO)_3(\mu-1\kappa^3N,2\kappa^P-L^2')\}_2 \{Re(CO)_2Br_2\}]Br$.

Neben den Untersuchungen zur Koordinationschemie von L^1 und L^2 wurde das Phosphanoxid L^2 zum Phosphan L^2' reduziert. Der Phosphan-Ligand L^2' reagierte mit der Re(I) Verbindung $[Re(CO)_5Br]$ zu einem trinuklearen Komplexkation, welches zwei L^2' Liganden enthält (siehe Schema 9^{a)}).

5. References

- [1] Martins, L. M. D. R. S.; Pombeiro, A. J. L. *Coord. Chem. Rev.* **2014**, *265*, 74–88.
- [2] Young, C. G. *Eur. J. Inorg. Chem.* **2016**, 2357–2376.
- [3] Silva, T. F. S.; Luzyanin, K. V.; Kirillova M. V.; Guedes da Silva, M. F.; Martins, L. M. D. R. S. Pombeiro, A. J. L. *Adv. Synth. Catal.* **2010**, *352*, 171-187.
- [4] Martins, L. M. D. R. S.; Pombeiro, A. J. L. *Eur. J. Inorg. Chem.* **2016**, 2236–2252.
- [5] Alegria, E. C. B.; Martins, L. M. D. R. S.; Haukka, M.; Pombeiro, A. J. L. *Dalton Trans.* **2006**, 4954–4961.
- [6] Kimblin, C.; Allen, W. E.; Parkin, G. *J. Chem. Soc. Chem. Commun.* **1995**, 1813–1815.
- [7] Read, R. J.; James, M. N. G.; *J. Am. Chem. Soc.* **1981**, *103*, 6947–6952.
- [8] Park, H.; Baus, J. S.; Lindeman, S. V.; Fiedler, A. T. *Inorg. Chem.* **2011**, *50*, 11978–11989
- [9] Otero, A.; Fernandez-Baeza, J.; Lara-Sanchez, A.; Sanchez-Barba, L. F. *Coord. Chem. Rev.* **2013**, *257*, 1806–1868.
- [10] Trofimenko, S. *J. Am. Chem. Soc.* **1966**, *88*, 1842-1844.
- [11] Trofimenko, S. *Chem. Rev.* **1993**, *93*, 943-980.
- [12] Gorrell, I. B.; Parkin, G. *Inorg. Chem.* **1990**, *29*, 2452-2456.
- [13] Naglav, D.; Tobey, B.; Wolper, C.; Blaser, D.; Jansen, G.; Schulz, S. *Eur. J. Inorg. Chem.* **2016**, 2424–2431.
- [14] Han, R.; Looney, A.; Parkin, G. *J. Am. Chem. Soc.* **1989**, *111*, 7216-7278.
- [15] Degnan, I. A.; Herrmann, W. A.; Herdtweck, E.; *Chem. Ber.* **1990**, *123*, 1347-1349.
- [16] Mlateček, M.; Dostál, L.; Růžičková, Z.; Honzíček, J.; Holubová J.; Erben, M. *Dalton Trans.* **2015**, *44*, 20242–20253.
- [17] Jeong, S. Y.; Lalancette, R. A.; Lin, H.; Lupinska P.; Shipman, P. O.; John, A.; Sheridan, J. B.; Jaekle, F. *Inorg. Chem.* **2016**, *55*, 3605–3615.
- [18] Alegria, E. C. B.; Martins, L. M. D. R. S.; Haukkac, M.; Pombeiro, A. J. L. *Dalton Trans.* **2006**, 4954–4961.

- [19] van Assema, S. G. A.; Tazelaar, C. G. J.; de Jong, G. B.; van Maarseveen, J. H.; Schakel, M.; Lutz, M.; Spek, A. L.; Slootweg, J. C.; Lammertsma, K. *Organometallics*. **2008**, *27*, 3210–3215.
- [20] Tazelaar, C. G. J.; Slootweg, J. C.; Lammertsma, K.; *Coord. Chem. Rev.* **2018**, *356*, 115–126.
- [21] Kraszewski, A.; Stawinski, J. *Tetrahedron Lett.* **1980**, *21*, 2935–2936.
- [22] Froehler, B. C.; Ng, P. G.; Matteucci, M. D. *Nucleic Acids Res.* **1986**, *14*, 5399–5407.
- [23] Pongracz, K.; Kaur, S.; Burlingame, A. L.; Bodell, W. J. *Carcinogenesis*. **1989**, *10*, 1009–1013.
- [24] Hovinen, J.; Azhayeva, E.; Azhayev, A.; Guzaev, A.; Loenberg, H. *J. Chem. Soc. Perkin Trans.* **1994**, 211–217.
- [25] Wada, T.; Moriguchi, T.; Sekine, M. *J. Am. Chem. Soc.* **1994**, *116*, 9901–9911.
- [26] Ora, M.; Maeki; E., Poijaervi, P.; Neuvonen, K.; Oivanen, M.; Loennberg, H. H. *J. Chem. Soc. Perkin Trans.* **2001**, *2*, 881–885.
- [27] Tazelaar, C. G. J.; Lyaskovskyy, V.; van Doorn, I. M.; Schaapkens, X.; Lutz, M.; Ehlers, A. W.; Slootweg, J. C.; Lammertsma, K. *Eur. J. Inorg. Chem.* **2014**, 1836–1842.
- [28] Frauhiger, B. E.; White, P. S.; Templeton, J. L. *Organometallics*, **2012**, *31*, 225–237.
- [29] Frauhiger, B. E.; Templeton, J. L. *Organometallics*, **2012**, *31*, 2770–2784.
- [30] Zink, D. M.; Baumann, T.; Nieger, M.; Braese. *Eur. J. Org. Chem.* **2011**, 1432–1437.
- [31] Hildebrandt, S. *PhD thesis*, Freie Universität Berlin, Berlin, **2018**.
- [32] Morais, M.; Paulo, A.; Gano, L.; Santos, I.; D. G. Correia. *J. Organomet. Chem.* **2013**, *744*, 125-139.
- [33] Coogan, M. P.; Doyle, R. P.; Valliant, J. F.; Babich, J. W.; Zubietta, J. J. *Label Compd. Radiopharm*, **2014**, *57*, 255–261.
- [34] Vucina, J.; Han R. *Med. Pregl.* **2003**, *56*, 362-365.
- [35] Kunz, P. C.; Huber, W.; Rojas, A.; Schatzschneider, U.; Spangler, B. *Eur. J. Inorg. Chem.* **2009**, 5358–5366

- [36] Botha, J. M.; Roodt A. *Metal-Based Drugs*, **2008**, 1-9.
- [37] The Cambridge Structural Database. CSD version 5.41, 2016–2020.
- [38] Kluba, C. A.; Mindt, T. L. *Molecules*, **2013**, *18*, 3206-3226.
- [39] Kromer, L.; Spingler, B.; Alberto, R. *J. Organomet. Chem.* **2007**, *692*, 1372-1376.
- [40] Kromer, L.; Spingler, B.; Alberto, R. *Dalton Trans.* **2008**, 5800–5806.
- [41] Eremenko, I. L.; Berke, H.; Kolobkov, B. I.; Novotortsev, V. M. *Organometallics*, **1994**, *13*, 244–252.
- [42] Uguagliati P.; Zingales, F.; Trovati, A.; Cariati. F. *Inorg. Chem.* **1971**, *10*, 507–510.
- [43] Garcia, R.; Xing, Y. H.; Domingos, A.; Paulo, A.; Santos, I. *Inorg. Chim. Acta*, **2003**, *343*, 27-32.
- [44] Tooyama, Y.; Braband, H.; Spingler, B.; Abram, U.; Alberto, R. *Inorg. Chem.* **2008**, *47*, 257-264.
- [45] Cowley, A. R.; Dilworth, J. R.; Salichou, M. *Dalton Trans.* **2007**, 1621–1629.
- [46] Robinson, P. L.; Evans, S. A., Jr.; Kelly, J. W. *Phosphorus Sulfur Relat. Elem.* **1986**, *26*, 15–24.
- [47] Yang, Z. Y. *J. Org. Chem.* **1995**, *60*, 5696–5698.
- [48] MestReNova, Version 14.1, **2020**.
- [49] von A.F. Shihada, Z. *Anorg. Allg. Chem.* **1981**, *472*, 102-108.
- [50] Beckmann. J.; Dakternieks D.; Duthie, A.; Jurkschat, K.; Mehring Michael.; Mitchell Cassandra.; Schürmann M. *Eur. J. Inorg. Chem.* **2003**, 4356-4360.
- [51] Schiller, A.; Scopelliti, R.; Benmelouka, M.; Severin K. *Inorg. Chem.* **2005**, *44*, 6482-6492.
- [52] Zubkevich, S. V.; Gagieva, S. Ch.; Tuskaev, V. A.; Dorovatovskii, P. V.; Khrustalev, V. N.; Sizov, A. I.; Bulychev, B. M. *Inorg. Chim. Acta*, **2017**, *458*, 58-67.
- [53] Fujisawa, K.; Tobita, K.; Sakuma S.; Savard D.; Leznoffc D. B. *Inorg. Chim. Acta*, **2019**, *486*, 582-588.
- [54] Wei, C.; He, Y.; Shi X.; Song Z. *Coord. Chem. Rev.* **2019**, *385*, 1–19.
- [55] Alberto, R.; Schibli, R.; Egli, A.; Schubiger, P. A.; Herrmann, W. A.; Artus, G.; Abram, U.; Kaden, T. A. *J. Organomet. Chem.* **1995**, *493*, 119-127.

- [56] Angelici, J. *Inorg. Synth.* **1990**, *28*, 162-163.
- [57] Wilkening, I.; del Signore, G.; Hackenberger, C. P. R. *Chem. Commun.* **2011**, *47*, 349–351.
- [58] L. J. Farrugia. *J. Appl. Cryst.* **2012**, *45*, 849-854.
- [59] SHELXS and SHELXL, Sheldrick, G. M. *Acta Cryst.* **2008**, *A64*, 112-122.
- [60] Sheldrick, G. M. SADABS, Universität Göttingen, Germany, **2014**.
- [61] Diamond Crystal and Molecular Structure Visualization; Crystal Impact – version 4.0, Dr. H. Putz and Dr. K. Brandenburg GbR, Bonn Germany.

6. Appendix

6.1 Crystallographic Data

Table S1. Crystal data and structure refinement for **1 · 0.5 CH₃OH**

Empirical formula	C _{27.5} H ₁₉ BrN ₉ O _{4.5} PRe
Formula weight (g/mol)	844.60
Temperature	100 K
Wavelength	0.71073 Å
Crystal system	Triclinic
Space group	P $\bar{1}$
Unit cell dimensions	a = 9.332(2) Å α = 83.129(5) $^{\circ}$ b = 12.189(2) Å β = 84.851(6) $^{\circ}$ c = 15.242(2) Å γ = 82.389(4) $^{\circ}$
Volume	1701.1(5) Å ³
Z	2
Density (calculated)	1.649 g/cm ³
Absorption coefficient	4.839 mm ⁻¹
F(000)	816
Crystal size	0.170 x 0.070 x 0.040 mm ³
Theta range for data collection	2.500 – 24.999 $^{\circ}$
Index ranges	-11 \leq h \leq 11, -14 \leq k \leq 14, -18 \leq l \leq 18
Reflections collected	23159
Independent reflections	5969 [R(int) = 0.0346]
Completeness to theta = 25.242 $^{\circ}$	99.7 %
Absorption correction	Semi-empirical
Refinement method	Full-matrix least-squares on F ²
Data / restraints / parameters	5969/2/379
Goodness-of-fit on F ²	1.111
Final R indices [I>2sigma(I)]	R1 = 0.0344 wR2 = 0.0880
R indices (all data)	R1 = 0.0408 wR2 = 0.0933

Table S2. Atomic coordinates ($x \times 10^4$) and equivalent isotropic displacement parameters ($\text{\AA}^2 \times 10^3$) for **1** · 0.5 CH₃OH. U(eq) is defined as one third of the trace of the orthogonalized U_{ij} tensor.

	x	y	z	U(eq)
C(1)	3625(6)	5680(5)	3556(4)	23(2)
C(2)	3028(6)	5962(5)	4366(4)	23(2)
C(10)	2558(6)	5415(5)	383(4)	25(2)
C(11)	422(6)	6455(5)	4933(4)	24(2)
C(12)	-995(6)	6491(5)	4724(4)	29(2)
C(13)	-2098(7)	6860(6)	5338(4)	34(2)
C(14)	-1782(7)	7177(5)	6123(4)	32(2)
C(15)	-368(7)	7123(6)	6326(4)	40(2)
C(16)	755(7)	6755(6)	5725(4)	38(2)
C(20)	623(6)	4986(5)	1771(4)	27(2)
C(21)	5634(6)	6097(5)	2106(4)	23(2)
C(22)	6714(6)	6664(5)	1696(4)	25(2)
C(30)	3330(6)	3896(6)	1759(4)	23(2)
C(31)	7028(9)	7632(7)	154(5)	52.5(9)
C(32)	8465(9)	7267(8)	-89(5)	52.5(9)
C(33)	9157(9)	7875(7)	-789(5)	52.5(9)
C(34)	8444(9)	8783(7)	-1216(5)	52.5(9)
C(35)	7013(9)	9141(8)	-971(5)	52.5(9)
C(36)	6284(9)	8563(7)	-273(5)	52.5(9)
C(41)	5875(6)	3990(5)	3076(4)	23(2)
C(42)	6590(6)	3480(5)	2388(4)	24(2)
C(51)	7235(6)	1468(5)	2164(4)	30(2)
C(52)	7149(7)	1585(6)	1253(5)	35(2)
C(53)	7756(7)	717(6)	769(5)	42(2)
C(54)	8414(7)	-240(6)	1212(5)	44(2)
C(55)	8474(8)	-352(6)	2122(6)	49(2)
C(56)	7889(7)	512(6)	2605(5)	40(2)
Br(1)	1421.3(8)	7536.6(6)	1473.4(5)	42.0(2)
N(3)	2495(5)	5668(4)	3039(3)	21(1)
N(4)	1254(5)	5929(4)	3486(3)	23(1)

N(5)	1577(5)	6098(4)	4299(3)	23(1)
N(23)	4610(5)	6130(4)	1512(3)	22(1)
N(24)	5008(5)	6689(4)	759(3)	24(1)
N(25)	6295(5)	7015(4)	874(3)	25(1)
N(43)	5540(5)	3192(4)	3742(3)	30(2)
N(44)	6004(6)	2214(4)	3479(4)	32(2)
N(45)	6649(5)	2394(4)	2649(3)	27(2)
O(1)	6421(4)	5812(4)	3825(3)	29.9(9)
O(10)	2582(5)	5389(4)	-373(3)	35(1)
O(20)	-526(4)	4724(4)	1849(3)	39(2)
O(30)	3740(5)	3040(4)	1819(3)	33(1)
P(1)	5502(2)	5429(2)	3216(1)	21.8(3)
Re(1)	2512.9(2)	5467.2(2)	1631.7(2)	21.67(9)
O(3)	5570(50)	11090(20)	-2990(20)	121(9)
C(4)	7500(60)	10550(30)	-4490(40)	121(9)
C(3)	4990(70)	11220(30)	-3830(30)	121(9)
O(4)	8580(40)	10600(20)	-3900(20)	121(9)

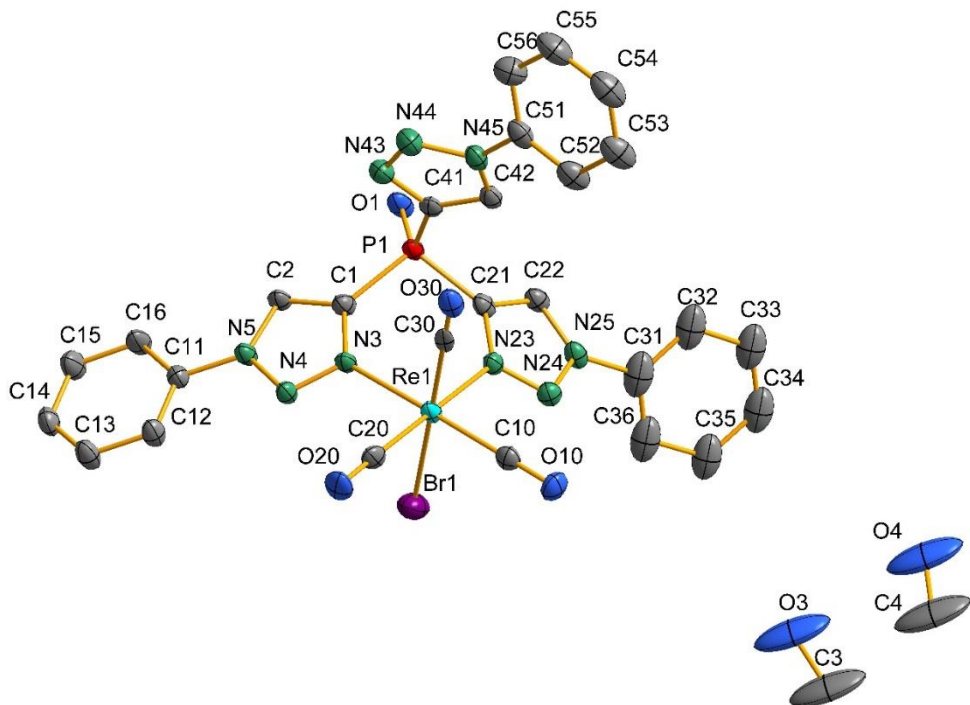


Figure S1. Ellipsoid representation of the asymmetric unit of **1** · 0.5 CH₃OH. Thermal ellipsoids represent 50% probability. Hydrogen atoms have been omitted for the sake of clarity.

Table S3. Crystal data and structure refinement for **2 · CHCl₃**.

Empirical formula	C ₃₄ H ₁₉ Br ₃ Cl ₃ N ₉ O ₁₀ PR ₃
Formula weight (g/mol)	1649.23
Temperature	100(2) K
Wavelength	0.71073 Å
Crystal system	Monoclinic
Space group	P2 ₁ /c
Unit cell dimensions	a = 13.291(1) Å α = 90° b = 20.079(2) Å β = 109.135(3)° c = 17.475(2) Å γ = 90°
Volume	4405.7(6) Å ³
Z	4
Density (calculated)	2.486 g/cm ³
Absorption coefficient	11.226 mm ⁻¹
F(000)	3048
Crystal size	0.160 x 0.014 x 0.010 mm ³
Theta range for data collection	2.374 to 27.149°
Index ranges	-17<=h<=17, -25<=k<=25, -22<=l<=22
Reflections collected	135112
Independent reflections	9754 [R(int) = 0.0839]
Completeness to theta = 25.242°	99.7 %
Absorption correction	Semi-empirical
Refinement method	Full-matrix least-squares on F ²
Data / restraints / parameters	9754/174/351
Goodness-of-fit on F ²	1.034
Final R indices [I>2sigma(I)]	R1 = 0.0941 wR2 = 0.2071
R indices (all data)	R1 = 0.1002 wR2 = 0.2119

Table S4. Atomic coordinates ($x \times 10^4$) and equivalent isotropic displacement parameters ($\text{\AA}^2 \times 10^3$) for **2** · CHCl₃. U(eq) is defined as one third of the trace of the orthogonalized Uij tensor.

	x	y	z	U(eq)
Re(1)	3344.8(5)	4250.2(3)	3047.2(4)	10.2(2)
Re(2)	615.9(5)	1515.6(3)	3068.5(4)	10.2(2)
Re(3)	2853.5(5)	643.7(3)	4154.7(4)	10.2(2)
Br(3)	2531(2)	1934(1)	3905(2)	28.5(4)
Br(1)	1737(2)	640(2)	2604(2)	34.6(5)
Br(2)	1002(2)	715(2)	4255(2)	52.6(7)
P(1)	945(3)	4150(2)	1362(2)	4.1(7)
Cl(3)	6342(5)	3188(2)	6174(3)	32(2)
Cl(1)	5451(5)	1924(3)	6398(5)	45(2)
Cl(2)	7699(5)	2167(3)	7140(4)	44(2)
O(1)	-78(8)	4086(5)	695(6)	7(2)
N(3)	2809(9)	3505(6)	2113(7)	4(2)
O(20)	5541(10)	4299(6)	2831(7)	16(2)
O(10)	3909(10)	5321(6)	4382(7)	15(2)
O(30)	4327(10)	3164(6)	4315(8)	19(3)
N(4)	3363(10)	2950(6)	2120(8)	7(2)
N(43)	1698(11)	4190(7)	3038(8)	9(3)
O(80)	3862(11)	744(8)	5990(9)	29(3)
N(5)	2786(10)	2602(6)	1454(7)	6(2)
O(60)	-1478(10)	847(7)	2127(8)	23(3)
N(44)	1398(11)	4197(7)	3685(8)	9(3)
C(22)	1622(12)	5435(7)	948(9)	6(3)
N(24)	3106(10)	5529(6)	2018(8)	8(2)
N(23)	2670(10)	4949(6)	2068(7)	6(2)
N(25)	2467(10)	5821(6)	1337(7)	5(2)
N(45)	324(11)	4166(7)	3408(8)	9(2)
C(2)	1883(12)	2916(8)	1031(9)	9(3)
C(1)	1899(12)	3494(7)	1455(9)	6(3)
C(14)	3828(13)	684(8)	1128(10)	13(3)
O(90)	2936(15)	-869(8)	4275(12)	45(4)

O(70)	5074(11)	655(9)	3995(9)	31(3)
C(20)	4739(11)	4296(7)	2918(9)	5(3)
C(41)	808(11)	4155(7)	2352(8)	4(3)
C(21)	1739(11)	4883(7)	1413(9)	6(3)
C(12)	3688(14)	1571(9)	2021(10)	15(3)
C(80)	3497(16)	708(10)	5295(12)	24(3)
C(15)	3266(13)	1071(8)	462(10)	13(3)
C(10)	3712(11)	4935(7)	3874(8)	4(2)
C(16)	2943(13)	1714(8)	563(10)	13(3)
O(40)	204(13)	2454(9)	1636(11)	37(4)
C(42)	-69(12)	4132(7)	2595(9)	8(3)
C(11)	3148(12)	1945(7)	1345(9)	7(3)
C(30)	3943(11)	3573(7)	3861(8)	3(2)
C(70)	4235(14)	640(11)	4051(11)	22(3)
C(31)	2722(11)	6487(7)	1134(9)	6(3)
C(51)	-250(12)	4177(8)	3992(9)	9(3)
C(52)	-1349(14)	4246(9)	3709(11)	17(3)
O(50)	-382(14)	2570(8)	3852(11)	37(4)
C(60)	-698(14)	1112(9)	2498(11)	17(3)
C(56)	326(14)	4121(9)	4815(11)	16(3)
C(34)	3238(14)	7744(9)	750(10)	16(3)
C(13)	4028(14)	943(9)	1905(11)	18(3)
C(32)	2057(13)	6795(8)	447(10)	13(3)
C(53)	-1883(15)	4262(9)	4274(11)	19(4)
C(55)	-240(14)	4137(9)	5354(11)	17(3)
C(33)	2328(15)	7434(9)	269(11)	20(4)
C(90)	2928(17)	-289(11)	4241(13)	28(4)
C(40)	401(15)	2096(10)	2192(13)	23(3)
C(36)	3629(15)	6799(9)	1632(11)	18(4)
C(54)	-1347(15)	4205(9)	5093(11)	18(4)
C(35)	3890(15)	7426(9)	1438(11)	20(4)
C(50)	-39(15)	2166(10)	3541(12)	23(3)
C(6)	6560(15)	2330(10)	6291(13)	24(3)

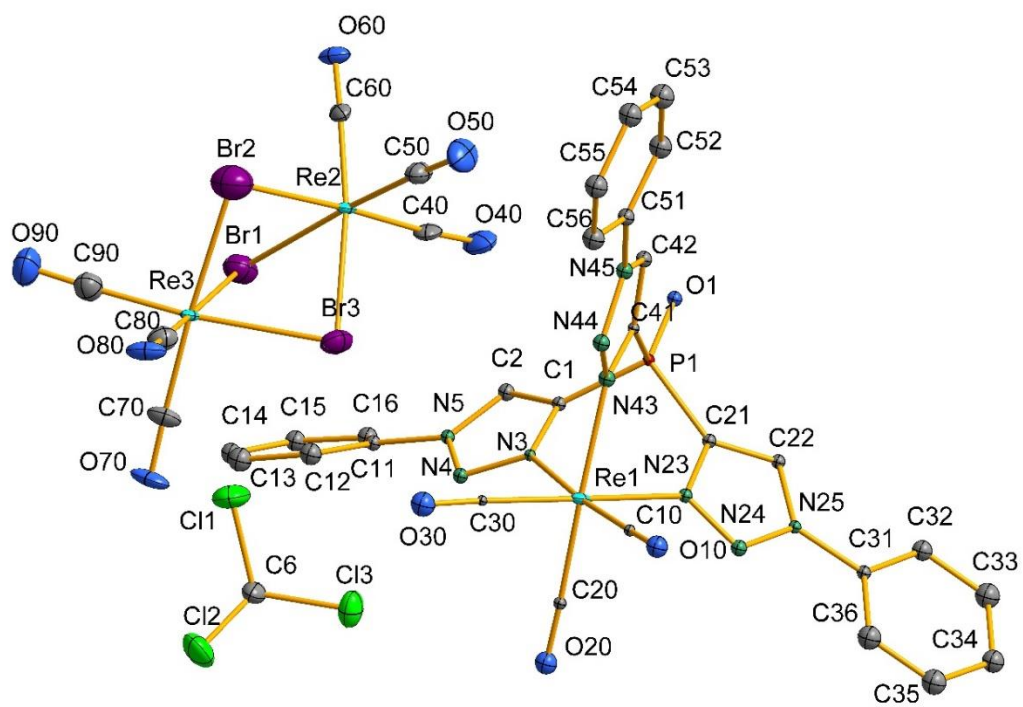


Figure S2. Ellipsoid representation of the asymmetric unit of **2** · CHCl₃. Thermal ellipsoids represent 50% probability. Hydrogen atoms have been omitted for the sake of clarity.

Table S5. Crystal data and structure refinement for 0.3 **3a** · 0.7 **3b**

Empirical formula	C ₃₀ H ₂₄ Br _{0.3} Cl _{0.7} N ₉ O ₄ PRe
Formula weight (g/mol)	840.54
Temperature	100(2) K
Wavelength	0.71073 Å
Crystal system	triclinic
Space group	P $\bar{1}$
Unit cell dimensions	a = 8.6892(7) Å α = 65.490(3) $^{\circ}$ b = 14.544(1) Å β = 76.819(3) $^{\circ}$ c = 14.696(1) Å γ = 85.154(3) $^{\circ}$
Volume	1645.2(2) Å ³
Z	2
Density (calculated)	1.697 g/cm ³
Absorption coefficient	4.212 mm ⁻¹
F(000)	823
Crystal size	0.5 x 0.19 x 0.4 mm ³
Theta range for data collection	2.408 - 25.000 $^{\circ}$
Index ranges	-10 \leq h \leq 10, -17 \leq k \leq 17, -17 \leq l \leq 17
Reflections collected	23771
Independent reflections	5791 [R(int) = 0.0367]
Completeness to theta = 25.242 $^{\circ}$	99.8 %
Absorption correction	Semi-empirical
Refinement method	Full-matrix least-squares on F ²
Data / restraints / parameters	5791 / 0 / 424
Goodness-of-fit on F ²	1.042
Final R indices [I>2sigma(I)]	R ₁ = 0.0237, wR ₂ = 0.0569
R indices (all data)	R ₁ = 0.0260, wR ₂ = 0.0581

Table S6. Atomic coordinates ($x \times 10^4$) and equivalent isotropic displacement parameters ($\text{\AA}^2 \times 10^3$) for 0.3 **3a** · 0.7 **3b**. U(eq) is defined as one third of the trace of the orthogonalized U_{ij} tensor.

	x	y	z	U(eq)
C(4)	4439(4)	8897(3)	2412(3)	19(1)
C(5)	7346(4)	8120(3)	2107(3)	16(1)
C(6)	5437(4)	8415(3)	779(3)	24(1)
C(11)	3673(4)	6443(3)	4632(3)	15(1)
C(12)	4131(4)	5982(3)	5553(3)	17(1)
C(13)	6763(4)	5888(3)	6041(3)	19(1)
C(14)	6512(4)	6655(3)	6508(3)	23(1)
C(15)	5735(6)	6376(4)	7525(4)	36(1)
C(16)	5476(7)	7099(5)	7947(5)	54(2)
C(17)	5977(6)	8085(5)	7348(6)	52(2)
C(18)	6751(7)	8374(4)	6319(6)	55(2)
C(19)	7030(6)	7655(4)	5894(4)	41(1)
C(21)	1264(4)	7886(3)	4284(3)	17(1)
C(22)	447(4)	8604(3)	3612(3)	19(1)
C(23)	-222(6)	10439(3)	3347(3)	31(1)
C(24)	-573(5)	10620(3)	2325(3)	21(1)
C(25)	-2119(5)	10747(3)	2198(3)	30(1)
C(26)	-2440(5)	10949(3)	1239(4)	33(1)
C(27)	-1217(6)	10999(3)	430(3)	30(1)
C(28)	329(5)	10868(3)	564(3)	30(1)
C(29)	656(5)	10680(3)	1506(3)	25(1)
C(31)	1743(4)	6622(2)	3244(3)	14(1)
C(32)	638(4)	6258(3)	2933(3)	16(1)
C(33)	523(5)	6317(3)	1186(3)	21(1)
C(34)	816(5)	5272(3)	1223(3)	24(1)
C(35)	18(6)	4439(3)	2068(4)	37(1)
C(36)	182(8)	3476(4)	2070(5)	52(2)
C(37)	1097(9)	3343(4)	1238(5)	56(2)
C(38)	1905(8)	4135(5)	413(5)	55(2)
C(39)	1767(7)	5129(4)	395(4)	42(1)

N(11)	5004(3)	6832(2)	3885(2)	15(1)
N(12)	6251(3)	6625(2)	4304(2)	17(1)
N(13)	5710(3)	6114(2)	5313(2)	17(1)
N(21)	1742(4)	8315(3)	4851(3)	25(1)
N(22)	1275(4)	9235(3)	4560(3)	25(1)
N(23)	472(4)	9427(2)	3812(2)	21(1)
N(31)	2951(3)	7059(2)	2404(2)	15(1)
N(32)	2621(4)	6985(2)	1603(2)	18(1)
N(33)	1223(3)	6500(2)	1932(2)	16(1)
O(1)	617(3)	5833(2)	5329(2)	20(1)
O(4)	4001(3)	9618(2)	2504(2)	29(1)
O(5)	8634(3)	8341(2)	2020(2)	21(1)
O(6)	5558(4)	8855(3)	-87(2)	37(1)
P(1)	1678(1)	6611(1)	4475(1)	14(1)
Re(1)	5252(1)	7700(1)	2237(1)	15(1)
Br(1)	6236(18)	6043(10)	2045(11)	16(2)
Cl(1)	6325(18)	6125(10)	2112(11)	13(1)

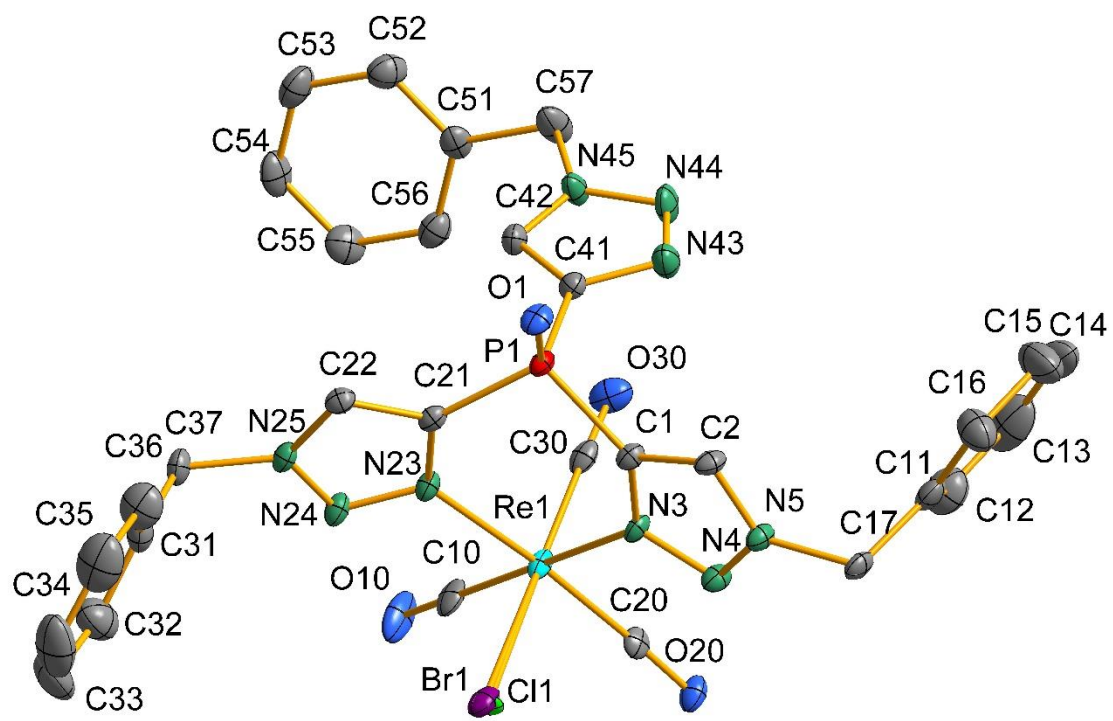


Figure S3. Ellipsoid representation of the asymmetric unit of $0.3 \mathbf{3a} \cdot 0.7 \mathbf{3b}$. Thermal ellipsoids represent 50% probability. Hydrogen atoms have been omitted for the sake of clarity.

Table S7. Crystal data and structure refinement for **4 · CH₂Cl₂**.

Empirical formula	C ₃₁ H ₂₆ BrCl ₂ N ₉ O ₄ PRe
Formula weight (g/mol)	956.59
Temperature	100.09 K
Wavelength	0.71073 Å
Crystal system	Monoclinic
Space group	C2/c
Unit cell dimensions	a = 20.134(4) Å α = 90° b = 11.689(2) Å β = 92.658(6)° c = 29.980(6) Å γ = 90°
Volume	7048(2) Å ³
Z	8
Density (calculated)	1.803 g/cm ³
Absorption coefficient	4.829 mm ⁻¹
F(000)	3728
Crystal size	0.3 x 0.4 x 0.6 mm ³
Theta range for data collection	2.387 - 27.950°
Index ranges	-26<=h<=26, -15<=k<=15, -39<=l<=39
Reflections collected	104071
Independent reflections	8454 [R(int) = 0.0412]
Completeness to theta = 25.242°	99.8 %
Absorption correction	Semi-empirical
Refinement method	Full-matrix least-squares on F ²
Data / restraints / parameters	8454/420/366
Goodness-of-fit on F ²	1.054
Final R indices [I>2sigma(I)]	R ₁ = 0.0349 wR ₂ = 0.0727
R indices (all data)	R ₁ = 0.0398 wR ₂ = 0.0748

Table S8. Atomic coordinates ($x \times 10^4$) and equivalent isotropic displacement parameters ($\text{\AA}^2 \times 10^3$) for **4** · CH_2Cl_2 . U(eq) is defined as one third of the trace of the orthogonalized U_{ij} tensor.

	x	y	z	U(eq)
Re(1)	7522.6(2)	3949.7(2)	3127.3(2)	7.57(5)
Br(1)	9219.9(3)	6480.1(4)	5194.6(2)	26.4(2)
P(1)	7563.5(5)	4191.3(9)	4316.1(3)	9.6(2)
O(30)	7892(2)	5921(3)	2509(2)	25.6(7)
O(1)	7577(2)	4264(3)	4807.6(9)	15.0(6)
O(10)	8355(2)	2414(3)	2534(2)	21.8(7)
O(20)	6267(2)	3442(3)	2539(2)	24.8(7)
N(44)	7082(2)	1626(3)	3535(2)	10.9(6)
N(3)	6979(2)	5084(3)	3557(2)	9.0(6)
N(45)	6995(2)	1124(3)	3929(1)	13.6(7)
N(43)	7285(2)	2671(3)	3628(2)	9.4(6)
N(23)	8355(2)	4319(3)	3600(2)	9.7(6)
N(4)	6564(2)	5864(3)	3391(2)	11.3(6)
C(30)	7748(2)	5188(4)	2736(2)	13.5(8)
N(5)	6347(2)	6436(3)	3744(2)	11.1(6)
C(42)	7136(2)	1828(4)	4276(2)	12.7(7)
N(25)	9325(2)	4735(3)	3855(2)	11.3(6)
N(24)	8966(2)	4504(3)	3478(2)	11.5(6)
C(10)	8039(2)	2958(4)	2764(2)	12.6(8)
C(20)	6739(2)	3624(4)	2755(2)	14.2(8)
C(21)	8332(2)	4432(3)	4055(2)	9.5(7)
C(41)	7319(2)	2838(3)	4081(2)	10.4(7)
C(22)	8957(2)	4701(3)	4221(2)	12.8(8)
C(1)	7021(2)	5156(3)	4014(2)	10.2(7)
C(2)	6612(2)	6040(4)	4135(2)	12.5(7)
C(52)	7313(3)	-923(5)	3909(2)	34.8(5)
C(12)	5158(3)	6846(4)	3583(2)	30.7(5)
C(51)	6758(2)	-70(4)	3936(2)	18.1(9)
C(17)	4986(3)	6339(4)	3172(2)	30.7(5)
C(31)	10034(2)	5016(4)	3830(2)	14.2(8)

C(32)	10150(3)	6285(5)	3802(2)	37.5(5)
C(57)	7487(3)	-1340(5)	3502(2)	34.8(5)
C(11)	5845(2)	7340(3)	3666(2)	13.3(8)
C(37)	9999(3)	6873(5)	3404(2)	37.5(5)
C(16)	4356(2)	5853(4)	3099(2)	30.7(5)
C(56)	8009(3)	-2119(5)	3475(2)	34.8(5)
C(13)	4705(2)	6873(4)	3918(2)	30.7(5)
C(53)	7641(3)	-1313(5)	4289(2)	34.8(5)
C(15)	3910(3)	5878(4)	3426(2)	30.7(5)
C(33)	10400(3)	6867(5)	4168(2)	37.5(5)
C(36)	10106(3)	8036(5)	3378(2)	37.5(5)
C(54)	8154(3)	-2094(5)	4265(2)	34.8(5)
C(55)	8344(3)	-2474(5)	3853(2)	34.8(5)
C(14)	4072(3)	6384(4)	3832(2)	30.7(5)
C(35)	10369(3)	8608(5)	3737(2)	37.5(5)
C(34)	10523(3)	8048(5)	4130(2)	37.5(5)
Cl(3)	9322.0(7)	4752(2)	2303.1(4)	35.8(3)
C(8)	10000	3914(7)	2500	47(2)
Cl(1)	8810(2)	10146(2)	4866.8(8)	28.3(5)
Cl(2)	10264(2)	10079(3)	4926(2)	49.7(8)
C(3)	9531(5)	9444(9)	4691(4)	29(2)

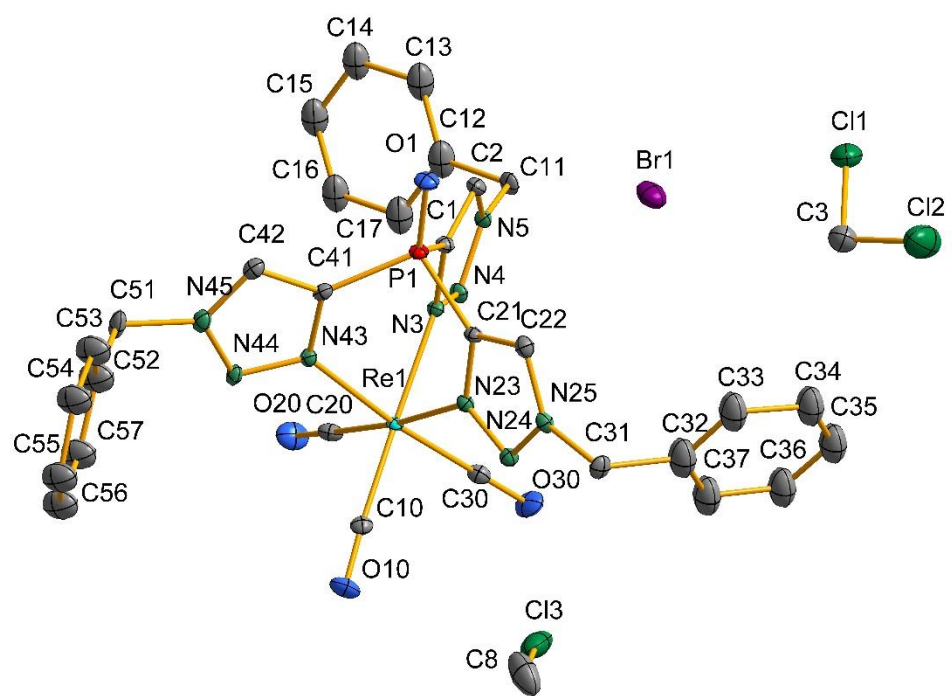


Figure S4. Ellipsoid representation of the asymmetric unit of $4 \cdot \text{CH}_2\text{Cl}_2$. Thermal ellipsoids represent 50% probability. Hydrogen atoms have been omitted for the sake of clarity.

Table S9. Crystal data and structure refinement for **5 · 2.5 H₂O**.

Empirical formula	C ₂₇ H ₂₃ ClN ₉ O _{6.5} PTc
Formula weight (g/mol)	741.96
Temperature	100(2) K
Wavelength	0.71073 Å
Crystal system	tetragonal
Space group	I4 ₁ cd
Unit cell dimensions	a = 32.557(2) Å α = 90° b = 32.557(2) Å β = 90° c = 11.694(1) Å γ = 90°
Volume	12395.2(2) Å ³
Z	16
Density (calculated)	1.590 g/cm ³
Absorption coefficient	0.661 mm ⁻¹
F(000)	6000.0
Crystal size	0.19 x 0.17 x 0.12 mm ³
Theta range for data collection	2.234 - 26.449°
Index ranges	-40<=h<=40, -40<=k<=40, -13<=l<=14
Reflections collected	126266
Independent reflections	6002 [R(int) = 0.0798]
Completeness to theta = 25.242°	99.8 %
Absorption correction	Semi-empirical
Refinement method	Full-matrix least-squares on F ²
Data / restraints / parameters	6002/0/395
Goodness-of-fit on F ²	1.089
Final R indices [I>2sigma(I)]	R ₁ = 0.0379 wR ₂ = 0.0890
R indices (all data)	R ₁ = 0.0444 wR ₂ = 0.0941

Table S10. Atomic coordinates ($\text{\AA} \times 10^4$) and equivalent isotropic displacement parameters ($\text{\AA}^2 \times 10^3$) for **5** · 2.5 H₂O. U(eq) is defined as one third of the trace of the orthogonalized Uij tensor.

	x	y	z	U(eq)
Tc(1)	811.5(2)	385.8(2)	3864(6)	13.7(2)
P(1)	1498.3(5)	1154.2(5)	2953(6)	17.0(3)
O(1)	1786(2)	1472(2)	2577(7)	21(1)
O(10)	409(2)	-249(2)	2300(7)	25(1)
O(20)	-28(2)	525(2)	4982(7)	23(1)
O(30)	990.(2)	-303(2)	5555(7)	25(2)
N(3)	1152(2)	831(2)	4882(7)	16(2)
N(4)	1140(2)	861 (2)	6006(7)	16(2)
N(5)	1413(2)	1155(2)	6272(8)	17(2)
N(23)	1394(2)	326 (2)	2946(8)	17(2)
N(24)	1536 (2)	-23(2)	2547(7)	17(2)
N(25)	1854(2)	79(2)	1868(7)	19(2)
N(43)	704(2)	907(2)	2715(7)	16(2)
N(44)	354(2)	987(2)	2193(7)	16(2)
N(45)	419(2)	1335(2)	1604(7)	17(2)
C(10)	552(2)	-9(2)	2868(8)	18(2)
C(20)	288(2)	475(2)	4593(8)	21(2)
C(30)	924(2)	-46(2)	4915(8)	19(2)
C(1)	1427(2)	1107(2)	4444(8)	17(2)
C(2)	1595(2)	1314(2)	5332(8)	18(2)
C(11)	1461(2)	1279(2)	7443(8)	20(2)
C(16)	1334(3)	1033(2)	8304(9)	29(2)
C(15)	1387(3)	1158(2)	9425(9)	32(2)
C(14)	1571(2)	1526(2)	9660(9)	27(2)
C(13)	1695(2)	1772(2)	8775(9)	28(2)
C(12)	1646(2)	1653(2)	7644(9)	23(2)
C(21)	1622(2)	646(2)	2530(8)	18(2)
C(22)	1917(2)	489(2)	1824(8)	18(2)
C(31)	2082(2)	-235(2)	1299(9)	22(2)
C(32)	2177(2)	-181(2)	155(8)	27(2)

C(33)	2404(2)	-477(3)	-394(9)	33(2)
C(34)	2532(2)	-822(3)	199(9)	36(2)
C(35)	2441(2)	-865(2)	1350(2)	32(2)
C(36)	2215(2)	-568(2)	1912(9)	26(2)
C(41)	988(2)	1200(2)	2439(8)	16(2)
C(42)	806(2)	1476(2)	1745(8)	17(1)
C(51)	105(2)	1505(2)	893(8)	20(1)
C(56)	219(2)	1675(2)	-146(9)	26(2)
C(55)	-76(3)	1854(2)	-820(8)	30(2)
C(54)	-485(2)	1860(2)	-455(9)	29(2)
C(53)	-591(2)	1689(2)	569(9)	26(2)
C(52)	-295(2)	1505.3(19)	1264(9)	22(2)
Cl(1)	2522.7(5)	849.1(6)	9675(6)	31.7(4)
O(2)	1759.9	2339	2465.59	64(2)
O(4)	2283.91	1940.6	4904.39	64(2)
O(3)	1525.8	2326.09	5355.8	64(2)
O(5)	2230.3	2451.3	10375.19	64(2)

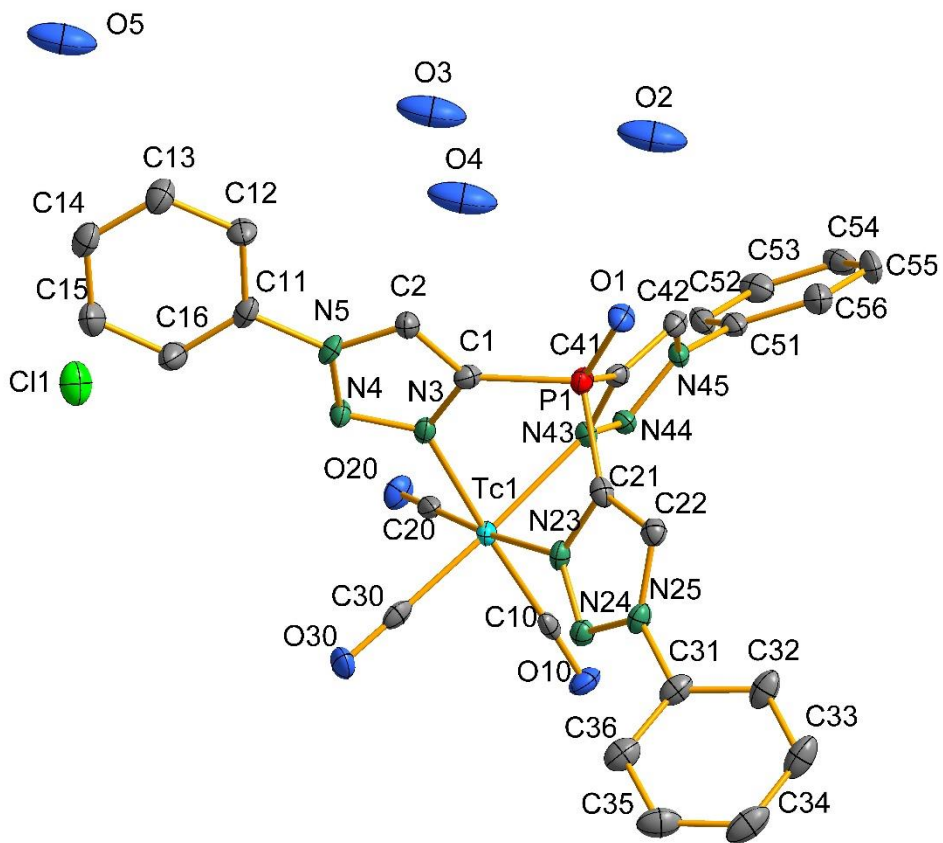


Figure S5. Ellipsoid representation of the asymmetric unit of **5** · 2.5 H₂O. Thermal ellipsoids represent 50% probability. Hydrogen atoms have been omitted for the sake of clarity.

Table S11. Crystal data and structure refinement for **6 · H₂O**.

Empirical formula	C ₃₀ H ₂₆ ClN ₉ O ₅ PTc
Formula weight	757.02
Temperature	100.05 K
Wavelength	0.71073 Å
Crystal system	monoclinic
Space group	C2/c
Unit cell dimensions	a = 11.644(1) Å α = 90° b = 20.063(2) Å β = 96.41(3)° c = 28.668(2) Å γ = 90°
Volume	6655(1) Å ³
Z	8
Density (calculated)	1.511 g/cm ³
Absorption coefficient	0.614 mm ⁻¹
F(000)	3072
Crystal size	0.16 x 0.13 x 0.12 mm ³
Theta range for data collection	2.369 - 27.154°
Index ranges	-13<=h<=14, -24<=k<=25, -36<=l<=36
Reflections collected	46432
Independent reflections	7342 [R(int) = 0.0459]
Completeness to theta = 25.242°	99.9 %
Absorption correction	Semi-empirical
Refinement method	Full-matrix least-squares on F ²
Data / restraints / parameters	7342/2/440
Goodness-of-fit on F ²	1.132
Final R indices [I>2sigma(I)]	R1 = 0.0535, wR2 = 0.1216
R indices (all data)	R1 = 0.0676, wR2 = 0.1293

Table S12. Atomic coordinates ($x \times 10^4$) and equivalent isotropic displacement parameters ($\text{\AA}^2 \times 10^3$) for **6** · H₂O. U(eq) is defined as one third of the trace of the orthogonalized Uij tensor.

	x	y	z	U(eq)
C10A	1628(9)	579(9)	5113(5)	26(2)
O10A	881(8)	763(5)	4862(3)	43(2)
C10B	1357(9)	468(9)	5212(5)	26(2)
O10B	480(8)	618(5)	5004(3)	43(2)
C30	3702(5)	785(2)	5118(2)	47(2)
C20	3032(4)	-506(2)	5193(2)	36(2)
O30	4144(5)	1082(2)	4852(2)	84(2)
O20	3091(4)	-974(2)	4972(2)	59(2)
C37	14(4)	2632(2)	5641(2)	38(2)
C1	4435(3)	197(2)	6534(2)	17.6(7)
C2	5523(3)	26(2)	6728(2)	23.6(8)
C11	7286(3)	-367(2)	6359(2)	39(2)
C12	8130(3)	202(2)	6409(2)	21.9(7)
C13	8390(5)	503(3)	6834(2)	46(2)
C14	9119(6)	1057(4)	6870(3)	75(2)
C15	9590(5)	1283(3)	6480(3)	68(2)
C16	9381(5)	961(3)	6070(3)	65(2)
C17	8643(4)	423(3)	6028(2)	43(2)
C21	2821(3)	1211(2)	6462(2)	17.2(7)
C22	2605(3)	1855(2)	6583(2)	21.2(7)
C41	2119(3)	-102(2)	6550(2)	21.8(7)
C42	1347(4)	-507(2)	6742(2)	34(1)
C51	-173(4)	-1317(2)	6360(3)	56(2)
C52	230(4)	-2018(2)	6284(2)	41(2)
C57	98(4)	-2277(2)	5837(2)	47(2)
C56	483(5)	-2913(3)	5752(2)	51(2)
C55	980(5)	-3295(2)	6110(2)	49(1)
C54	1112(5)	-3049(3)	6559(2)	56(1)
C53	740(5)	-2408(3)	6651(2)	51(2)
N3	4396(2)	120(2)	6056(1)	16.6(6)

N4	5410(3)	-85(2)	5949(2)	22.0(6)
N5	6081(3)	-141(2)	6359(2)	23.9(7)
N23	2683(3)	1178(2)	5980(1)	18.6(6)
N24	2391(3)	1768(2)	5804(2)	23.0(7)
N25	2347(3)	2176(2)	6172(2)	20.3(6)
N43	1966(3)	-203(2)	6073(2)	21.8(6)
N44	1146(3)	-650(2)	5966(2)	32.1(8)
N45	778(3)	-827(2)	6371(2)	36.6(9)
O1	3318(3)	555.2(15)	7305.5(9)	31.5(7)
P1	3196.4(8)	473.6(5)	6793.5(3)	17.8(2)
Tc1	2875.7(3)	300.7(2)	5552.0(2)	23.0(1)
C32	654(3)	2912(2)	6036(2)	28.3(9)
C33	105(4)	3225(2)	6373(2)	45(2)
C36	-1177(4)	2661(3)	5594(2)	57(2)
C35	-1724(5)	2973(3)	5933(3)	64(2)
C34	-1112(5)	3259(3)	6319(3)	68(2)
C31	1951(3)	2865(2)	6090(2)	24.5(8)
Cl1	7959(3)	8408(2)	7255.5(8)	56.4(7)
Cl1A	7165(7)	8239(4)	7358(2)	56.4(7)
Cl1B	7574(9)	8686(4)	7254(3)	56.4(7)
O3	6155(12)	7356(4)	7469(4)	104(3)
O4	9520(20)	8920(8)	7394(8)	104(3)
O2	5000	-956(6)	7500	104(3)

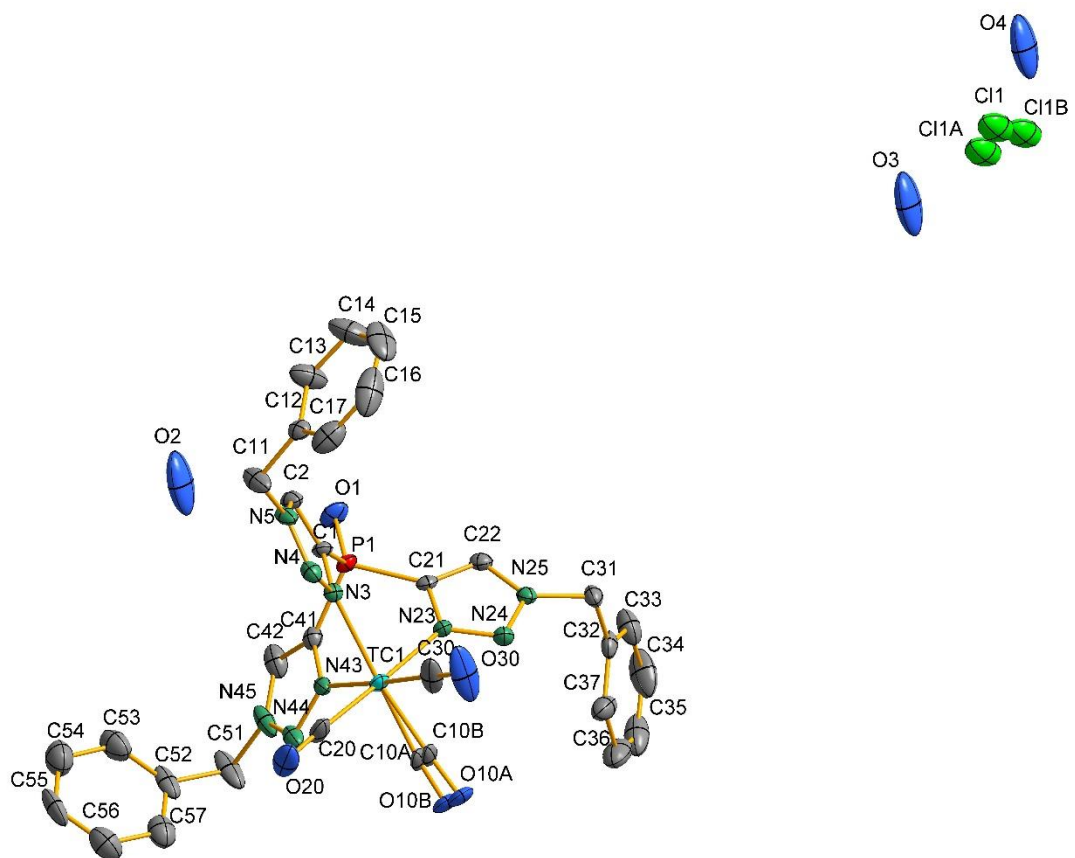


Figure S6. Ellipsoid representation of the asymmetric unit of **6** · H₂O. Thermal ellipsoids represent 50% probability. Hydrogen atoms have been omitted for the sake of clarity.

Table S13. Crystal data and structure refinement for $7 \cdot 2\text{C}_3\text{H}_6\text{O} \cdot 1.5\text{CH}_2\text{Cl}_2 \cdot \text{H}_2\text{O}$.

Empirical formula	$\text{C}_{69.5}\text{H}_{63}\text{Br}_3\text{Cl}_3\text{N}_{18}\text{O}_{11}\text{P}_2\text{Re}_3$
Formula weight (g/mol)	2293.00
Temperature	100(2) K
Wavelength	0.71073 Å
Crystal system	Triclinic
Space group	P1
Unit cell dimensions	$a = 11.515(6)$ Å $\alpha = 83.34(2)^\circ$ $b = 11.556(6)$ Å $\beta = 78.96(1)^\circ$ $c = 17.871(9)$ Å $\gamma = 60.28(1)^\circ$
Volume	2026.4(18) Å ³
Z	1
Density (calculated)	1.879 g/cm ³
Absorption coefficient	6.154 mm ⁻¹
F(000)	1105
Crystal size	0.15 x 0.42 x 0.50 mm ³
Theta range for data collection	2.189 to 27.970°
Index ranges	-15≤h≤15, -15≤k≤14, -23≤l≤23
Reflections collected	32375
Independent reflections	16752 [R(int) = 0.0358]
Completeness to theta = 25.242°	99.6 %
Absorption correction	Semi-empirical
Refinement method	Full-matrix least-squares on F ²
Flack x parameter	0.059
Data / restraints / parameters	16752 / 6 / 582
Goodness-of-fit on F ²	0.788
Final R indices [I>2sigma(I)]	R1 = 0.0421 wR2 = 0.1069
R indices (all data)	R1 = 0.0435 wR2 = 0.1082
Largest diff. peak and hole	2.460 and -2.185 e·Å ⁻³

Table S14. Atomic coordinates ($x \cdot 10^4$) and equivalent isotropic displacement parameters ($\text{\AA}^2 \times 10^3$) for $7 \cdot 2 \text{C}_3\text{H}_6\text{O} \cdot 1.5 \text{CH}_2\text{Cl}_2 \cdot \text{H}_2\text{O}$. U(eq) is defined as one third of the trace of the orthogonalized U_{ij} tensor.

	x	y	z	U(eq)
C(1)	6368(13)	3281(14)	2073(6)	20(1)
C(2)	4449(13)	5855(14)	1930(7)	20(1)
C(3)	7082(13)	5220(14)	1694(6)	20(1)
C(4)	7457(13)	4745(14)	5807(6)	20(1)
C(5)	5763(13)	3754(14)	5949(6)	20(1)
C(6)	4921(13)	7018(14)	9881(6)	20(1)
C(7)	5369(13)	4505(14)	9950(6)	20(1)
C(8)	2768(13)	6633(14)	9972(6)	20(1)
C(11)	7276(12)	4159(11)	4018(6)	14(2)
C(12)	8501(12)	3275(12)	4235(7)	17(2)
C(13)	10746(15)	1591(14)	3483(9)	30(1)
C(14)	10949(16)	259(15)	3361(9)	30(1)
C(15)	11234(15)	-717(15)	3955(9)	30(1)
C(16)	11419(15)	-1973(15)	3819(9)	30(1)
C(17)	11288(16)	-2255(15)	3125(9)	30(1)
C(18)	11055(16)	-1305(15)	2521(9)	30(1)
C(19)	10903(16)	-64(15)	2652(8)	30(1)
C(21)	5305(12)	6775(11)	3883(7)	16(2)
C(22)	4928(13)	8070(12)	4032(7)	20(2)
C(23)	4470(20)	10103(17)	3188(11)	42(2)
C(24)	5310(20)	10464(17)	3552(11)	42(2)
C(25)	6490(20)	10376(17)	3150(11)	42(2)
C(26)	7300(20)	10677(17)	3523(11)	42(2)
C(27)	6870(20)	11059(17)	4283(11)	42(2)
C(28)	5700(20)	11147(17)	4654(11)	42(2)
C(29)	4950(20)	10822(18)	4309(11)	42(2)
C(31)	4569(12)	4840(12)	4266(6)	16(1)
C(32)	3598(12)	4556(12)	4690(7)	16(1)
C(33)	2001(15)	3870(16)	4310(9)	31(1)
C(34)	769(16)	4872(16)	3968(9)	31(1)

C(35)	-260(15)	5923(16)	4385(9)	31(1)
C(36)	-1402(15)	6855(16)	4060(9)	31(1)
C(37)	-1522(15)	6694(16)	3342(9)	31(1)
C(38)	-479(15)	5598(16)	2895(9)	31(1)
C(39)	674(15)	4693(16)	3241(9)	31(1)
C(41)	6529(11)	5389(11)	7714(6)	11(1)
C(42)	7877(11)	4980(11)	7460(6)	11(1)
C(43)	9835(14)	4306(14)	8190(9)	29(1)
C(44)	10029(14)	5426(14)	8377(9)	29(1)
C(45)	9638(14)	5853(14)	9119(9)	29(1)
C(46)	9903(14)	6875(14)	9303(9)	29(1)
C(47)	10378(14)	7489(14)	8723(9)	29(1)
C(48)	10724(14)	7098(14)	8000(9)	29(1)
C(49)	10602(14)	6032(14)	7816(9)	29(1)
C(51)	4430(11)	4843(11)	7774(6)	10(1)
C(52)	4021(11)	3994(11)	7555(6)	10(1)
C(53)	3160(13)	2504(13)	8315(8)	22(1)
C(54)	4370(13)	1108(13)	8279(8)	22(1)
C(55)	4995(13)	554(13)	8915(8)	22(1)
C(56)	6125(13)	-718(13)	8873(8)	22(1)
C(57)	6625(13)	-1416(13)	8205(8)	22(1)
C(58)	5993(13)	-859(13)	7574(8)	22(1)
C(59)	4840(13)	425(14)	7608(8)	22(1)
C(61)	3930(11)	7414(11)	7653(6)	11(1)
C(62)	3127(11)	8666(11)	7349(6)	11(1)
C(63)	1476(18)	10880(20)	7965(15)	56(2)
C(67)	-2587(9)	11659(14)	8007(8)	56(2)
C(68)	-2064(11)	11386(14)	8685(7)	56(2)
C(69)	-748(12)	11135(14)	8675(7)	56(2)
C(64)	44(9)	11156(14)	7986(8)	56(2)
C(65)	-480(11)	11429(14)	7308(7)	56(2)
C(66)	-1795(12)	11680(14)	7319(7)	56(2)
C(91)	6830(20)	-1470(20)	1058(11)	50(5)

C(72)	848(16)	1491(15)	10255(8)	28(3)
C(73)	2093(17)	250(16)	10460(9)	35(3)
C(71)	-470(19)	1900(20)	10740(10)	49(5)
C(82)	12220(18)	3222(17)	1392(9)	36(4)
C(81)	13310(20)	3440(20)	1564(15)	60(6)
C(83)	11450(20)	4090(20)	768(11)	51(5)
Br(1)	2928(1)	6987(2)	5902(1)	27(1)
Br(2)	5658(2)	7830(2)	5802(1)	41(1)
Br(3)	2216(1)	2961(2)	6340(1)	27(1)
N(11)	7401(10)	3975(10)	3250(5)	15(2)
N(12)	8653(10)	3038(11)	2991(6)	18(2)
N(13)	9310(10)	2629(10)	3593(6)	17(2)
N(21)	5380(9)	6710(9)	3133(5)	12(2)
N(22)	5083(11)	7889(11)	2784(7)	22(2)
N(23)	4816(10)	8689(10)	3344(6)	17(2)
N(31)	4587(11)	4671(11)	3525(6)	16(1)
N(32)	3677(10)	4316(10)	3458(6)	16(1)
N(33)	3080(10)	4265(10)	4175(6)	16(1)
N(41)	6326(9)	5407(10)	8498(5)	11(1)
N(42)	7492(9)	5024(9)	8744(5)	11(1)
N(43)	8420(9)	4770(9)	8097(5)	11(1)
N(51)	4173(9)	4843(9)	8564(5)	10(1)
N(52)	3675(9)	4036(9)	8833(5)	10(1)
N(53)	3596(9)	3518(9)	8220(5)	10(1)
N(61)	3651(9)	7551(10)	8435(5)	11(1)
N(62)	2761(9)	8783(9)	8608(5)	11(1)
N(63)	2459(9)	9452(9)	7947(5)	11(1)
O(1)	6665(11)	2310(12)	1805(6)	32(1)
O(2)	3612(11)	6397(12)	1533(6)	32(1)
O(3)	7798(11)	5367(11)	1199(6)	32(1)
O(4)	8643(11)	4268(12)	5750(6)	32(1)
O(5)	5939(11)	2854(12)	5975(6)	32(1)
O(6)	5188(11)	7575(11)	10240(6)	32(1)

O(7)	5913(11)	3589(11)	10340(6)	32(1)
O(8)	1761(11)	7012(12)	10379(6)	32(1)
O(81)	11921(15)	2425(13)	1754(7)	48(3)
O(71)	974(12)	2112(11)	9668(6)	36(3)
P(1)	5687(3)	5356(3)	4544(2)	13(1)
P(2)	5119(3)	5828(3)	7216(2)	11(1)
Re(1)	5880(1)	4946(1)	2520(1)	15(1)
Re(2)	5564(1)	5570(1)	5862(1)	13(1)
Re(3)	4493(1)	6001(1)	9294(1)	10(1)
Cl(1)	8365(6)	-1870(7)	1360(4)	73(2)
Cl(2)	5841(8)	179(6)	905(4)	74(2)
Cl(32)	-670(14)	10330(14)	5774(7)	71(2)
Cl(31)	-984(14)	7939(14)	6049(7)	71(2)
O(20)	1900(40)	10940(40)	5250(20)	71(2)
O(30)	-800(40)	6910(40)	6300(20)	71(2)
C(30)	-1530(60)	9370(60)	5640(30)	71(2)

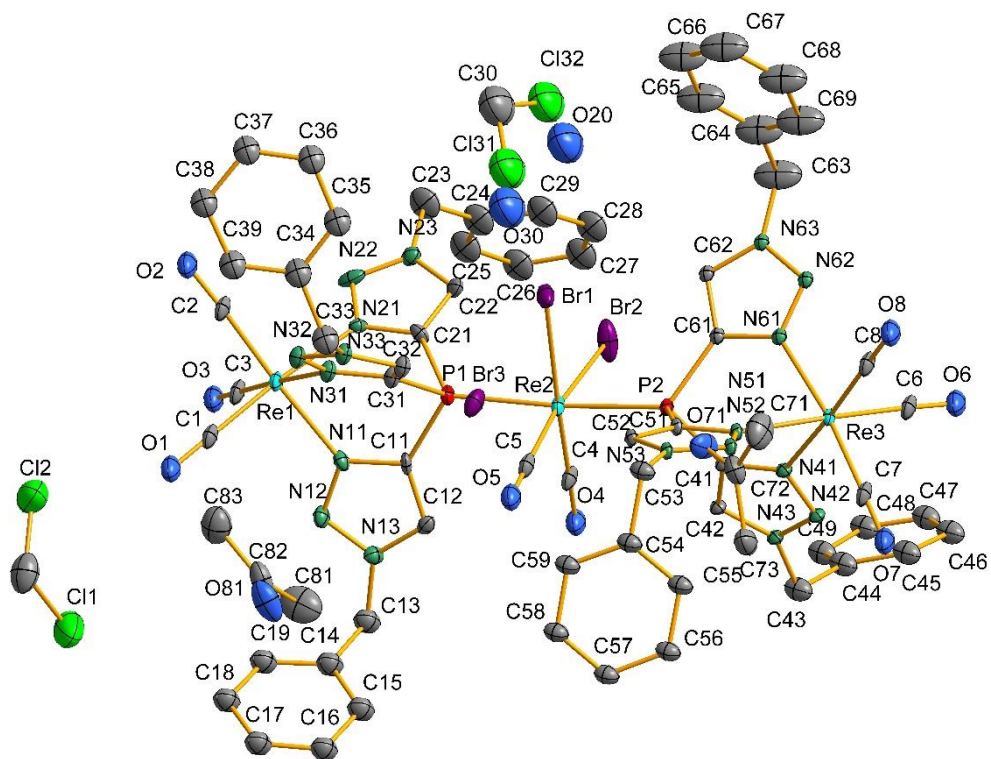


Figure S7. Ellipsoid representation of the asymmetric unit of $7 \cdot 2 \text{C}_3\text{H}_6\text{O} \cdot 1.5 \text{CH}_2\text{Cl}_2 \cdot \text{H}_2\text{O}$. Thermal ellipsoids represent 50% probability. Hydrogen atoms have been omitted for the sake of clarity.

Table S15. Crystal data and structure refinement for **8 · 2 CH₂Cl₂**.

Empirical formula	C ₄₂ H ₅₈ Cl ₉ N ₁₀ O ₄ PRE ₂
Formula weight (g/mol)	1489.40
Temperature	100(2) K
Wavelength	0.71073 Å
Crystal system	Monoclinic
Space group	P2 ₁ /n
Unit cell dimensions	a = 23.159(1) Å α = 90° b = 19.570(1) Å β = 99.78(1)° c = 24.909(1) Å γ = 90°
Volume	11125.2(9) Å ³
Z	8
Density (calculated)	1.778 g/cm ³
Absorption coefficient	4.858 mm ⁻¹
F(000)	5840
Crystal size	0.250 x 0.180 x 0.050 mm ³
Theta range for data collection	2.221 to 26.390°
Index ranges	-28<=h<=28, -24<=k<=24, -31<=l<=30
Reflections collected	118447
Independent reflections	22738 [R(int) = 0.0583]
Completeness to theta = 25.242°	99.9 %
Absorption correction	Semi-empirical
Refinement method	Full-matrix least-squares on F ²
Data / restraints / parameters	22738 / 43 / 1218
Goodness-of-fit on F ²	1.052
Final R indices [I>2sigma(I)]	R1 = 0.0340, wR2 = 0.0592
R indices (all data)	R1 = 0.0578, wR2 = 0.0668

Table S16. Atomic coordinates ($x \times 10^4$) and equivalent isotropic displacement parameters ($\text{\AA}^2 \times 10^3$) for $\mathbf{8} \cdot 2 \text{CH}_2\text{Cl}_2$. U(eq) is defined as one third of the trace of the orthogonalized U_{ij} tensor.

	x	y	z	U(eq)
Re(3)	4187(1)	4019(1)	6479(1)	11(1)
Re(2)	1032(1)	1030(1)	3468(1)	9(1)
Re(1)	3155(1)	1006(1)	2059(1)	12(1)
Re(4)	2053(1)	3885(1)	7857(1)	13(1)
Cl(15)	343(1)	144(1)	3270(1)	16(1)
P(1)	2031(1)	993(1)	2736(1)	9(1)
Cl(14)	304(1)	1858(1)	3223(1)	17(1)
Cl(21)	2116(1)	2664(1)	7800(1)	18(1)
Cl(12)	4084(1)	1093(1)	2618(1)	18(1)
Cl(22)	1144(1)	3828(1)	7271(1)	18(1)
Cl(11)	3052(1)	2227(1)	2069(1)	19(1)
Cl(24)	4843(1)	4927(1)	6711(1)	19(1)
Cl(13)	3198(1)	-209(1)	2180(1)	20(1)
Cl(25)	4943(1)	3228(1)	6732(1)	18(1)
Cl(23)	2037(1)	5110(1)	7768(1)	21(1)
P(2)	3198(1)	3955(1)	7210(1)	11(1)
Cl(81)	2181(1)	3899(1)	5599(1)	28(1)
Cl(52)	3196(1)	965(1)	4293(1)	35(1)
Cl(82)	1271(1)	4822(1)	5862(1)	35(1)
Cl(71)	1014(1)	2333(1)	5450(1)	38(1)
Cl(51)	3995(1)	-85(1)	4021(1)	54(1)
Cl(72)	727(1)	3438(1)	4664(1)	69(1)
O(6)	3924(1)	4010(2)	7176(1)	12(1)
O(2)	2723(1)	1004(2)	2678(1)	11(1)
O(7)	2498(1)	3902(2)	7254(1)	11(1)
O(3)	1302(1)	988(2)	2780(1)	10(1)
O(4)	1103(1)	1063(2)	4157(1)	14(1)
O(5)	4125(1)	4016(2)	5790(1)	15(1)
N(24)	3464(2)	4717(2)	6391(2)	13(1)
N(14)	1691(2)	1805(2)	3503(2)	12(1)
N(13)	2349(2)	-490(2)	3826(2)	12(1)
N(26)	2807(2)	5455(2)	6144(2)	12(1)
N(27)	2945(2)	3929(2)	8241(2)	12(1)
N(17)	2260(2)	953(2)	1693(2)	12(1)
N(21)	3556(2)	3210(2)	6417(2)	13(1)
N(11)	1727(2)	286(2)	3571(2)	11(1)
N(19)	1451(2)	955(2)	1150(2)	12(1)
N(25)	3300(2)	5177(2)	6012(2)	14(1)

N(3)	5022(2)	6935(2)	7591(2)	16(1)
O(8)	1876(1)	3892(2)	8488(1)	19(1)
N(12)	1872(2)	-173(2)	3954(2)	12(1)
N(29)	3740(2)	3995(2)	8801(2)	12(1)
N(15)	1806(2)	2325(2)	3838(2)	14(1)
N(16)	2302(2)	2602(2)	3714(2)	15(1)
N(18)	2044(2)	951(2)	1175(2)	13(1)
C(210)	2661(2)	5162(2)	6593(2)	15(1)
N(22)	3448(2)	2712(2)	6059(2)	15(1)
N(23)	2981(2)	2381(2)	6198(2)	12(1)
C(11)	2108(2)	282(2)	3205(2)	9(1)
C(117)	1827(2)	961(2)	2007(2)	14(1)
O(1)	3323(1)	979(2)	1427(1)	20(1)
C(12)	2514(2)	-220(2)	3375(2)	13(1)
N(28)	3147(2)	3954(2)	8765(2)	14(1)
C(118)	1306(2)	964(2)	1653(2)	13(1)
C(217)	3383(2)	3962(2)	7938(2)	11(1)
C(22)	2796(2)	2675(2)	6629(2)	13(1)
C(23)	2720(2)	1822(2)	5869(2)	13(1)
C(218)	3901(2)	4006(2)	8303(2)	13(1)
C(220)	4695(2)	3985(3)	9388(2)	16(1)
N(4)	5174(2)	-865(2)	2457(2)	28(1)
C(219)	4094(2)	4063(2)	9337(2)	15(1)
C(29)	3082(2)	4685(2)	6753(2)	12(1)
C(124)	1082(2)	975(2)	625(2)	12(1)
C(21)	3167(2)	3209(2)	6778(2)	12(1)
C(110)	2495(2)	2255(2)	3309(2)	14(1)
C(211)	2532(2)	6015(2)	5824(2)	13(1)
C(26)	2163(2)	780(3)	5252(2)	19(1)
C(13)	2622(2)	-1028(2)	4178(2)	14(1)
C(221)	5041(2)	4068(2)	9894(2)	17(1)
C(19)	2094(2)	1741(2)	3163(2)	11(1)
C(310)	5817(2)	6803(3)	6990(2)	24(1)
C(120)	143(2)	828(3)	73(2)	21(1)
C(14)	2724(2)	-1647(2)	3939(2)	17(1)
C(28)	2667(2)	1198(2)	6111(2)	22(1)
C(313)	5393(2)	7323(3)	8060(2)	19(1)
C(24)	2511(2)	1931(2)	5327(2)	19(1)
C(18)	2783(2)	-904(3)	4726(2)	21(1)
C(216)	2293(2)	5909(3)	5283(2)	18(1)
C(222)	4784(2)	4236(2)	10345(2)	18(1)
C(39)	5396(2)	6459(3)	7314(2)	22(1)

C(111)	2560(2)	3184(3)	4020(2)	19(1)
C(25)	2235(2)	1399(3)	5021(2)	22(1)
C(119)	494(2)	801(3)	585(2)	18(1)
C(116)	2285(3)	3808(3)	3961(2)	30(1)
C(49)	5374(3)	-1490(3)	2177(3)	40(2)
C(31)	4730(2)	7479(3)	7197(2)	21(1)
C(27)	2389(3)	669(3)	5792(2)	26(1)
C(121)	366(2)	1023(3)	-378(2)	22(1)
C(214)	2033(2)	7102(3)	5219(2)	25(1)
C(224)	3834(2)	4215(3)	9784(2)	19(1)
C(314)	5745(2)	6880(3)	8499(2)	23(1)
C(215)	2040(2)	6465(3)	4980(2)	23(1)
C(123)	1316(2)	1158(3)	169(2)	15(1)
C(45)	5158(2)	-227(3)	2096(3)	26(1)
C(223)	4182(2)	4309(3)	10284(2)	22(1)
C(32)	4318(2)	7206(3)	6703(2)	30(1)
C(413)	5597(3)	-738(3)	2980(3)	40(2)
C(311)	6197(3)	6261(3)	6781(3)	43(2)
C(17)	3052(2)	-1420(3)	5058(2)	23(1)
C(122)	961(2)	1193(3)	-334(2)	21(1)
C(15)	2998(2)	-2161(3)	4280(2)	26(1)
C(213)	2275(2)	7195(3)	5761(2)	26(1)
C(113)	3340(3)	3642(3)	4663(3)	39(2)
C(115)	2554(3)	4361(3)	4254(3)	38(2)
C(16)	3164(2)	-2045(3)	4831(2)	23(1)
C(112)	3085(3)	3093(3)	4367(2)	30(1)
C(8)	1611(2)	4013(3)	5995(2)	25(1)
C(114)	3068(3)	4275(3)	4606(3)	40(2)
C(315)	6015(2)	7321(3)	8986(2)	29(1)
C(411)	6115(3)	-2093(3)	1718(3)	44(2)
C(312)	6602(3)	5931(4)	7206(3)	59(2)
C(47)	4741(3)	396(3)	1248(3)	35(2)
C(410)	5992(3)	-1456(3)	2045(3)	48(2)
C(414)	5451(3)	-154(5)	3337(3)	58(2)
C(46)	4813(3)	-297(3)	1526(3)	37(2)
C(316)	5571(3)	7605(3)	9315(2)	31(1)
C(48)	4430(3)	338(4)	662(3)	58(2)
C(7)	847(4)	2564(3)	4751(3)	48(2)
C(5)	3733(3)	764(4)	3890(3)	46(2)
C(412)	5810(3)	-2080(4)	1138(3)	55(2)
C(6A)	4757(3)	2398(4)	5478(3)	60(2)
Cl(6A)	4309(3)	2243(5)	4865(4)	54(1)

Cl(6C)	5411(3)	1702(5)	5571(3)	54(1)
C(6B)	4757(3)	2398(4)	5478(3)	60(2)
Cl(6B)	4244(1)	1900(2)	5058(1)	54(1)
Cl(6D)	5451(1)	2190(2)	5513(1)	54(1)
C(33)	4170(3)	7786(4)	6288(3)	46(2)
C(34)	4669(4)	7976(4)	5996(3)	59(2)
C(35)	4569(2)	6481(3)	7795(2)	22(1)
C(36A)	4172(2)	6837(3)	8135(3)	27(1)
C(37A)	3625(4)	6405(4)	8183(4)	27(1)
C(38A)	3775(3)	5708(4)	8450(3)	27(1)
C(36B)	4172(2)	6837(3)	8135(3)	27(1)
C(37B)	3805(11)	6239(13)	8318(11)	27(1)
C(38B)	3436(9)	5886(11)	7864(10)	27(1)
C(45A)	5887(4)	-146(6)	3873(4)	85(3)
C(4AA)	5853(7)	-561(11)	4268(7)	85(3)
C(45B)	5887(4)	-146(6)	3873(4)	85(3)
C(4BB)	5744(7)	186(11)	4294(7)	85(3)
C(212)	2524(2)	6649(3)	6070(2)	23(1)
C(41A)	4550(2)	-991(3)	2572(3)	37(2)
C(4F)	3893(3)	-1621(4)	3125(4)	23(1)
C(4G)	3595(4)	-2070(4)	2664(4)	23(1)
C(4H)	4537(3)	-1451(4)	3099(4)	23(1)
C(41B)	4550(2)	-991(3)	2572(3)	37(2)
C(4E)	3642(7)	-2447(8)	3026(7)	23(1)
C(4C)	4431(7)	-1668(8)	2785(8)	23(1)
C(4D)	3774(7)	-1762(9)	2805(8)	23(1)
C(4AA)	5853(7)	-561(11)	4268(7)	85(3)
C(45B)	5887(4)	-146(6)	3873(4)	85(3)
C(4BB)	5744(7)	186(11)	4294(7)	85(3)
C(212)	2524(2)	6649(3)	6070(2)	23(1)
C(41A)	4550(2)	-991(3)	2572(3)	37(2)
C(4F)	3893(3)	-1621(4)	3125(4)	23(1)
C(4G)	3595(4)	-2070(4)	2664(4)	23(1)
C(4H)	4537(3)	-1451(4)	3099(4)	23(1)
C(41B)	4550(2)	-991(3)	2572(3)	37(2)
C(4E)	3642(7)	-2447(8)	3026(7)	23(1)
C(4C)	4431(7)	-1668(8)	2785(8)	23(1)
C(4D)	3774(7)	-1762(9)	2805(8)	23(1)

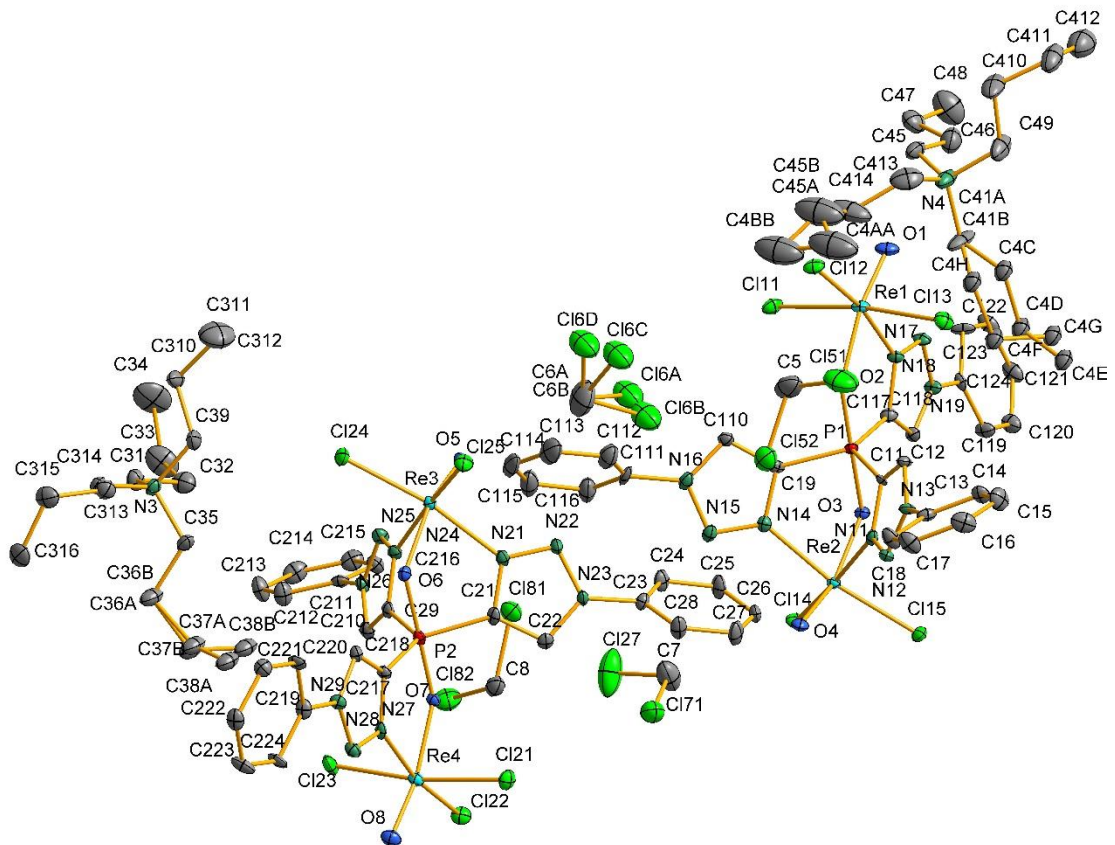


Figure S8. Ellipsoid representation of the asymmetric unit of **8** · 2 CH₂Cl₂. Thermal ellipsoids represent 50% probability. Hydrogen atoms have been omitted for the sake of clarity.

Table S17. Crystal data and structure refinement for **9**.

Empirical formula	C ₃₂ H ₄₈ Cl ₃ N ₇ O ₃ PRe
Formula weight (g/mol)	902.29
Temperature	100(2) K
Wavelength	0.71073 Å
Crystal system	Triclinic
Space group	P $\bar{1}$
Unit cell dimensions	a = 11.020(1) Å α = 77.117(4) $^{\circ}$ b = 12.779(1) Å β = 76.522(4) $^{\circ}$ c = 14.670(2) Å γ = 70.798(4) $^{\circ}$
Volume	1873.0(4) Å ³
Z	2
Density (calculated)	1.600 g/cm ³
Absorption coefficient	3.543 mm ⁻¹
F(000)	908
Crystal size	0.4 x 0.3 x 0.3 mm ³
Theta range for data collection	2.246 to 26.447 $^{\circ}$
Index ranges	-13 \leq h \leq 13, -15 \leq k \leq 15, -18 \leq l \leq 18
Reflections collected	93103
Independent reflections	7697 [R(int) = 0.0434]
Completeness to theta = 25.242 $^{\circ}$	99.9 %
Absorption correction	Semi-empirical
Refinement method	Full-matrix least-squares on F ²
Data / restraints / parameters	7697 / 15 / 477
Goodness-of-fit on F ²	1.084
Final R indices [I>2sigma(I)]	R1 = 0.0204, wR2 = 0.0467
R indices (all data)	R1 = 0.0231, wR2 = 0.0482

Table S18. Atomic coordinates ($x \times 10^4$) and equivalent isotropic displacement parameters ($\text{\AA}^2 \times 10^3$) for **9**. U(eq) is defined as one third of the trace of the orthogonalized U_{ij} tensor.

	x	y	z	U(eq)
C(12)	4980(3)	3719(2)	6593(2)	26(1)
C(13)	3825(3)	4188(2)	6269(2)	26(1)
C(14)	1531(3)	4206(3)	7042(2)	31(1)
C(15)	768(3)	3843(2)	7860(2)	27(1)
C(16)	-561(3)	4092(3)	7886(2)	31(1)
C(17)	-1110(3)	4693(3)	7105(2)	42(1)
C(18)	-336(3)	5049(4)	6299(3)	73(2)
C(19)	998(3)	4813(4)	6252(2)	65(1)
C(21)	7285(3)	2678(3)	5329(2)	41(1)
C(22)	7780(3)	1545(3)	5500(2)	41(1)
C(311)	3946(3)	7131(2)	8691(2)	31(1)
C(321)	4924(3)	7452(2)	7000(2)	27(1)
C(322)	5287(3)	8244(3)	6117(2)	39(1)
C(323)	5761(4)	7638(3)	5253(2)	46(1)
C(324)	5844(4)	8463(3)	4327(2)	56(1)
C(341)	3870(3)	9086(2)	7864(2)	29(1)
N(3)	4668(2)	7865(2)	7948(1)	23(1)
N(11)	4694(2)	3218(2)	7514(2)	26(1)
N(12)	3441(2)	3340(2)	7772(2)	27(1)
N(13)	2915(2)	3936(2)	7005(2)	26(1)
O(1)	6892(2)	4716(2)	5757(1)	41(1)
O(2)	5016(2)	2174(2)	9292(1)	26(1)
O(3)	7198(2)	2932(2)	7074(1)	25(1)
P(1)	6674(1)	3616(1)	6172(1)	30(1)
Re(1)	6163(1)	2426(1)	8375(1)	20(1)
Cl(1)	5978(1)	4216(1)	8703(1)	30(1)
Cl(2)	8097(1)	1705(1)	8987(1)	25(1)
Cl(3)	6595(1)	699(1)	7820(1)	38(1)
C(31A)	5940(3)	7739(4)	8253(2)	63(1)
C(32A)	6917(6)	6784(5)	8391(5)	44(1)
C(33A)	8130(5)	6892(5)	8665(4)	39(1)

C(34A)	8925(8)	7498(9)	7896(6)	69(2)
C(31B)	5940(3)	7739(4)	8253(2)	63(1)
C(32B)	7041(6)	7868(6)	7610(6)	44(1)
C(33B)	8246(7)	7574(7)	8091(6)	39(1)
C(34B)	9310(8)	8016(10)	7433(7)	69(2)
C(32C)	2516(4)	7373(3)	8645(2)	46(1)
C(33C)	1805(5)	6580(4)	9289(3)	33(1)
C(34C)	2158(5)	5525(4)	8858(4)	46(1)
C(32D)	2516(4)	7373(3)	8645(2)	46(1)
C(33D)	2439(9)	6111(8)	9266(7)	33(1)
C(34D)	1077(9)	6041(8)	9322(8)	46(1)
C(32E)	3513(4)	9592(3)	8773(2)	39(1)
C(33E)	2162(7)	10602(5)	8715(4)	38(1)
C(34E)	1802(8)	11248(5)	9560(4)	44(2)
C(32F)	3513(4)	9592(3)	8773(2)	39(1)
C(33F)	2753(11)	10722(7)	8717(7)	38(1)
C(34F)	2482(13)	11132(9)	9658(7)	44(2)
N(21B)	7405(10)	3252(7)	4366(7)	35(1)
N(22B)	7875(9)	2406(6)	3911(6)	36(1)
N(23B)	8081(11)	1448(6)	4563(8)	24(1)
C(23B)	8583(8)	362(6)	4298(6)	23(1)
C(24B)	9238(7)	242(7)	3365(5)	34(1)
C(25B)	9677(8)	-794(8)	3107(6)	42(2)
C(26B)	9534(10)	-1726(10)	3747(8)	45(2)
C(27B)	8911(8)	-1633(7)	4679(6)	44(1)
C(28B)	8456(9)	-580(7)	4951(6)	29(1)
N(22A)	7789(7)	1877(5)	3994(4)	36(1)
N(21A)	7281(8)	2801(5)	4370(5)	35(1)
N(23A)	8123(8)	1010(5)	4704(6)	24(1)
C(23A)	8654(6)	-123(6)	4519(5)	23(1)
C(24A)	9151(6)	-323(6)	3575(4)	34(1)
C(25A)	9647(7)	-1419(8)	3408(5)	42(2)
C(26A)	9667(6)	-2310(6)	4163(5)	45(2)

C(27A)	9204(7)	-2096(6)	5078(5)	44(1)
C(28A)	8663(7)	-1001(5)	5278(4)	29(1)

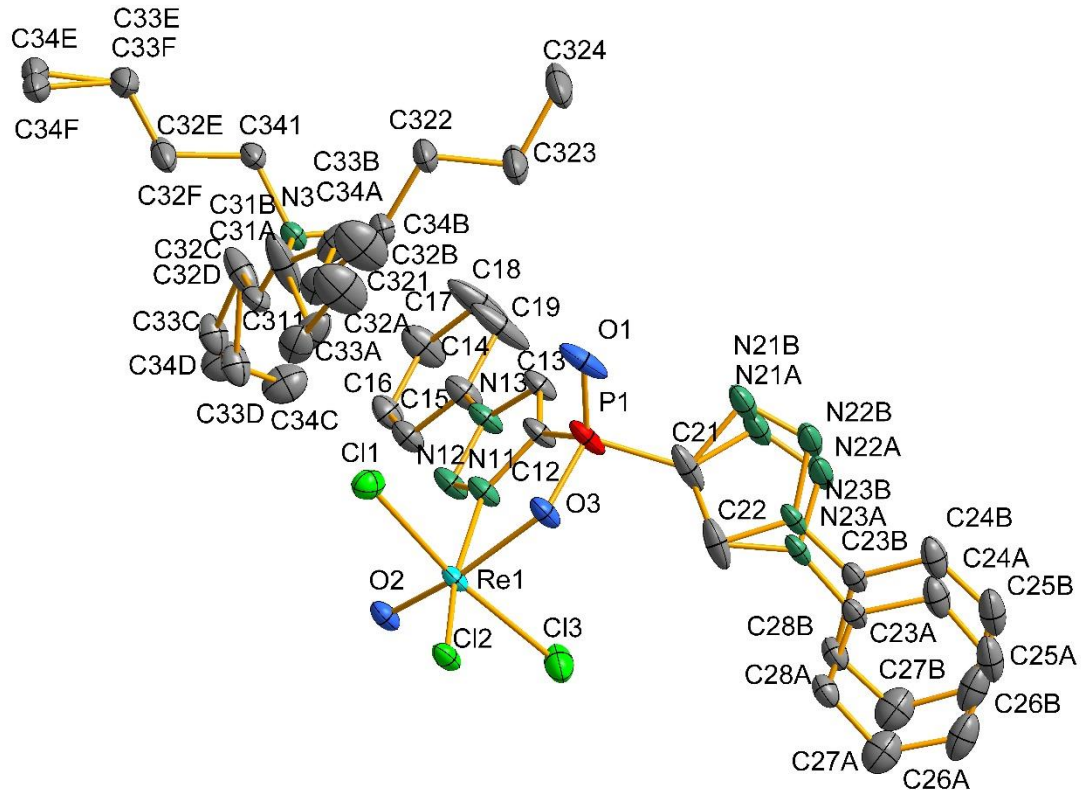


Figure S9. Ellipsoid representation of the asymmetric unit of **9**. Thermal ellipsoids represent 50% probability. Hydrogen atoms have been omitted for the sake of clarity.

Table S19. Crystal data and structure refinement for **10 · CH₂Cl₂**

Empirical formula	C ₈₈ H ₁₂₄ Cl ₁₄ N ₂₀ O ₈ P ₂ Re ₄
Formula weight (g/mol)	2893.10
Temperature	102(2) K
Wavelength	0.71073 Å
Crystal system	Orthorhombic
Space group	P2 ₁ 2 ₁ 2 ₁
Unit cell dimensions	a = 15.972(1) Å α = 90° b = 21.959(2) Å β = 90° c = 31.445(2) Å γ = 90°
Volume	11029(1) Å ³
Z	4
Density (calculated)	1.742 g/cm ³
Absorption coefficient	4.804 mm ⁻¹
F(000)	5696
Crystal size	0.48 x 0.12 x 0.03 mm ³
Theta range for data collection	2.153 to 27.187°
Index ranges	-20<=h<=20, -28<=k<=28, -40<=l<=40
Reflections collected	273295
Independent reflections	24451 [R(int) = 0.0409]
Completeness to theta = 25.242°	99.9 %
Absorption correction	Semi-empirical
Refinement method	Full-matrix least-squares on F ²
Flack x parameter	0.485
Data / restraints / parameters	24451 / 1 / 1220
Goodness-of-fit on F ²	1.035
Final R indices [I>2sigma(I)]	R1 = 0.0204, wR2 = 0.0497
R indices (all data)	R1 = 0.0216, wR2 = 0.0504

Table S20. Atomic coordinates ($x \times 10^4$) and equivalent isotropic displacement parameters ($\text{\AA}^2 \times 10^3$) for **10** · CH₂Cl₂. U(eq) is defined as one third of the trace of the orthogonalized Uij tensor.

	x	y	z	U(eq)
C(2)	1898(4)	8160(3)	3260(2)	35(1)
C(11)	6940(3)	4068(2)	5379(2)	13(1)
C(12)	6324(3)	4123(2)	5674(1)	15(1)
C(13)	4770(3)	4346(2)	5604(2)	17(1)
C(14)	4315(3)	3750(2)	5682(2)	16(1)
C(15)	3446(3)	3743(2)	5655(2)	23(1)
C(16)	2999(3)	3214(3)	5738(2)	26(1)
C(17)	3415(3)	2687(2)	5860(2)	22(1)
C(18)	4277(3)	2690(2)	5885(2)	23(1)
C(19)	4727(3)	3218(2)	5801(2)	20(1)
C(21)	8512(3)	4644(2)	5177(2)	14(1)
C(22)	9042(3)	5087(2)	5317(2)	16(1)
C(23)	9532(3)	6083(2)	4992(2)	21(1)
C(24)	9079(3)	6576(2)	5229(2)	17(1)
C(25)	8725(3)	7061(2)	5006(2)	18(1)
C(26)	8291(3)	7514(2)	5220(2)	22(1)
C(27)	8212(3)	7484(2)	5660(2)	22(1)
C(28)	8572(3)	7010(2)	5886(2)	21(1)
C(29)	9007(3)	6555(2)	5668(2)	20(1)
C(31)	8596(3)	3249(2)	5493(1)	13(1)
C(32)	8816(3)	2750(2)	5252(1)	13(1)
C(33)	9532(3)	1757(2)	5432(2)	20(1)
C(34)	9060(3)	1270(2)	5671(2)	22(1)
C(35)	8235(4)	1132(3)	5561(2)	36(1)
C(36)	7796(4)	701(3)	5793(3)	46(2)
C(37)	8157(4)	413(3)	6132(3)	41(2)
C(38)	8980(4)	541(3)	6242(2)	34(1)
C(39)	9436(3)	969(2)	6008(2)	24(1)
C(41)	2979(3)	5927(2)	4584(1)	12(1)
C(42)	3628(3)	5867(2)	4298(1)	14(1)

C(43)	5165(3)	5624(2)	4398(2)	19(1)
C(44)	5631(3)	6225(2)	4339(1)	17(1)
C(45)	5231(3)	6770(2)	4252(2)	21(1)
C(46)	5684(3)	7298(2)	4170(2)	24(1)
C(47)	6551(4)	7282(3)	4178(2)	27(1)
C(48)	6953(3)	6743(3)	4273(2)	31(1)
C(49)	6500(3)	6218(2)	4357(2)	24(1)
C(51)	1376(3)	5375(2)	4748(2)	15(1)
C(52)	842(3)	4939(2)	4591(2)	16(1)
C(53)	325(3)	3938(2)	4900(2)	20(1)
C(54)	829(3)	3428(2)	4699(2)	17(1)
C(55)	1180(3)	2977(2)	4954(2)	21(1)
C(56)	1646(3)	2516(2)	4771(2)	21(1)
C(57)	1765(3)	2509(2)	4334(2)	21(1)
C(58)	1414(3)	2955(2)	4081(2)	21(1)
C(59)	941(3)	3415(2)	4259(2)	19(1)
C(61)	1360(3)	6777(2)	4455(1)	13(1)
C(62)	1128(3)	7267(2)	4703(1)	14(1)
C(63)	423(3)	8271(2)	4529(2)	20(1)
C(64)	840(3)	8766(2)	4273(2)	21(1)
C(65)	405(3)	9038(2)	3943(2)	24(1)
C(66)	792(4)	9480(2)	3691(2)	32(1)
C(67)	1603(4)	9652(2)	3767(2)	33(1)
C(68)	2035(4)	9387(3)	4094(2)	36(1)
C(69)	1665(4)	8946(3)	4352(2)	32(1)
C(111)	1100(3)	4467(3)	7621(2)	25(1)
C(112)	240(4)	4182(3)	7661(2)	34(1)
C(113)	62(4)	3978(3)	8116(2)	37(1)
C(114)	-777(4)	3671(4)	8149(2)	48(2)
C(121)	795(3)	5014(2)	6940(2)	22(1)
C(122)	808(4)	5665(3)	7093(2)	33(1)
C(123)	68(4)	6013(3)	6887(2)	29(1)
C(124)	148(6)	6698(3)	6915(3)	65(3)

C(131)	1342(4)	3977(2)	6914(2)	23(1)
C(132)	1758(4)	3429(3)	7123(2)	32(1)
C(133)	1743(5)	2891(3)	6818(2)	45(2)
C(134)	2119(6)	2316(3)	7010(3)	63(2)
C(141)	2267(3)	4817(3)	7183(2)	29(1)
C(142)	2669(4)	4938(3)	6746(2)	34(1)
C(143)	3538(4)	5231(3)	6789(2)	35(1)
C(144)	3529(5)	5866(3)	6966(3)	54(2)
C(211)	-773(3)	5004(2)	3010(2)	20(1)
C(212)	-622(4)	4367(2)	2832(2)	27(1)
C(213)	21(4)	4041(3)	3105(2)	27(1)
C(214)	108(5)	3375(3)	3002(2)	46(2)
C(221)	-2169(3)	5090(3)	2651(2)	25(1)
C(222)	-2655(3)	4856(3)	3027(2)	29(1)
C(223)	-3432(3)	4523(3)	2868(2)	28(1)
C(224)	-4008(4)	4337(3)	3225(2)	37(1)
C(231)	-968(3)	5584(3)	2330(2)	22(1)
C(232)	-166(3)	5955(3)	2352(2)	26(1)
C(233)	68(4)	6200(3)	1917(2)	35(1)
C(234)	888(4)	6551(4)	1937(2)	48(2)
C(241)	-1499(3)	5980(2)	3022(2)	23(1)
C(242)	-1956(4)	6497(3)	2804(2)	30(1)
N(1)	1378(3)	4571(2)	7166(1)	22(1)
N(2)	-1352(3)	5410(2)	2753(1)	20(1)
N(11)	6596(2)	4194(2)	4993(1)	15(1)
N(12)	5791(2)	4321(2)	5031(1)	15(1)
N(13)	5624(2)	4266(2)	5451(1)	16(1)
N(21)	8234(3)	4819(2)	4785(1)	16(1)
N(22)	8554(3)	5350(2)	4679(1)	18(1)
N(23)	9060(3)	5501(2)	5003(1)	17(1)
N(31)	8848(2)	3122(2)	5898(1)	13(1)
N(32)	9207(3)	2586(2)	5923(1)	16(1)
N(33)	9184(2)	2366(2)	5522(1)	16(1)

N(41)	3302(2)	5780(2)	4975(1)	13(1)
N(42)	4100(2)	5647(2)	4950(1)	16(1)
N(43)	4294(2)	5705(2)	4533(1)	15(1)
N(51)	1642(3)	5182(2)	5138(1)	15(1)
N(52)	1301(3)	4650(2)	5233(1)	19(1)
N(53)	811(3)	4512(2)	4900(1)	18(1)
N(61)	1143(2)	6922(2)	4047(1)	14(1)
N(62)	787(3)	7459(2)	4028(1)	18(1)
N(63)	786(3)	7667(2)	4432(1)	16(1)
O(1)	6872(2)	4790(2)	4242(1)	23(1)
O(2)	7974(2)	3711(1)	4870(1)	11(1)
O(3)	8161(2)	4150(2)	5880(1)	14(1)
O(4)	9269(2)	3345(2)	6711(1)	21(1)
O(5)	2940(2)	5161(2)	5702(1)	23(1)
O(6)	1929(2)	6287(1)	5078(1)	13(1)
O(7)	1808(2)	5888(1)	4059(1)	13(1)
O(8)	778(2)	6739(2)	3225(1)	23(1)
P(1)	8062(1)	3950(1)	5385(1)	11(1)
P(2)	1870(1)	6066(1)	4558(1)	11(1)
Cl(1)	9193(2)	1840(1)	6979(1)	70(1)
Cl(3)	1042(1)	8200(1)	2918(1)	59(1)
Cl(4)	2726(1)	8629(1)	3090(1)	49(1)
Cl(11)	6682(1)	3362(1)	4168(1)	19(1)
Cl(12)	8496(1)	4047(1)	3954(1)	22(1)
Cl(13)	8535(1)	4692(1)	6773(1)	22(1)
Cl(14)	7377(1)	3458(1)	6598(1)	20(1)
Cl(15)	9986(1)	4216(1)	6062(1)	20(1)
Cl(21)	3202(1)	6571(1)	5818(1)	22(1)
Cl(22)	1331(1)	5930(1)	5974(1)	24(1)
Cl(23)	0(1)	5849(1)	3842(1)	20(1)
Cl(24)	1515(1)	5392(1)	3141(1)	21(1)
Cl(25)	2658(1)	6601(1)	3371(1)	20(1)
Re(1)	7418(1)	4195(1)	4448(1)	13(1)

Re(2)	8743(1)	3803(1)	6375(1)	14(1)
Re(3)	2443(1)	5775(1)	5501(1)	14(1)
Re(4)	1276(1)	6262(1)	3558(1)	14(1)
C(1A)	8206(5)	1897(4)	6729(2)	50(2)
Cl(2A)	7555(6)	1653(5)	7102(3)	68(1)
C(1B)	8206(5)	1897(4)	6729(2)	50(2)
Cl(2B)	7414(3)	1383(2)	6952(1)	68(1)
C(23A)	-2104(4)	7016(3)	3118(2)	40(2)
C(24A)	-1312(10)	7330(6)	3251(6)	59(3)
C(23B)	-2104(4)	7016(3)	3118(2)	40(2)
C(24B)	-2502(11)	7568(7)	2943(6)	59(3)
C(23A)	-2104(4)	7016(3)	3118(2)	40(2)
C(24A)	-1312(10)	7330(6)	3251(6)	59(3)
C(24B)	-2502(11)	7568(7)	2943(6)	59(3)

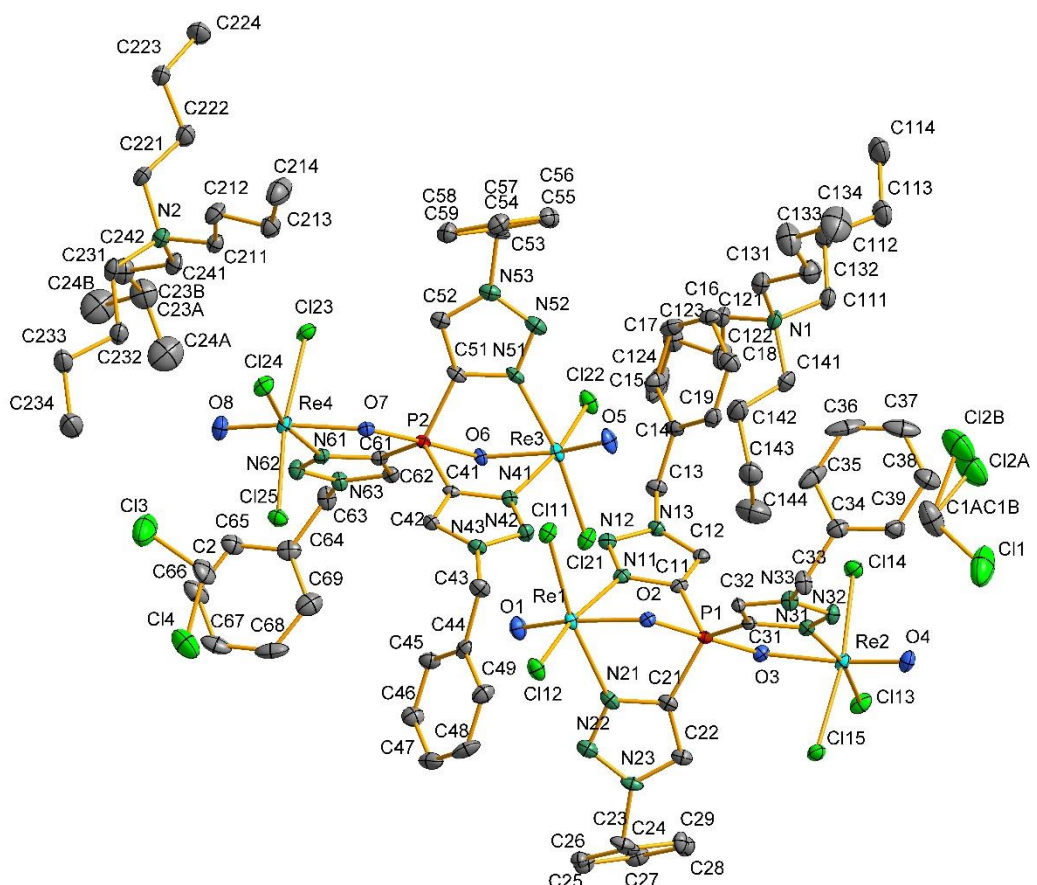


Figure S10. Ellipsoid representation of the asymmetric unit of **10** · CH_2Cl_2 . Thermal ellipsoids represent 50% probability. Hydrogen atoms have been omitted for the sake of clarity.

Table S21. Crystal data and structure refinement for **11**.

Empirical formula	C ₃₄ H ₅₂ Cl ₆ N ₇ O ₄ PR ₂
Formula weight (g/mol)	1238.89
Temperature	105(2) K
Wavelength	0.71073 Å
Crystal system	Monoclinic
Space group	P2 ₁ /c
Unit cell dimensions	a = 15.032(2) Å α = 90° b = 17.490(2) Å β = 99.052(4)° c = 17.121(2) Å γ = 90°
Volume	4445.3(8) Å ³
Z	4
Density (calculated)	1.851 g/cm ³
Absorption coefficient	5.882 mm ⁻¹
F(000)	2416
Crystal size	0.14 x 0.09 x 0.01 mm ³
Theta range for data collection	2.282 to 28.352°
Index ranges	-20<=h<=20, -23<=k<=23, -22<=l<=22
Reflections collected	144532
Independent reflections	11100 [R(int) = 0.0756]
Completeness to theta = 25.242°	100.0 %
Absorption correction	Semi-empirical
Refinement method	Full-matrix least-squares on F ²
Data / restraints / parameters	11100 / 0 / 487
Goodness-of-fit on F ²	1.033
Final R indices [I>2sigma(I)]	R1 = 0.0274, wR2 = 0.0457
R indices (all data)	R1 = 0.0408, wR2 = 0.0485
Largest diff. peak and hole	1.684 and -1.115 e·Å ⁻³

Table S22. Atomic coordinates ($x \times 10^4$) and equivalent isotropic displacement parameters ($\text{\AA}^2 \times 10^3$) for **11**. U(eq) is defined as one third of the trace of the orthogonalized U_{ij} tensor.

	x	y	z	U(eq)
C(11)	1272(2)	3003(2)	6717(2)	11(1)
C(12)	901(2)	2923(2)	5937(2)	11(1)
C(13)	1571(2)	3014(2)	4670(2)	14(1)
C(14)	1425(2)	3836(2)	4420(2)	15(1)
C(15)	563(3)	4145(2)	4321(2)	22(1)
C(16)	427(3)	4918(2)	4153(2)	29(1)
C(17)	1155(3)	5382(2)	4083(2)	33(1)
C(18)	2009(3)	5070(2)	4153(2)	31(1)
C(19)	2145(3)	4302(2)	4328(2)	25(1)
C(21)	263(2)	3925(2)	7711(2)	9(1)
C(22)	349(2)	4704(2)	7730(2)	10(1)
C(23)	-760(2)	5778(2)	7854(2)	14(1)
C(24)	-1067(2)	5916(2)	8641(2)	12(1)
C(25)	-462(2)	5835(2)	9339(2)	18(1)
C(26)	-763(3)	5904(2)	10061(2)	22(1)
C(27)	-1657(3)	6064(2)	10090(2)	21(1)
C(28)	-2250(3)	6180(2)	9396(2)	20(1)
C(29)	-1955(2)	6098(2)	8670(2)	15(1)
C(311)	4966(2)	1983(2)	6077(2)	17(1)
C(312)	5239(2)	2799(2)	5924(2)	20(1)
C(313)	4534(3)	3179(2)	5313(2)	24(1)
C(314)	4751(3)	4015(2)	5189(3)	35(1)
C(321)	6558(2)	1481(2)	6326(2)	17(1)
C(322)	6499(2)	1204(2)	5473(2)	20(1)
C(323)	7441(3)	1069(3)	5274(2)	29(1)
C(324)	7416(3)	828(2)	4424(2)	29(1)
C(331)	5325(2)	709(2)	6700(2)	17(1)
C(332)	4481(2)	608(2)	7076(2)	19(1)
C(333)	4400(3)	-221(2)	7322(3)	26(1)
C(334)	3571(3)	-356(2)	7711(3)	31(1)
C(341)	5798(2)	1917(2)	7438(2)	16(1)

C(342)	6319(2)	1465(2)	8117(2)	19(1)
C(343)	6503(3)	1960(2)	8860(2)	26(1)
C(344)	7083(3)	1549(3)	9538(2)	37(1)
Cl(11)	2585(1)	4614(1)	7600(1)	18(1)
Cl(12)	3797(1)	3673(1)	9051(1)	20(1)
Cl(13)	3322(1)	2039(1)	8135(1)	18(1)
Cl(21)	-802(1)	2683(1)	9207(1)	16(1)
Cl(22)	-1316(1)	1334(1)	7900(1)	17(1)
Cl(23)	-1117(1)	2503(1)	6442(1)	18(1)
N(3)	5655(2)	1524(2)	6631(2)	14(1)
N(11)	2186(2)	3079(2)	6737(2)	9(1)
N(12)	2384(2)	3055(2)	6016(2)	12(1)
N(13)	1600(2)	2961(2)	5538(2)	12(1)
N(21)	-615(2)	3775(2)	7777(2)	10(1)
N(22)	-1067(2)	4412(2)	7836(2)	11(1)
N(23)	-465(2)	4975(2)	7804(2)	11(1)
O(11)	3925(2)	3397(1)	7237(1)	18(1)
O(12)	1845(2)	3164(1)	8185(1)	10(1)
O(21)	-2180(2)	2987(1)	7717(1)	16(1)
O(22)	304(2)	2485(1)	7866(1)	10(1)
P(1)	938(1)	3096(1)	7667(1)	8(1)
Re(1)	3107(1)	3341(1)	7782(1)	10(1)
Re(2)	-1136(1)	2647(1)	7818(1)	10(1)

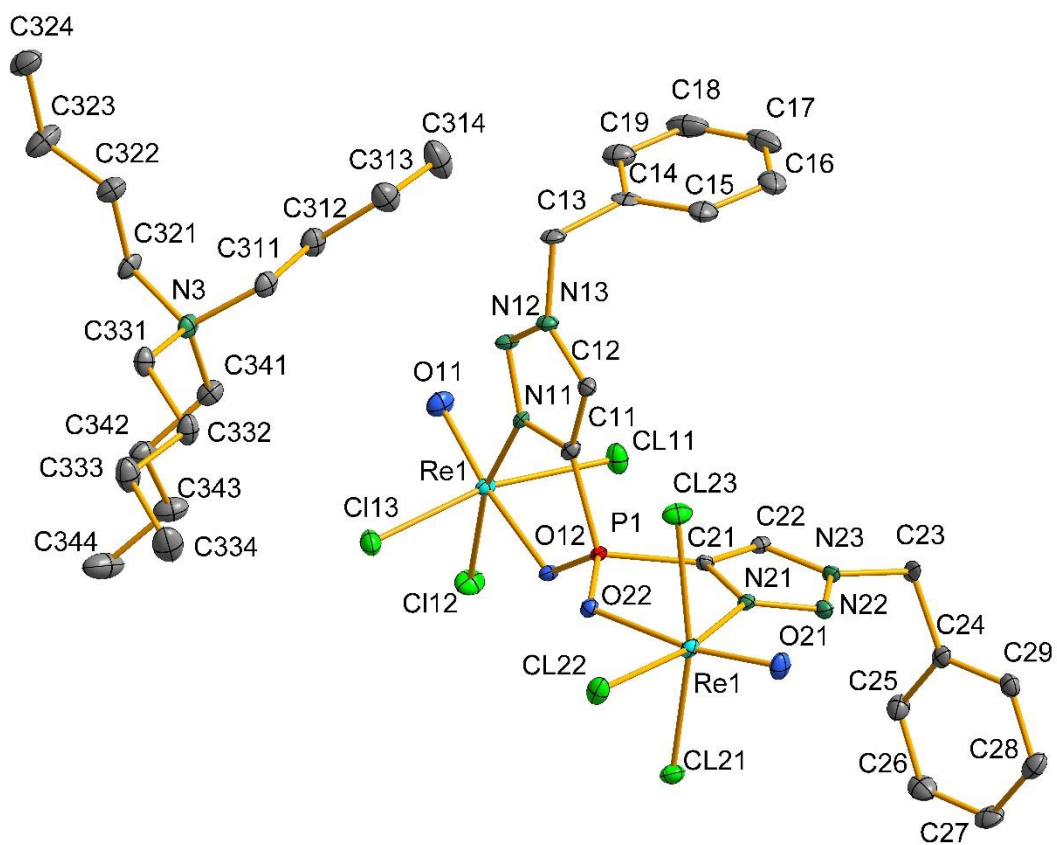


Figure S11. Ellipsoid representation of the asymmetric unit of **11**. Thermal ellipsoids represent 50% probability. Hydrogen atoms have been omitted for the sake of clarity.

Table S23. Crystal data and structure refinement for **12 · 2 CH₂Cl₂**.

Empirical formula	C ₅₆ H ₅₀ Cl ₄ CuN ₂₀ O ₈ P ₂
Formula weight (g/mol)	1398.44
Temperature	100(2) K
Wavelength	0.71073 Å
Crystal system	triclinic
Space group	P $\bar{1}$
Unit cell dimensions	a = 10.365(3) Å α = 107.55(2) $^{\circ}$ b = 11.277(3) Å β = 102.354(9) $^{\circ}$ c = 14.403(4) Å γ = 100.23(2) $^{\circ}$
Volume	1514.2(8) Å ³
Z	1
Density (calculated)	1.534 g/cm ³
Absorption coefficient	0.663 mm ⁻¹
F(000)	717
Crystal size	0.14 x 0.15 x 0.19 mm ³
Theta range for data collection	2.462 - 27.196 $^{\circ}$
Index ranges	-13<=h<=13, -14<=k<=14, -18<=l<=18
Reflections collected	54528
Independent reflections	6736 [R(int) = 0.2161]
Completeness to theta = 25.242 $^{\circ}$	99.9 %
Absorption correction	Semi-empirical
Refinement method	Full-matrix least-squares on F ²
Data / restraints / parameters	6736 / 0 / 412
Goodness-of-fit on F ²	1.010
Final R indices [I>2sigma(I)]	R ₁ = 0.0441, wR ₂ = 0.1140
R indices (all data)	R ₁ = 0.0761, wR ₂ = 0.1245

Table S24. Atomic coordinates ($x \times 10^4$) and equivalent isotropic displacement parameters ($\text{\AA}^2 \times 10^3$) for **12** · 2 CH₂Cl₂. U(eq) is defined as one third of the trace of the orthogonalized U_{ij} tensor.

	x	y	z	U(eq)
C(4)	523(3)	1263(3)	1210(2)	32(1)
C(11)	4752(3)	7359(2)	4478(2)	14(1)
C(12)	3949(2)	7696(2)	3769(2)	16(1)
C(13)	1887(3)	6380(2)	2247(2)	18(1)
C(14)	620(3)	6558(2)	2564(2)	17(1)
C(15)	436(3)	7785(3)	2934(2)	25(1)
C(16)	-759(3)	7944(3)	3189(2)	31(1)
C(17)	-1753(3)	6878(3)	3089(2)	31(1)
C(18)	-1554(3)	5669(3)	2747(2)	30(1)
C(19)	-381(3)	5502(3)	2476(2)	23(1)
C(21)	5560(2)	7715(2)	6523(2)	15(1)
C(22)	5617(3)	8339(3)	7524(2)	18(1)
C(23)	4972(3)	7426(3)	8836(2)	24(1)
C(24)	5853(3)	6682(3)	9274(2)	23(1)
C(25)	5423(3)	5345(3)	8939(2)	26(1)
C(26)	6236(3)	4659(3)	9322(2)	32(1)
C(27)	7497(4)	5294(3)	10031(2)	36(1)
C(28)	7919(4)	6607(3)	10368(2)	40(1)
C(29)	7098(3)	7316(3)	9993(2)	31(1)
C(31)	7480(3)	7523(2)	5440(2)	14(1)
C(32)	8840(3)	8012(2)	5616(2)	19(1)
C(33)	10772(3)	6908(3)	5453(2)	34(1)
C(34)	11774(3)	8114(3)	6214(2)	22(1)
C(35)	12408(3)	9047(3)	5894(2)	28(1)
C(36)	13273(3)	10174(3)	6590(3)	34(1)
C(37)	13536(3)	10401(3)	7618(3)	37(1)
C(38)	12930(3)	9479(3)	7945(2)	33(1)
C(39)	12052(3)	8331(3)	7247(2)	26(1)
Cl(41)	1403(1)	2791(1)	2137(1)	27(1)
Cl(42)	480(1)	28(1)	1729(1)	36(1)

Cu(1)	5000	5000	5000	15(1)
N(4)	7323(2)	11483(2)	9642(2)	25(1)
N(11)	4288(2)	6060(2)	4224(2)	14(1)
N(12)	3239(2)	5584(2)	3398(2)	16(1)
N(13)	3049(2)	6585(2)	3129(2)	14(1)
N(21)	5049(2)	6431(2)	6287(2)	16(1)
N(22)	4760(2)	6209(2)	7077(2)	19(1)
N(23)	5112(2)	7368(2)	7818(2)	17(1)
N(31)	7221(2)	6216(2)	5173(2)	17(1)
N(32)	8366(2)	5889(2)	5171(2)	22(1)
N(33)	9352(2)	6981(2)	5439(2)	23(1)
O(1)	6510(2)	9672(2)	5840(1)	18(1)
O(41)	7196(2)	10378(2)	9724(2)	41(1)
O(42)	6789(2)	11510(2)	8780(2)	42(1)
O(43)	7962(2)	12433(2)	10361(2)	49(1)
P(1)	6129(1)	8275(1)	5608(1)	14(1)

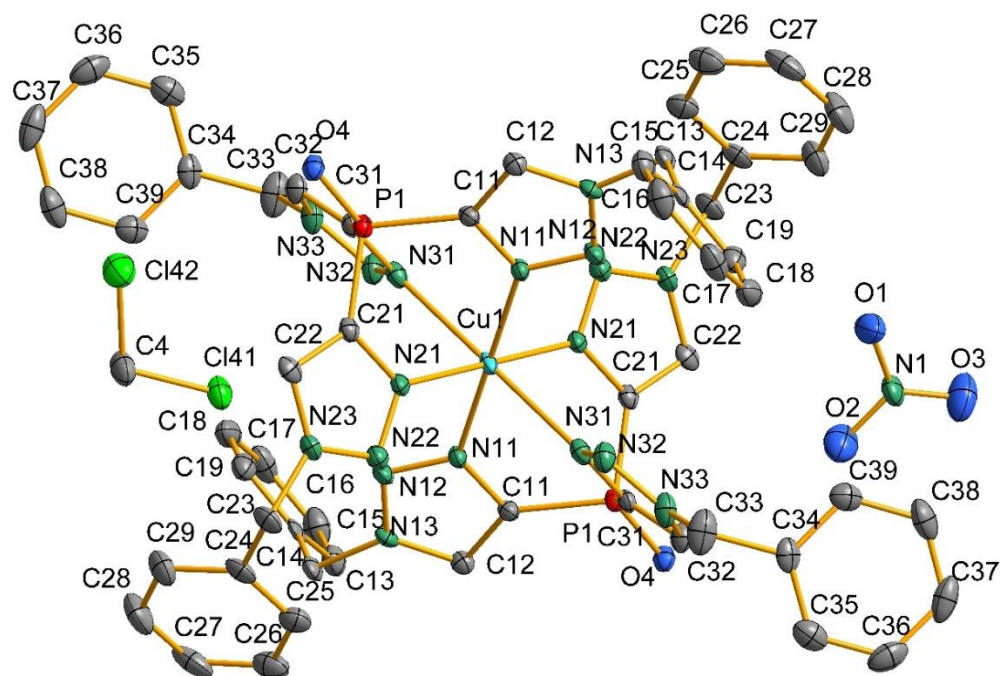


Figure S12. Ellipsoid representation of the asymmetric unit of **12** · 2 CH₂Cl₂. Thermal ellipsoids represent 50% probability. Hydrogen atoms have been omitted for the sake of clarity.

Table S25. Crystal data and structure refinement for **13 · 2 CH₂Cl₂**.

Empirical formula	C ₅₆ H ₅₀ Cl ₄ NiN ₂₀ O ₈ P ₂
Formula weight (g/mol)	1395.61
Temperature	100(2) K
Wavelength	1.54178 Å
Crystal system	Triclinic
Space group	P $\bar{1}$
Unit cell dimensions	a = 10.3210(7) Å α = 107.318(5) $^{\circ}$ b = 11.3520(7) Å β = 102.040(5) $^{\circ}$ c = 14.374(1) Å γ = 101.937(5) $^{\circ}$
Volume	1505.7(2) Å ³
Z	1
Density (calculated)	1.539 g/cm ³
Absorption coefficient	3.217 mm ⁻¹
F(000)	718
Crystal size	0.6 x 0.2 x 0.1 mm ³
Theta range for data collection	3.36 to 73.88 $^{\circ}$
Index ranges	-12 \leq h \leq 12, -14 \leq k \leq 14, -17 \leq l \leq 17
Reflections collected	33468
Independent reflections	6137 [R(int) = 0.1778]
Completeness to theta = 25.242 $^{\circ}$	99.9 %
Absorption correction	Semi-empirical
Refinement method	Full-matrix least-squares on F ²
Data / restraints / parameters	6137 / 0 / 412
Goodness-of-fit on F ²	1.011
Final R indices [I>2sigma(I)]	R1 = 0.0660, wR2 = 0.1462
R indices (all data)	R1 = 0.1167, wR2 = 0.1711
Largest diff. peak and hole	0.682 and -0.557 e·Å ⁻³

Table S26. Atomic coordinates ($x \times 10^4$) and equivalent isotropic displacement parameters ($\text{\AA}^2 \times 10^3$) for **13** · 2 CH₂Cl₂. U(eq) is defined as one third of the trace of the orthogonalized U_{ij} tensor.

	x	y	z	U(eq)
Ni(1)	5000	5000	5000	16(1)
P(1)	3913(1)	1724(1)	4326(1)	17(1)
Cl(03)	8531(1)	7185(1)	7909(1)	33(1)
Cl(04)	9458(2)	9947(1)	8252(1)	41(1)
O(4)	3429(3)	328(3)	4083(2)	23(1)
N(31)	5043(4)	3595(3)	3675(3)	18(1)
N(21)	5747(4)	3922(3)	5796(3)	18(1)
N(11)	2980(4)	3857(3)	4766(3)	17(1)
N(13)	813(4)	3175(3)	4471(3)	21(1)
N(32)	5316(4)	3843(3)	2893(3)	21(1)
N(23)	6953(4)	3351(3)	6868(3)	19(1)
O(2)	2763(4)	-364(4)	197(3)	42(1)
N(12)	1870(4)	4235(3)	4755(3)	21(1)
N(33)	4950(4)	2700(3)	2134(3)	21(1)
N(22)	6767(4)	4376(3)	6637(3)	20(1)
O(1)	1970(4)	-2431(3)	-419(3)	44(1)
N(1)	2675(4)	-1434(4)	304(3)	31(1)
O(3)	3314(5)	-1459(4)	1132(3)	50(1)
C(21)	5286(4)	2608(4)	5480(3)	18(1)
C(22)	6061(4)	2240(4)	6173(3)	19(1)
C(11)	2631(4)	2543(4)	4499(3)	18(1)
C(31)	4522(4)	2285(4)	3417(3)	20(1)
C(24)	9383(5)	3408(4)	7409(3)	21(1)
C(32)	4451(5)	1715(4)	2420(3)	21(1)
C(12)	1239(5)	2101(4)	4303(3)	21(1)
C(14)	-1665(4)	2024(4)	3753(4)	23(1)
C(23)	8110(5)	3528(4)	7737(3)	23(1)
C(25)	9584(5)	2203(5)	7020(4)	27(1)
C(34)	4160(5)	3379(5)	690(4)	26(1)
C(39)	4573(6)	4730(5)	1056(4)	30(1)

C(19)	-2225(5)	1198(5)	4204(4)	29(1)
C(29)	10360(5)	4499(5)	7491(4)	28(1)
C(15)	-2051(5)	1647(5)	2703(4)	26(1)
C(33)	5066(5)	2660(4)	1112(3)	26(1)
C(16)	-2960(5)	472(5)	2110(4)	32(1)
C(26)	10780(6)	2117(5)	6753(4)	35(1)
C(13)	-602(5)	3288(5)	4408(4)	29(1)
C(18)	-3157(5)	5(5)	3604(5)	35(1)
C(17)	-3523(5)	-368(5)	2545(4)	34(1)
C(38)	3744(6)	5387(5)	684(4)	33(1)
C(35)	2917(6)	2718(5)	-40(4)	33(1)
C(27)	11770(6)	3214(6)	6845(4)	39(1)
C(28)	11552(6)	4408(6)	7218(4)	39(1)
C(37)	2490(7)	4736(6)	-37(4)	40(1)
C(36)	2081(7)	3400(6)	-411(4)	43(1)
C(01A)	9415(6)	8741(5)	8814(4)	37(1)

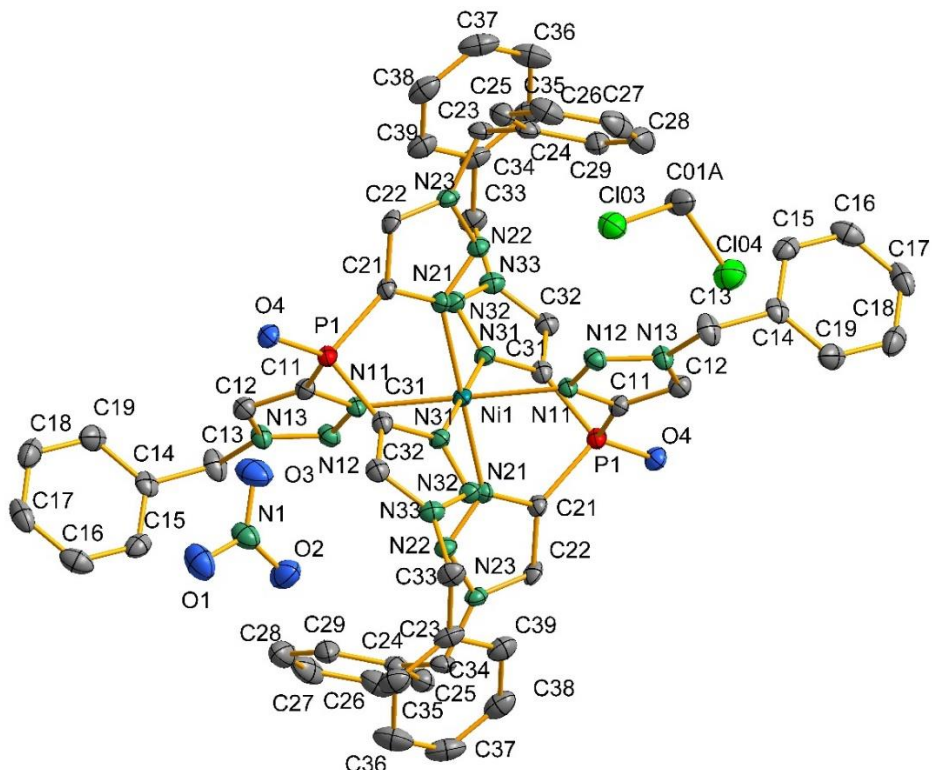


Figure S13. Ellipsoid representation of the asymmetric unit of **13** · 2CH₂Cl₂. Thermal ellipsoids represent 50% probability. Hydrogen atoms have been omitted for the sake of clarity.

6.2 Spectroscopic data

6.2.1 Spectroscopic data of L¹

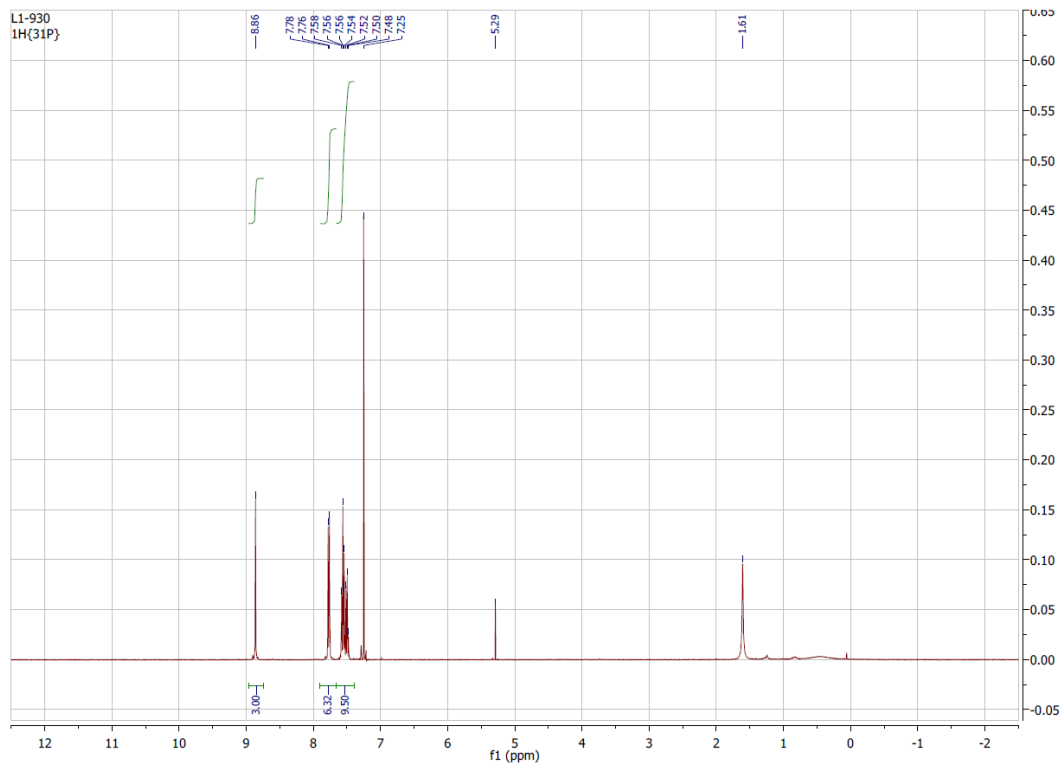


Figure S14. ¹H NMR spectrum of tris(1-phenyl-1H-1,2,3-triazol-4-yl)phosphine oxide (L¹) in CDCl₃.

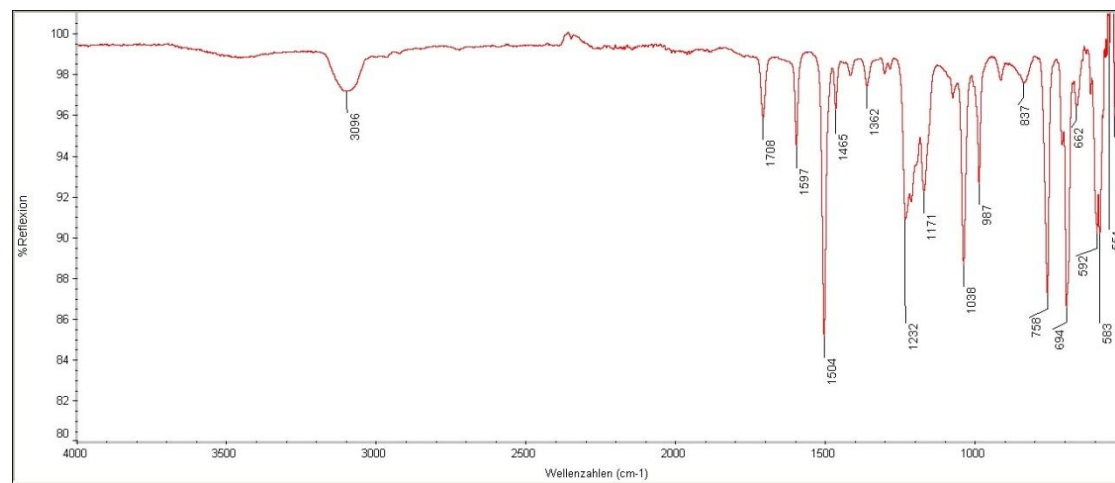


Figure S15. IR spectrum of tris(1-phenyl-1H-1,2,3-triazol-4-yl)phosphine oxide (L¹)

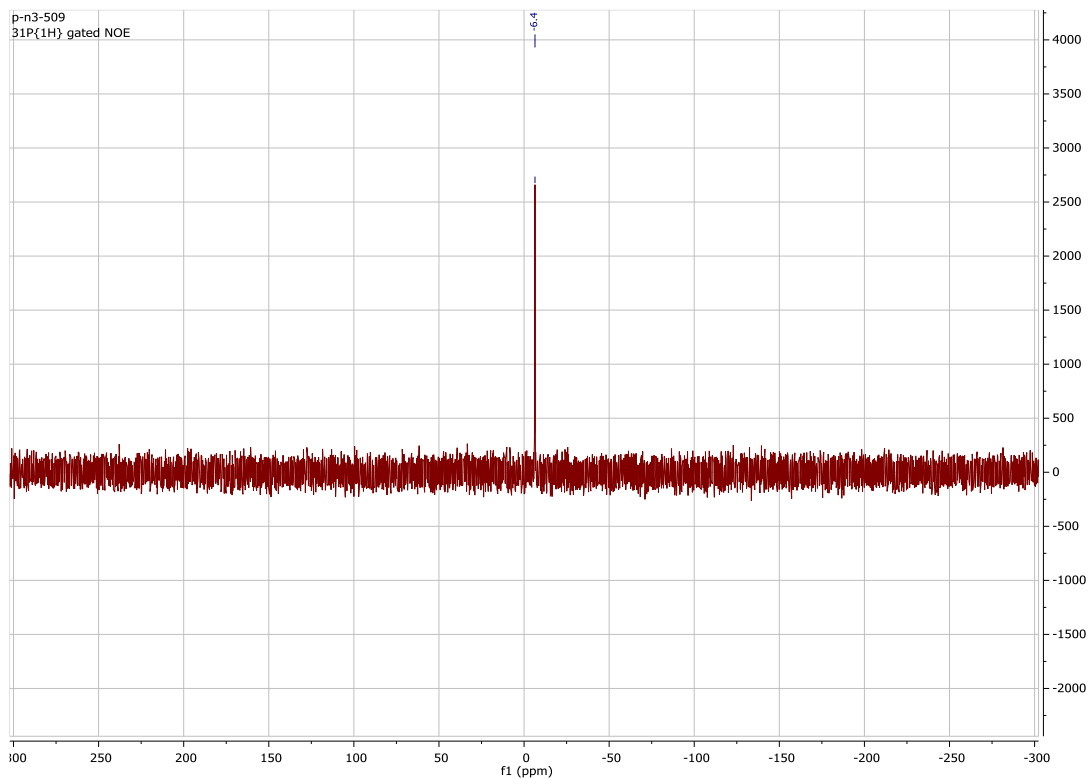


Figure S16. ^{31}P NMR spectrum of tris(1-phenyl-1H-1,2,3-triazol-4-yl)phosphine oxide (L^1) in CDCl_3 .

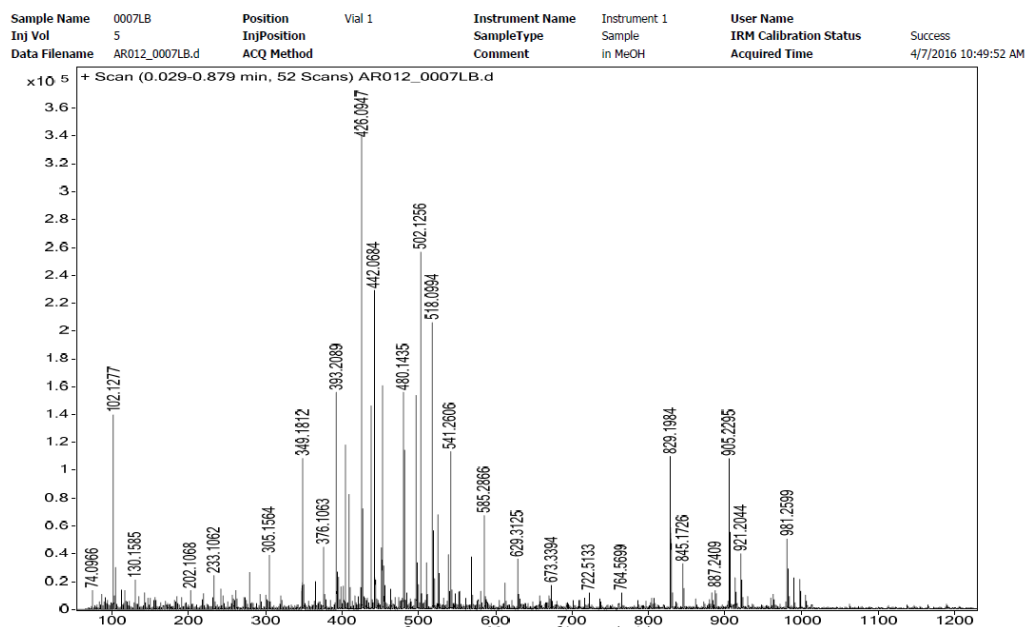


Figure S17. ESI+ mass spectrum of tris(1-phenyl-1H-1,2,3-triazol-4-yl)phosphine oxide (L^1)

6.2.2 Spectroscopic data of L²

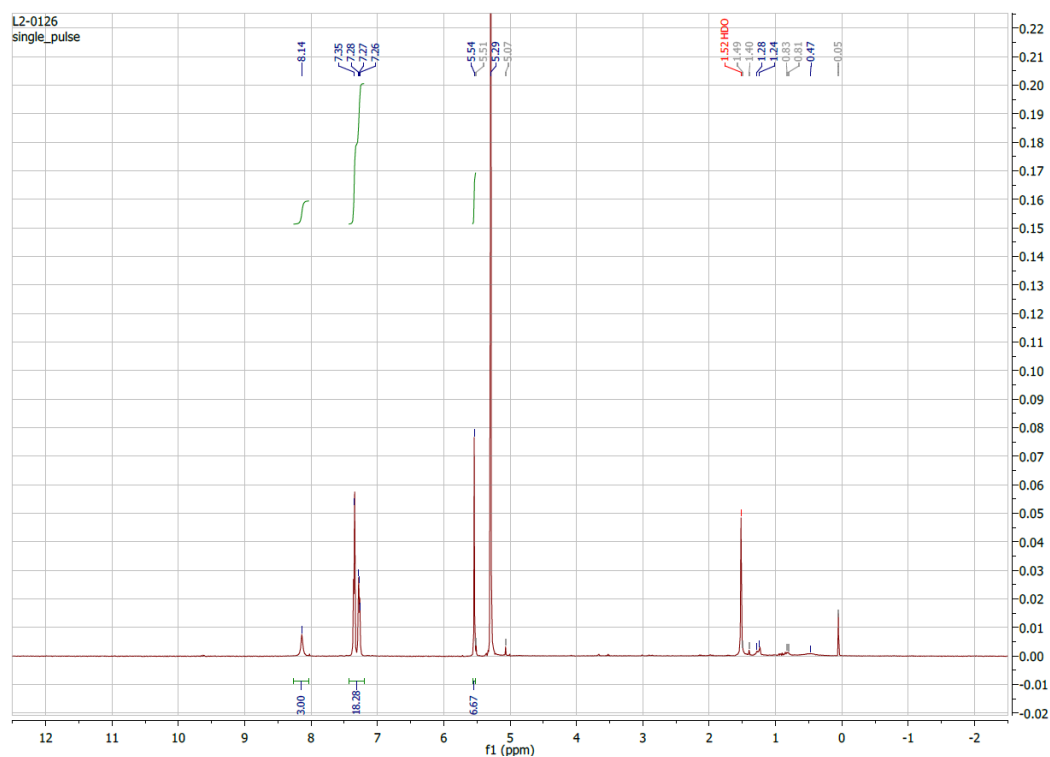


Figure S18. ^1H NMR spectrum of tris(1-benzyl-1H-1,2,3-triazol-4-yl)phosphine oxide (L^2) in CD_2Cl_2 .

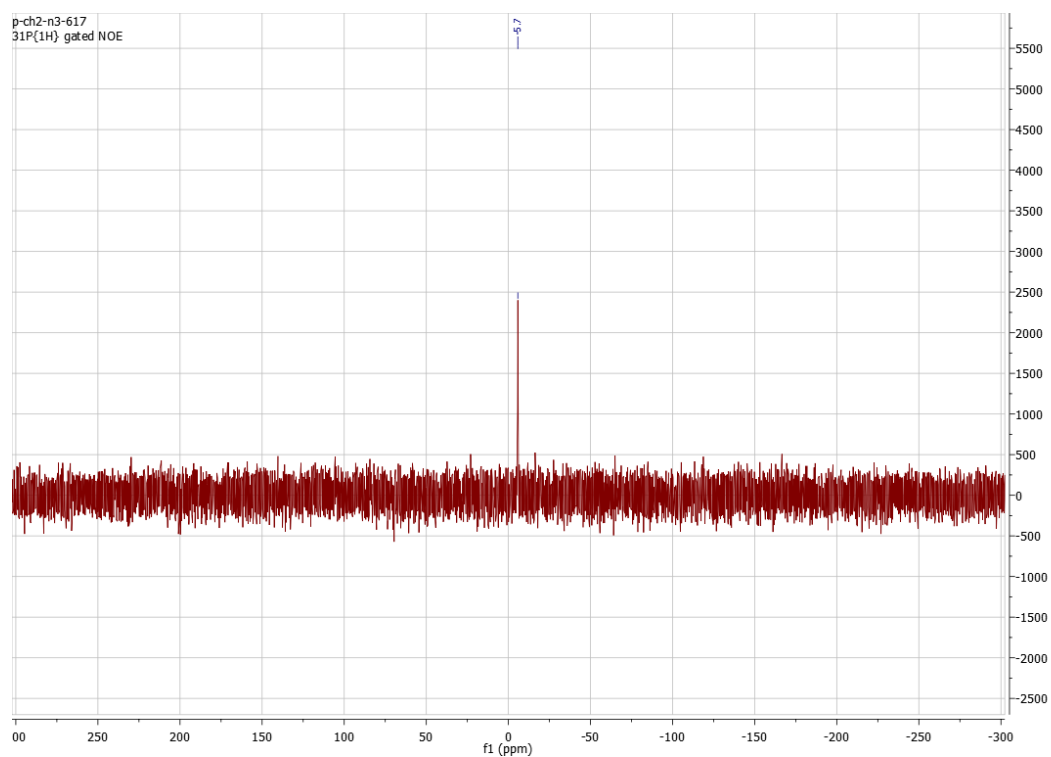


Figure S19. ^{31}P NMR spectrum of tris(1-benzyl-1H-1,2,3-triazol-4-yl)phosphine oxide (L^2) in CDCl_3 .

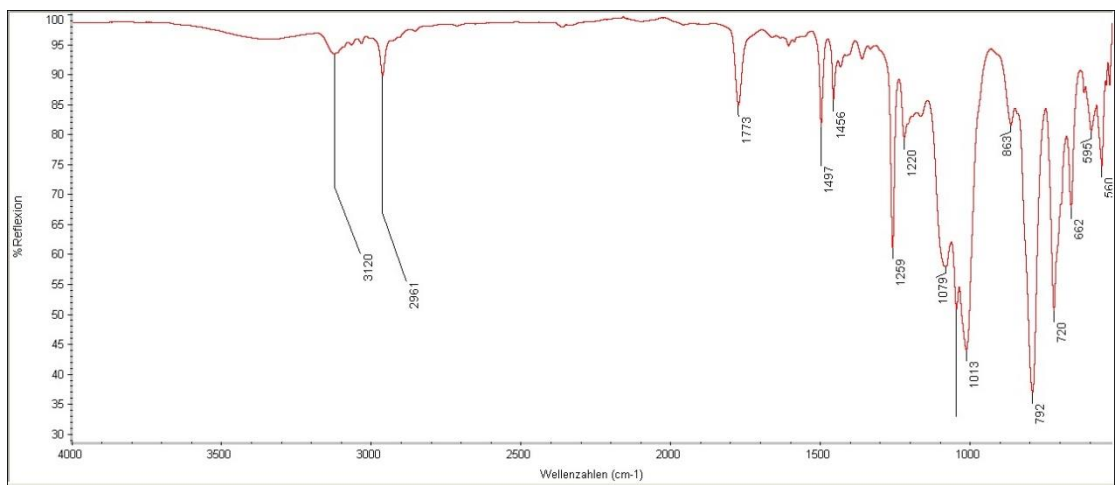


Figure S20. IR spectrum of tris(1-benzyl-1H-1,2,3-triazol-4-yl)phosphine oxide (L^2)

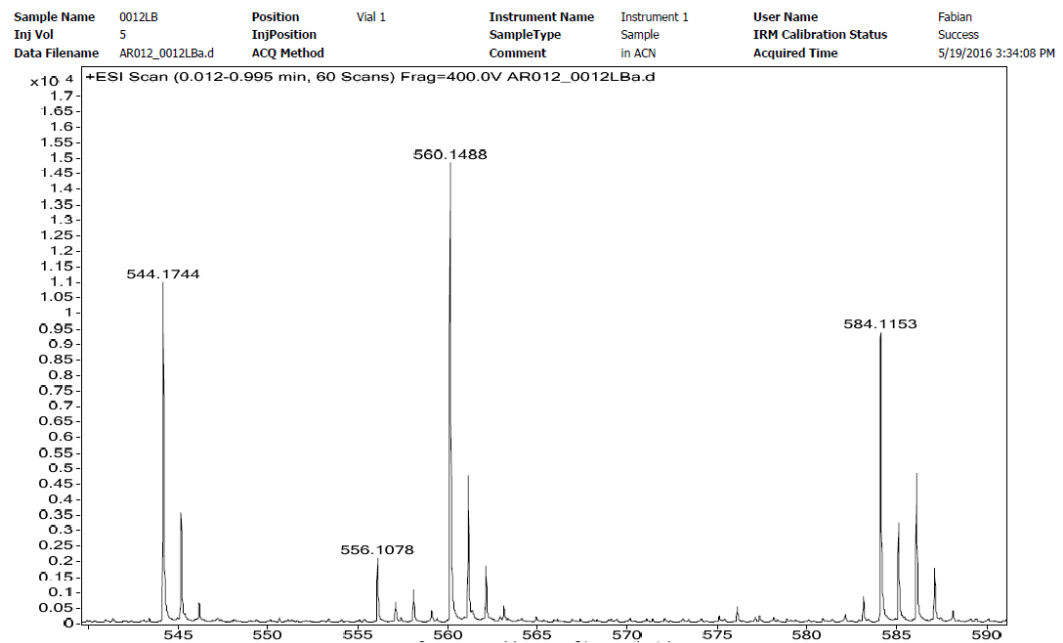


Figure S21. ESI+ mass spectrum of tris(1-benzyl-1H-1,2,3-triazol-4-yl)phosphine oxide (L^2).

6.2.4 Spectroscopic data of $[\text{Re}(\text{CO})_3\text{Br}(\kappa^2\text{N-L}^1)]$ (1)

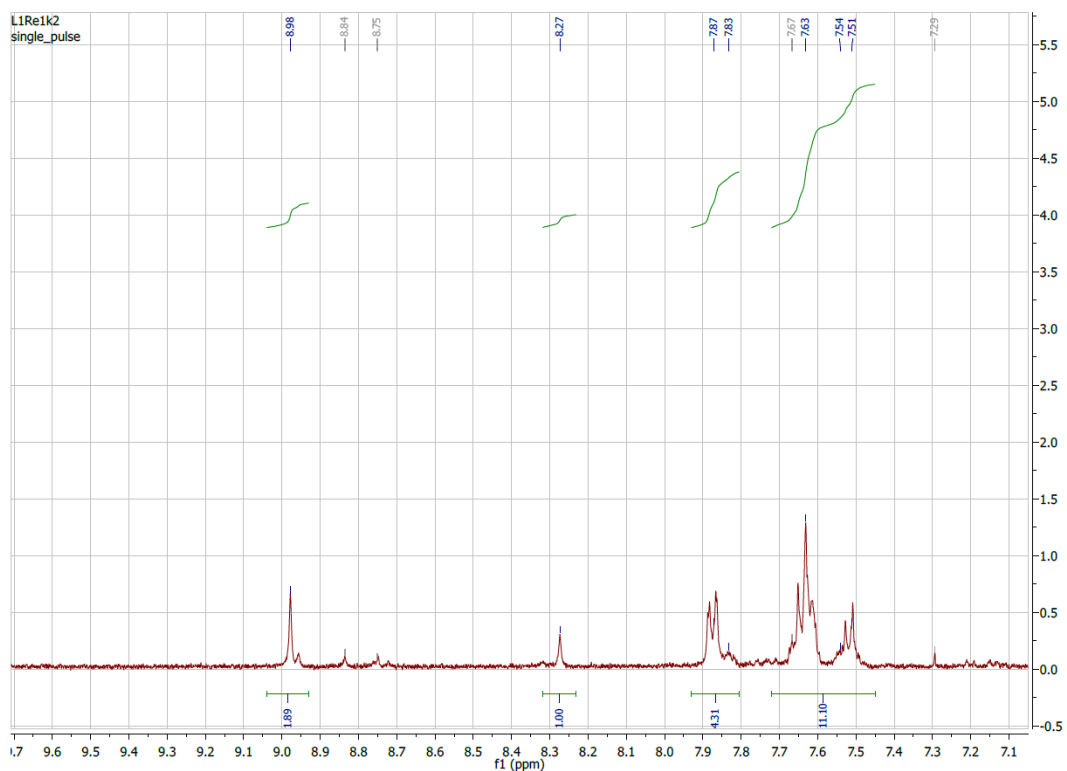


Figure S22. ^1H NMR spectrum of $[\text{Re}(\text{CO})_3\text{Br}(\kappa^2\text{N-L}^1)]$ (1) in CD_2Cl_2 .

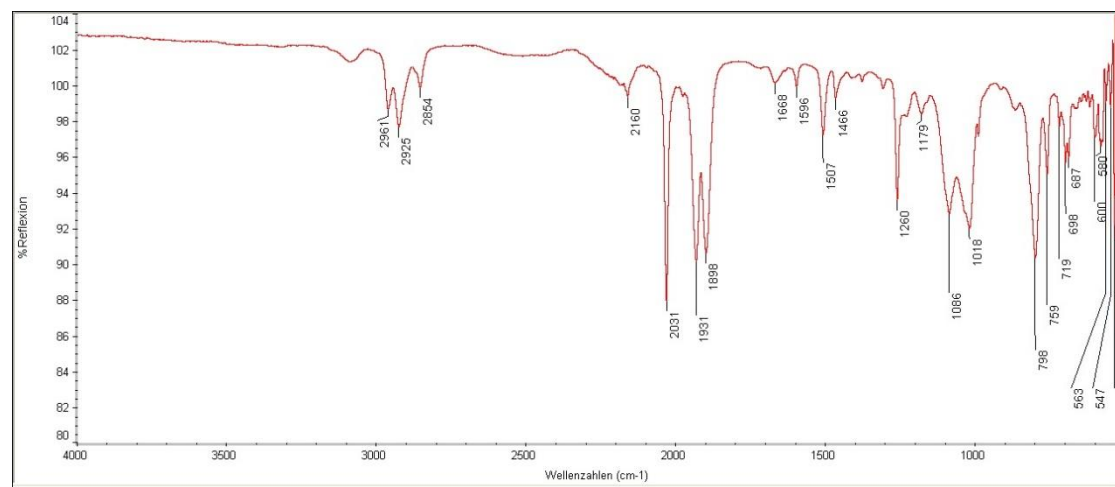


Figure S23. IR spectrum of $[\text{Re}(\text{CO})_3\text{Br}(\kappa^2\text{N-L}^1)]$ (1).

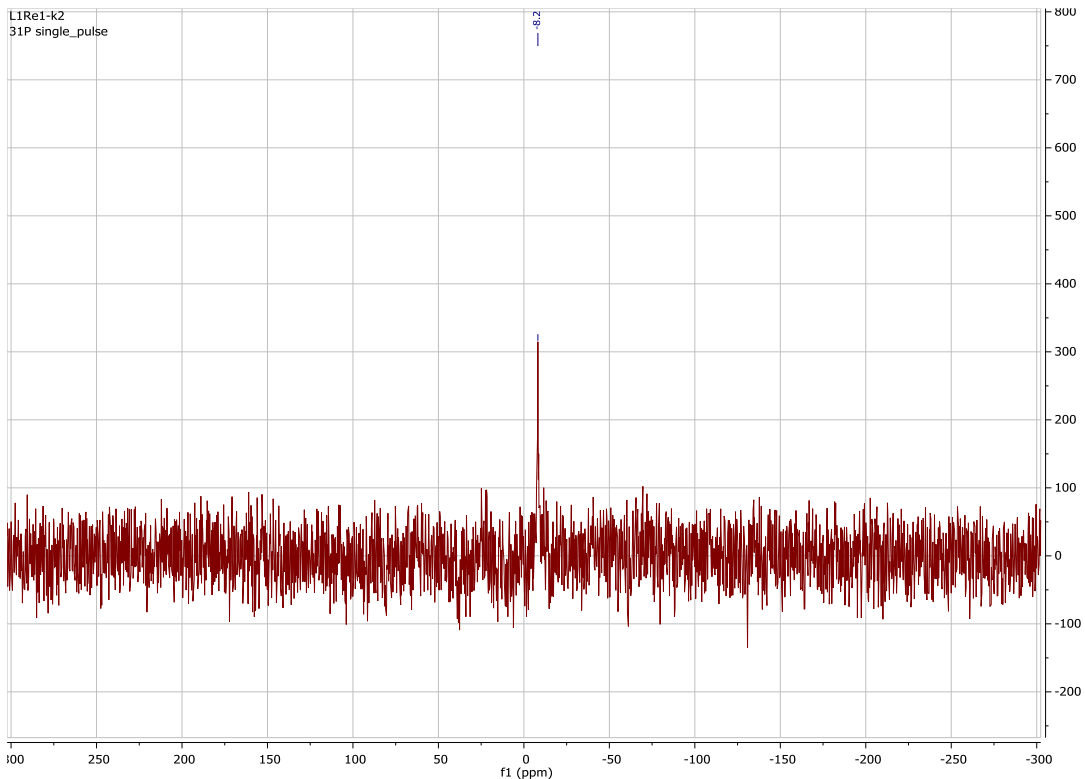


Figure S24. ^{31}P NMR spectrum of $[\text{Re}(\text{CO})_3\text{Br}(\kappa^2\text{N}-\text{L}^1)]$ (**1**) in CDCl_3 .

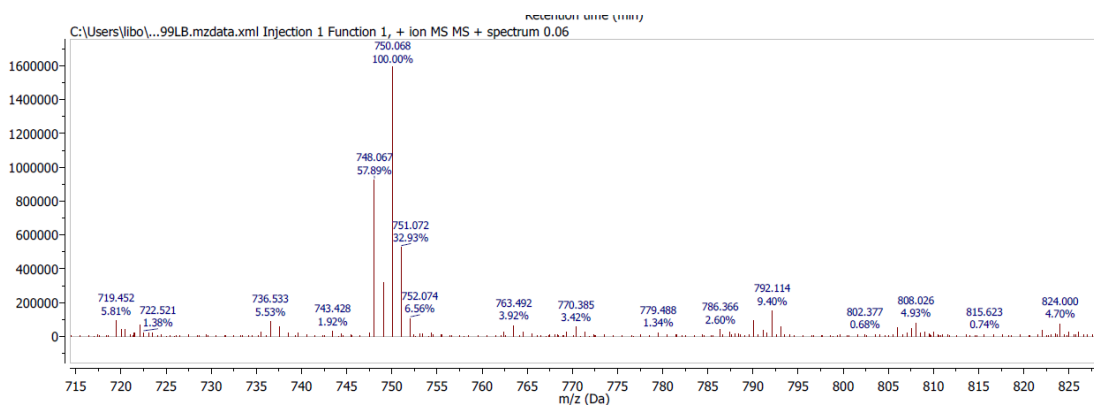


Figure S25. ESI+ mass spectrum spectrum of $[\text{Re}(\text{CO})_3\text{Br}(\kappa^2\text{N}-\text{L}^1)]$ (**1**).

6.2.5 Spectroscopic data of $[\text{Re}(\text{CO})_3(\kappa^3\text{N-L}^1)]$ (2)

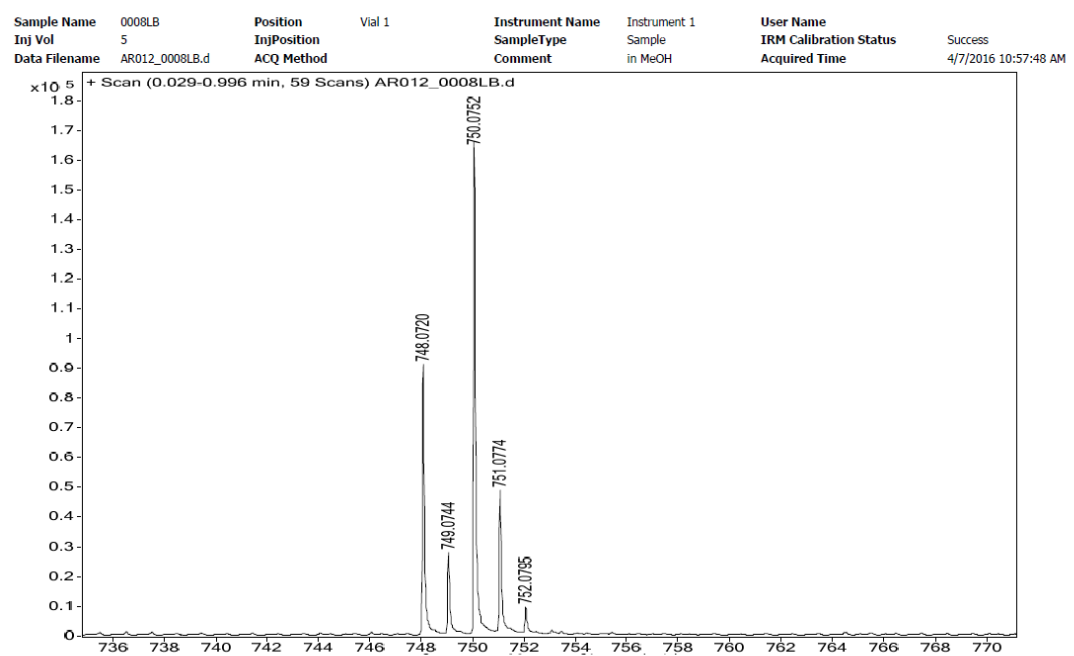


Figure S26. ESI+ mass spectrum of $[\text{Re}(\text{CO})_3(\kappa^3\text{N-L}^1)][\text{Re}_2(\text{CO})_6\text{Br}_2]$ (2).

6.2.5 Spectroscopic data of $[\text{Re}(\text{CO})_3\text{Br}(\kappa^2\text{N-L}^2)]$ and $[\text{Re}(\text{CO})_3\text{Cl}(\kappa^2\text{N-L}^2)]$ (3a and 3b)

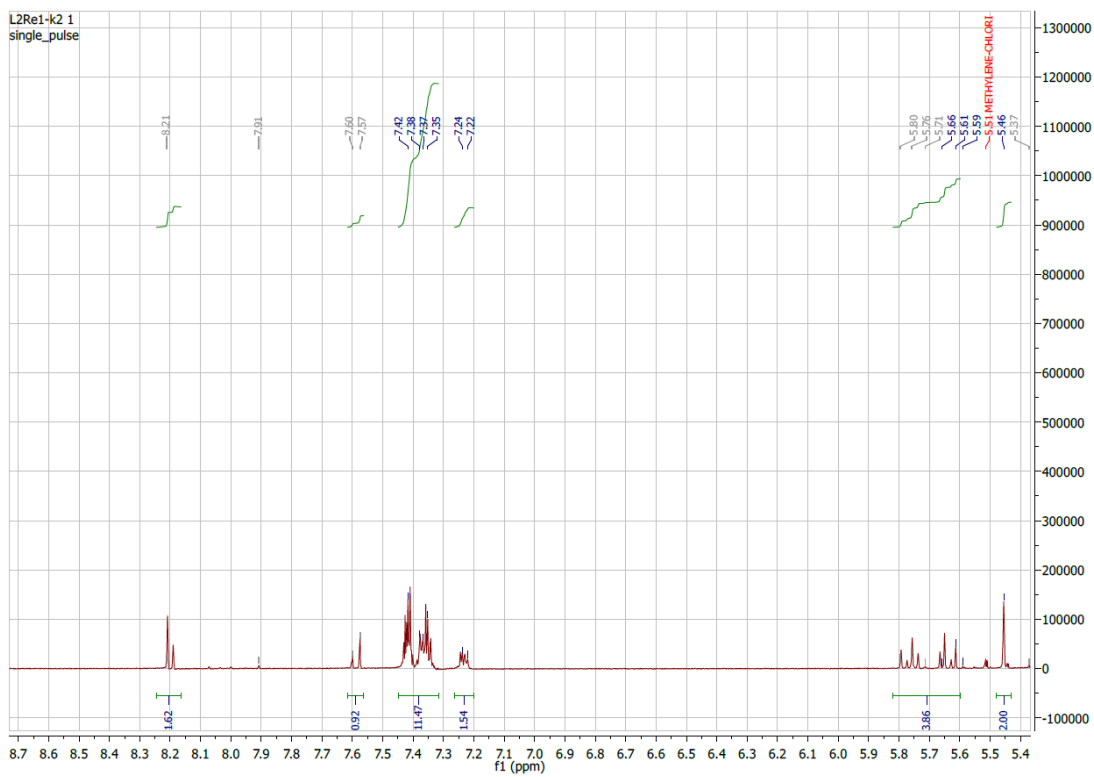


Figure S27. ^1H NMR spectrum of $[\text{Re}(\text{CO})_3\text{Br}(\kappa^2\text{N-L}^2)]$ and $[\text{Re}(\text{CO})_3\text{Cl}(\kappa^2\text{N-L}^2)]$ (3a and 3b) in CD_2Cl_2 .

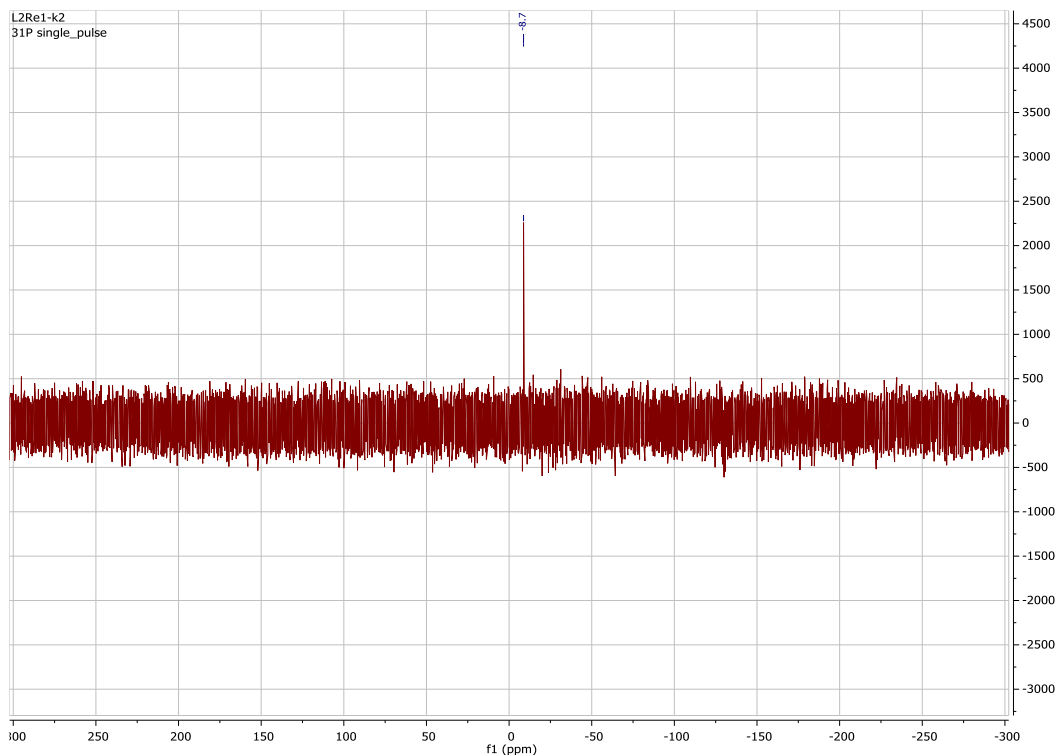


Figure S28. ^{31}P NMR spectrum of $[\text{Re}(\text{CO})_3\text{Br}(\kappa^2\text{N-L}^2)]$ and $[\text{Re}(\text{CO})_3\text{Cl}(\kappa^2\text{N-L}^2)]$ (3a and 3b) in CD_2Cl_2 .

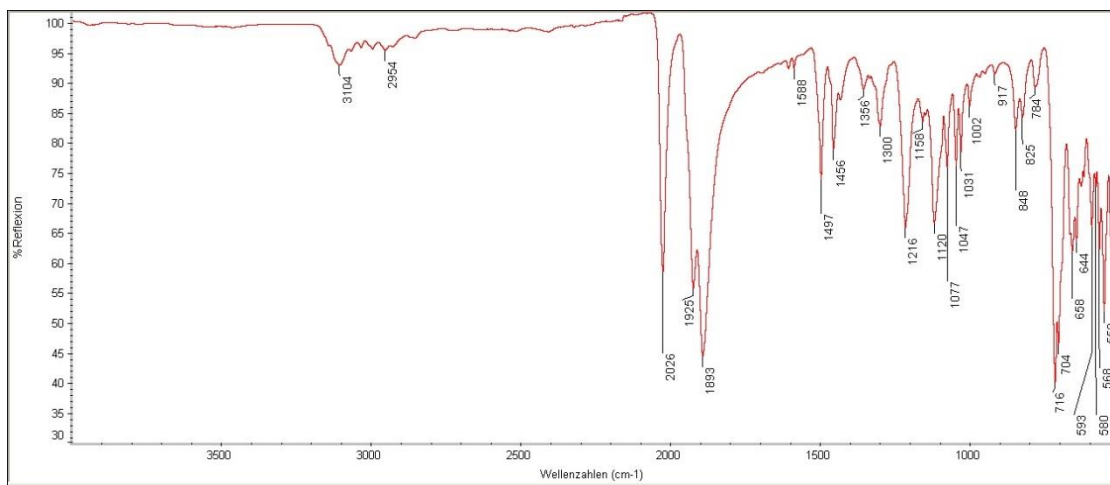


Figure S29. $[\text{Re}(\text{CO})_3\text{Br}(\kappa^2\text{N-L}^2)]$ and $[\text{Re}(\text{CO})_3\text{Cl}(\kappa^2\text{N-L}^2)]$ (**3a** and **3b**).

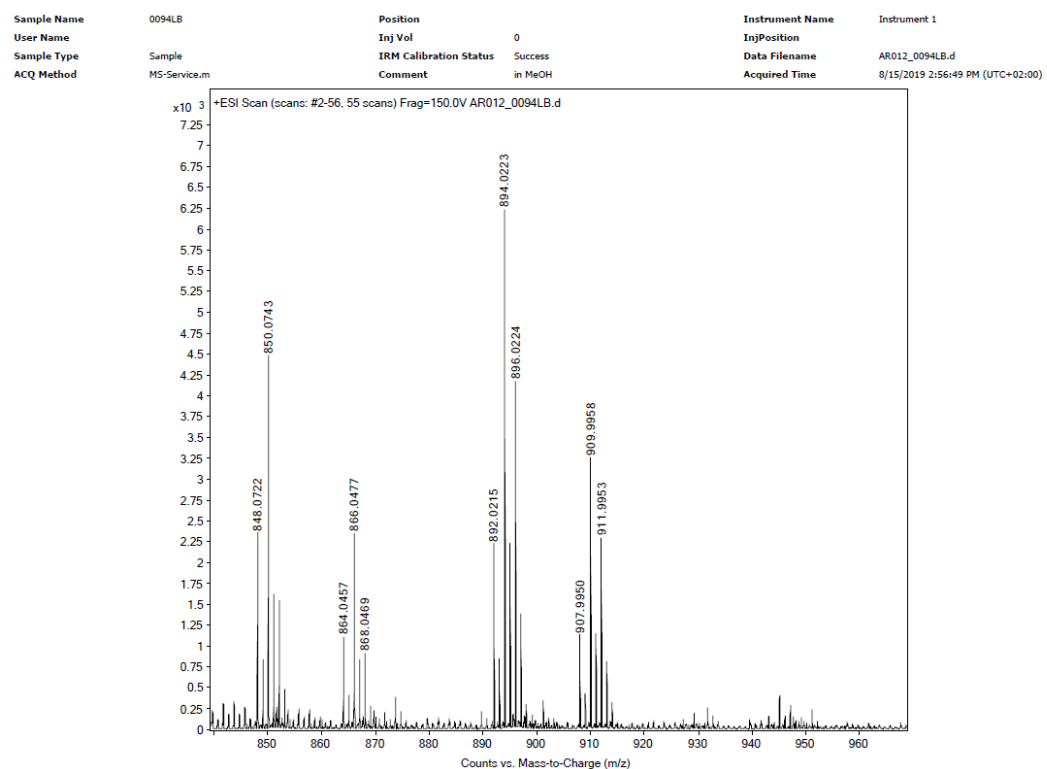


Figure S30. ESI+ mass spectrum of $[\text{Re}(\text{CO})_3\text{Br}(\kappa^2\text{N-L}^2)]$ (**3a**) and $[\text{Re}(\text{CO})_3\text{Cl}(\kappa^2\text{N-L}^2)]$ (**3b**).

6.2.6 Spectroscopic data of $[\text{Re}(\text{CO})_3(\kappa^3\text{N-L}^2)]\text{Br}$ (4)

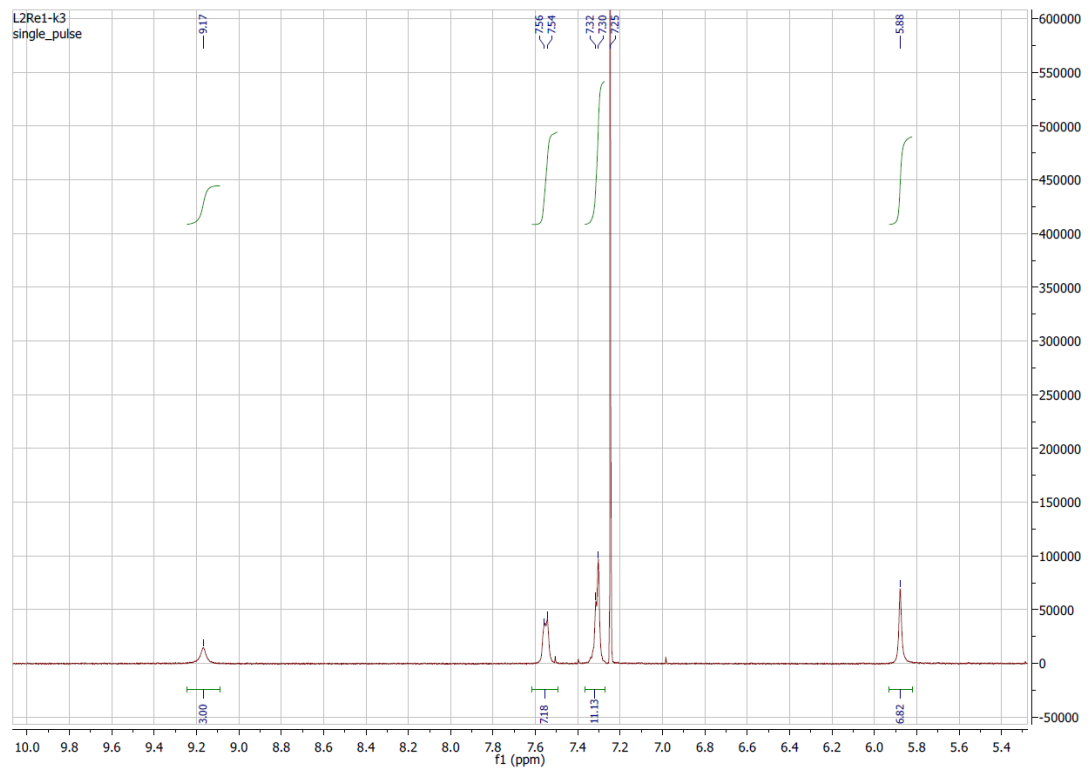


Figure S31. ^1H NMR spectrum of $[\text{Re}(\text{CO})_3(\kappa^3\text{N-L}^2)]\text{Br}$ (4) in CDCl_3 .

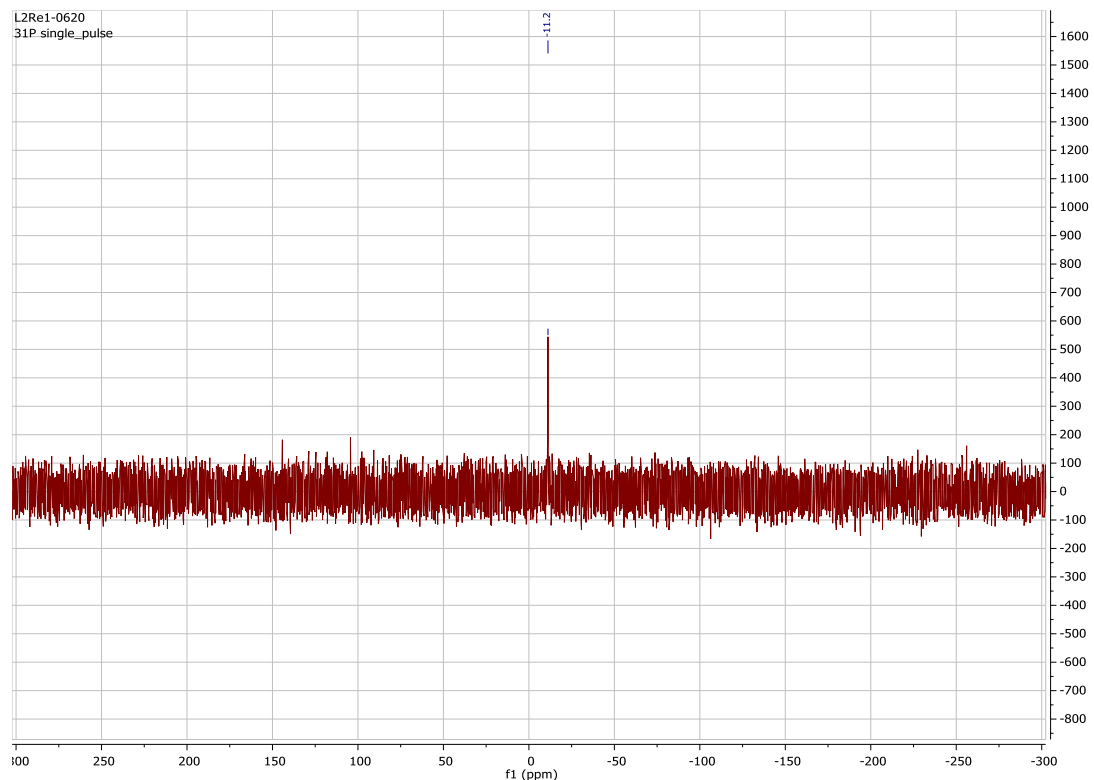


Figure S32. ^{31}P NMR spectrum of $[\text{Re}(\text{CO})_3(\kappa^3\text{N-L}^2)]\text{Br}$ in CD_2Cl_2 (4).

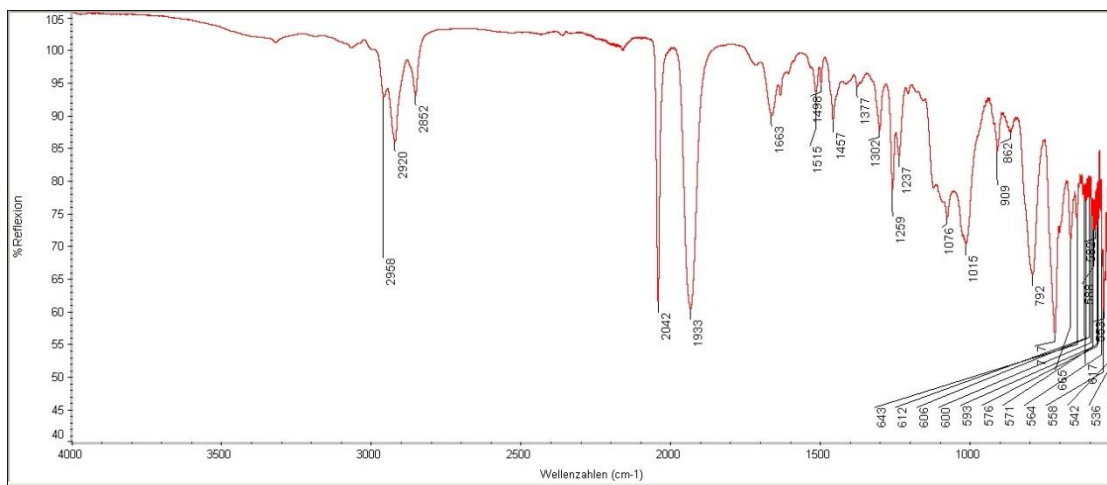


Figure S33. IR spectrum of $[\text{Re}(\text{CO})_3(\kappa^3\text{N}-\text{L}^2)]\text{Br}$ (**4**).

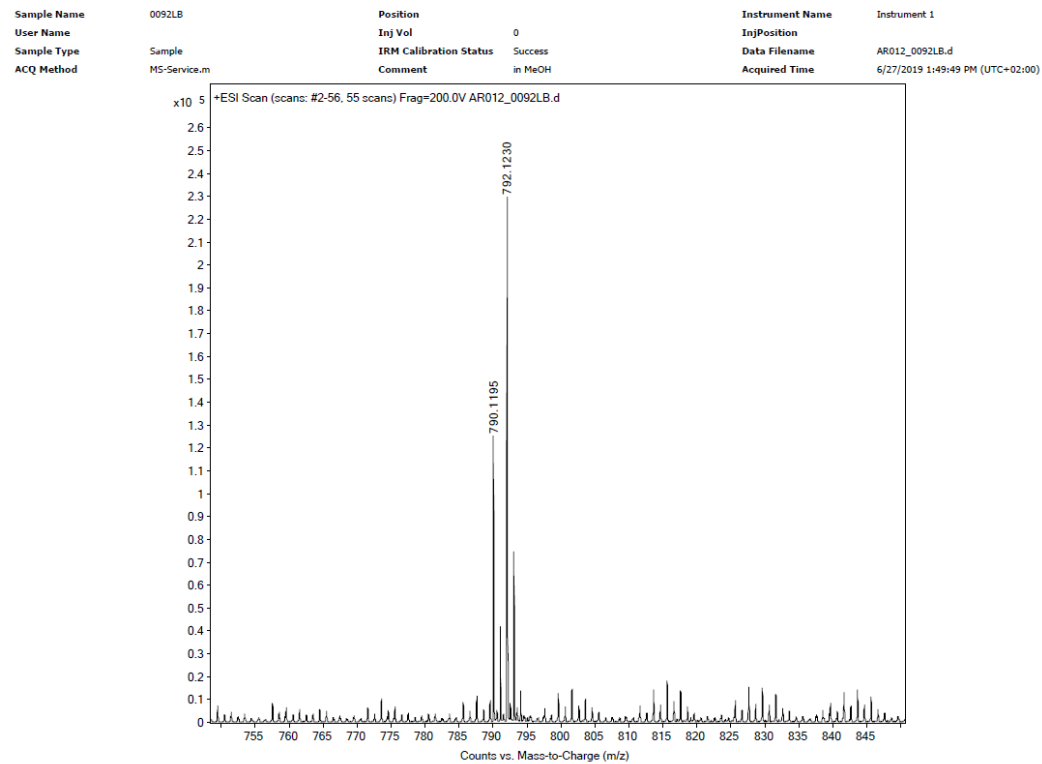


Figure S34. ESI⁺ mass spectrum of $[\text{Re}(\text{CO})_3(\kappa^3\text{N}-\text{L}^2)]\text{Br}$ (**4**).

6.2.7 Spectroscopic data of $[\{\text{Re}(\text{CO})_3(\mu\text{-1}\kappa^3\text{N}, 2\kappa^p\text{-L}2')\}2\{\text{Re}(\text{CO})_2\text{Br}_2\}]\text{Br}$ (7)

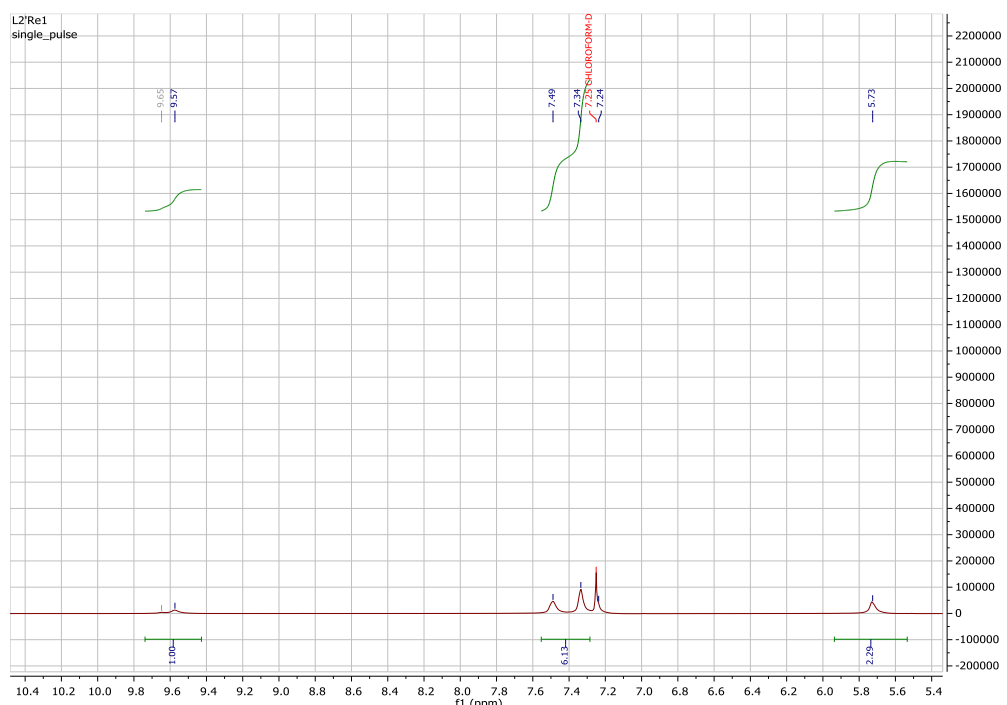


Figure S35. ^1H NMR spectrum of $[\{\text{Re}(\text{CO})_3(\mu-\text{l}\kappa^3\text{N}, \text{2}\kappa^{\text{P}}\text{-L}^2)\}_2\{\text{Re}(\text{CO})_2\text{Br}_2\}]\text{Br}$ (7) in CD_2Cl_2 .

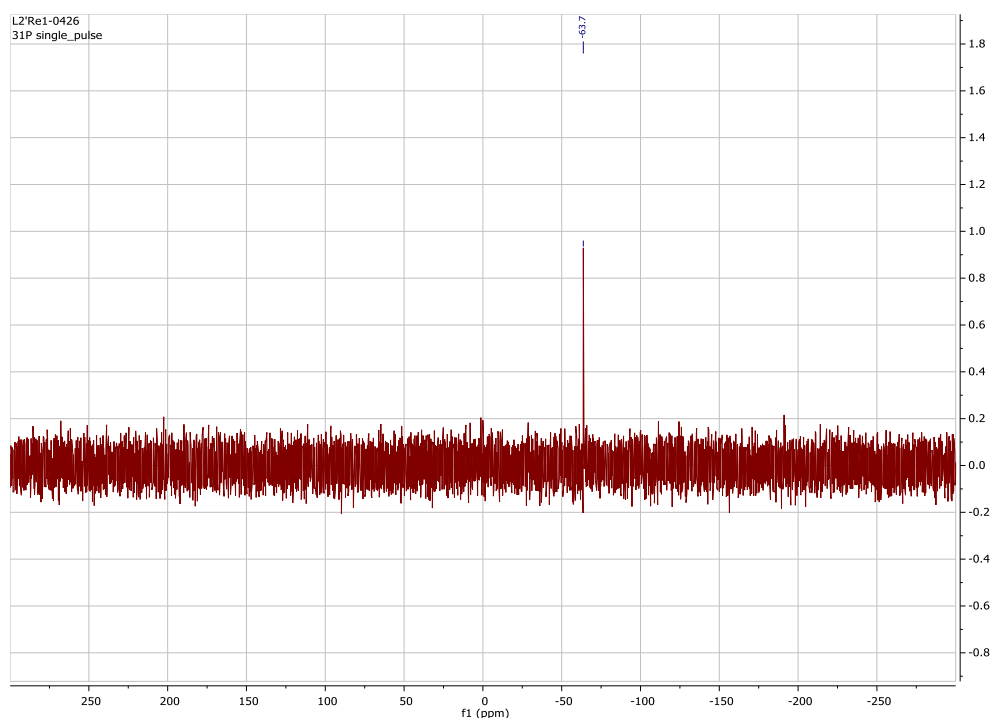


Figure S36. ^{31}P NMR spectrum of $[\{\text{Re}(\text{CO})_3(\mu\text{-1}\kappa^3\text{N}, 2\kappa^{\text{p}}\text{-L}^2)\}_2\{\text{Re}(\text{CO})_2\text{Br}_2\}]\text{Br}$ (7) in CD_2Cl_2 .

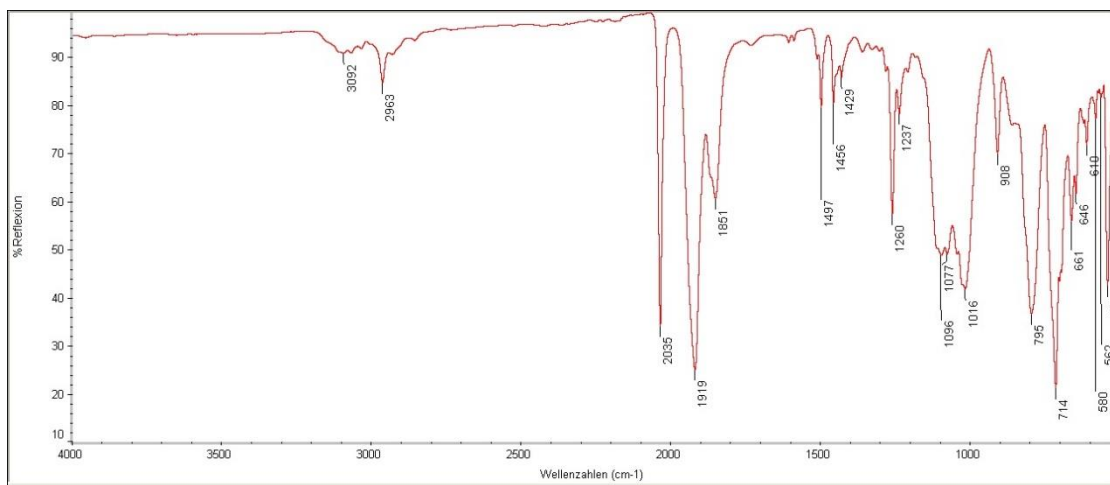


Figure S37. IR spectrum of $[\{\text{Re}(\text{CO})_3(\mu-\text{l}\kappa^3\text{N}, 2\kappa^0\text{-L}^2)\}_2\{\text{Re}(\text{CO})_2\text{Br}_2\}]\text{Br}$ (7).

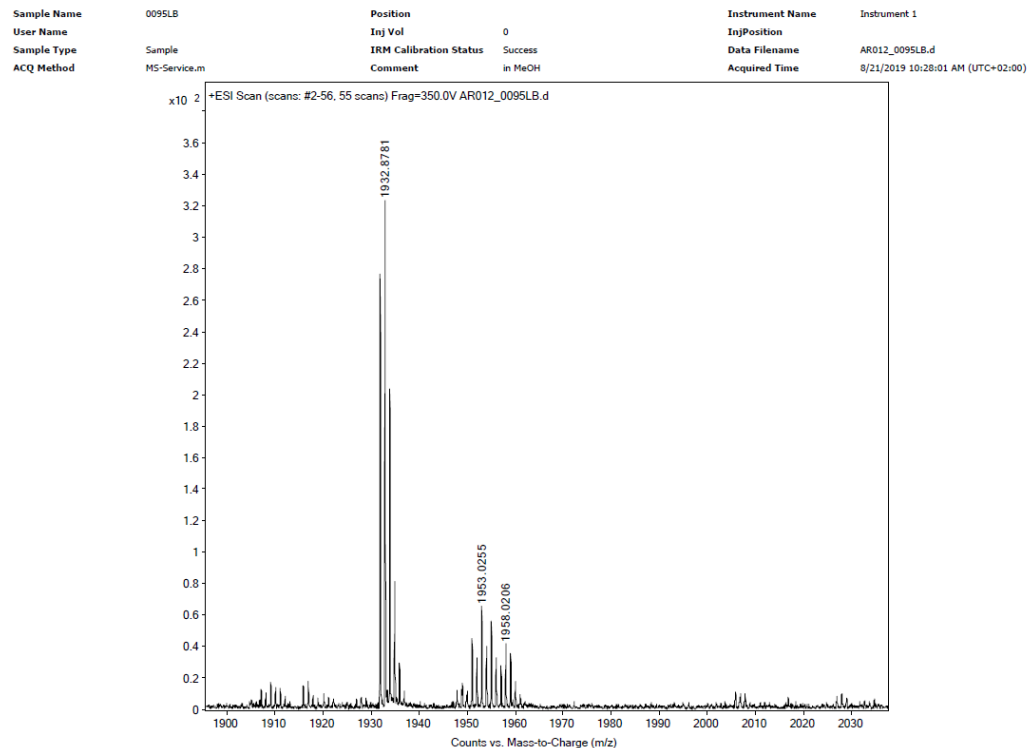


Figure S38. ESI+ mass spectrum of $[\{\text{Re}(\text{CO})_3(\mu-\text{l}\kappa^3\text{N}, 2\kappa^0\text{-L}^2)\}_2\{\text{Re}(\text{CO})_2\text{Br}_2\}]\text{Br}$ (7).

6.2.8 Spectroscopic data of $(\text{NBu}_4)[\text{Cl}_3(\text{O})\text{Re}\{\text{O}_2\text{P}^{(1,2,3}\text{Tz}^{1-\text{Ph})_3\}\text{Re}(\text{O})\text{Cl}_2]$ (8)

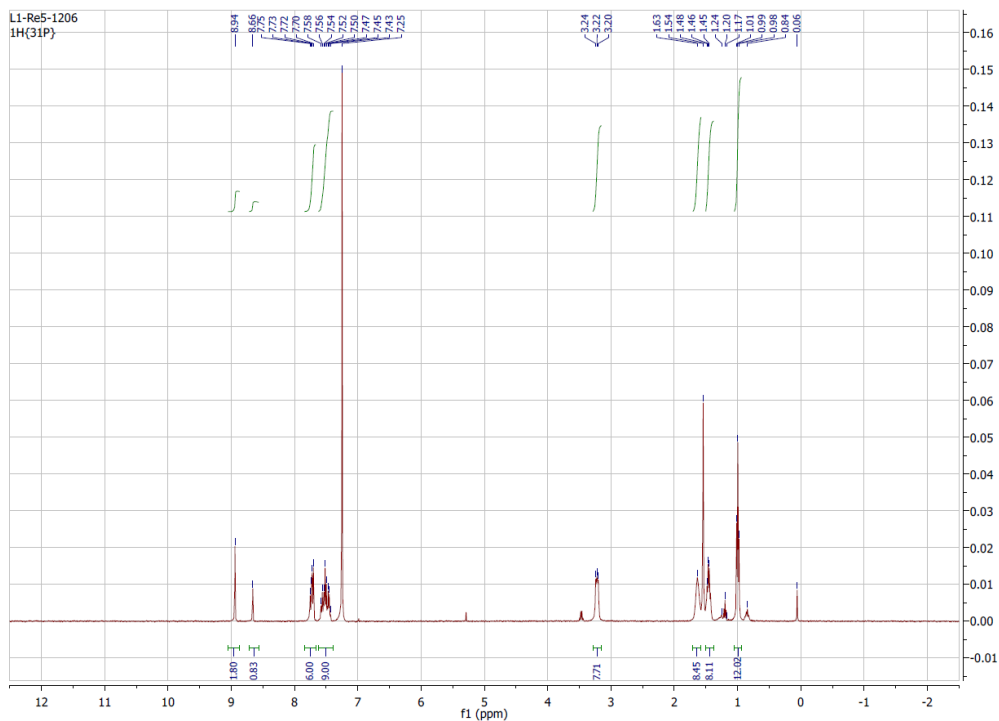


Figure S39. ^1H NMR spectrum of $(\text{NBu}_4)[\text{Cl}_3(\text{O})\text{Re}\{\text{O}_2\text{P}^{(1,2,3}\text{Tz}^{1-\text{Ph})_3\}\text{Re}(\text{O})\text{Cl}_2]$ (8) in CDCl_3 .

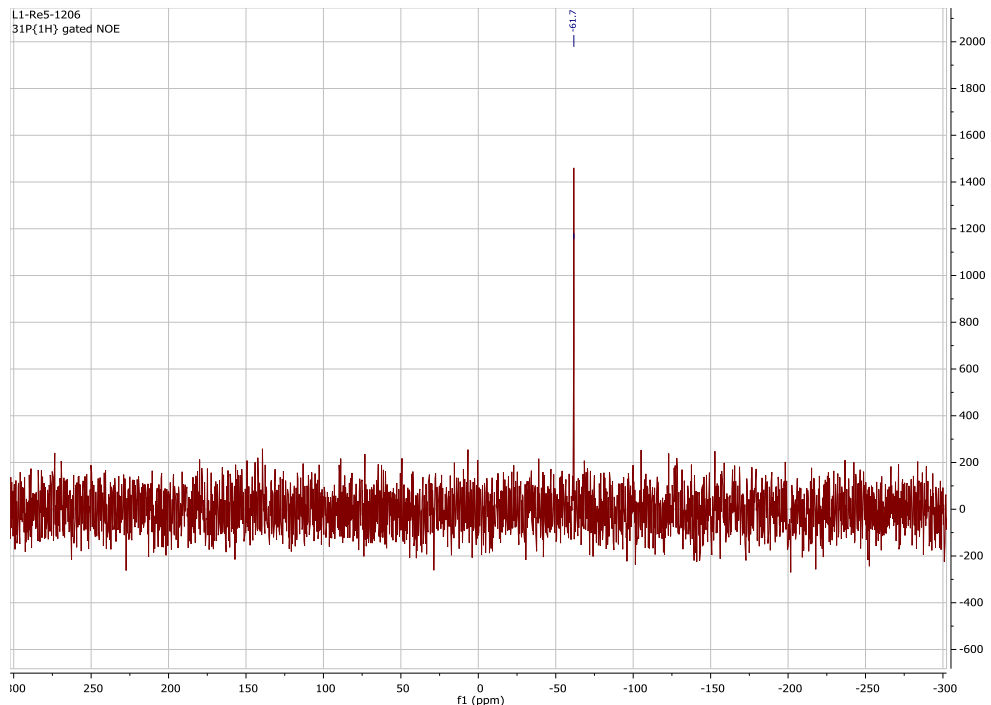


Figure S40. ^{31}P NMR spectrum of $(\text{NBu}_4)[\text{Cl}_3(\text{O})\text{Re}\{\text{O}_2\text{P}^{(1,2,3}\text{Tz}^{1-\text{Ph})_3\}\text{Re}(\text{O})\text{Cl}_2]$ (8) in CDCl_3 .

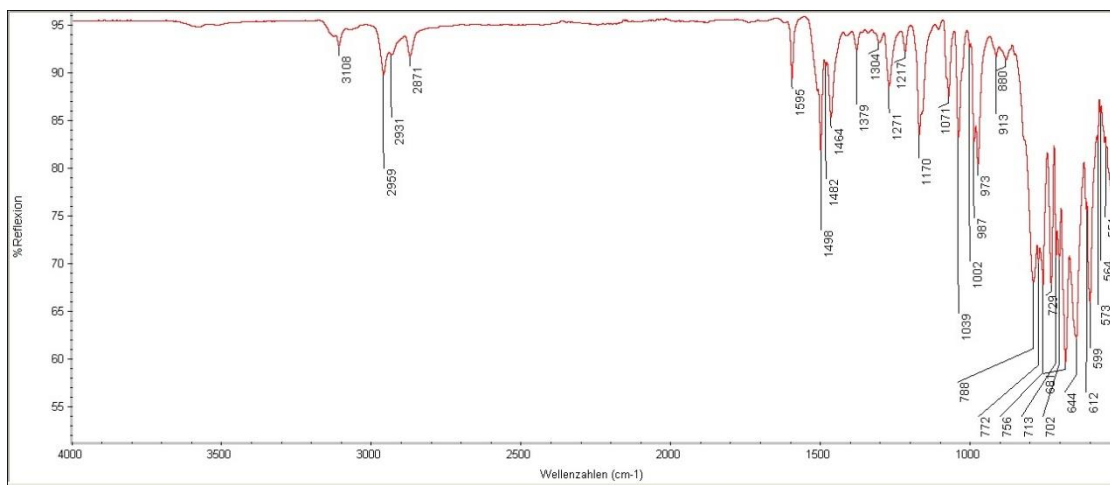


Figure S41. IR spectrum of (NBu₄)[Cl₃(O)Re{O₂P(^{1,2,3}Tz^{1-Ph})₃}Re(O)Cl₂] (**8**).

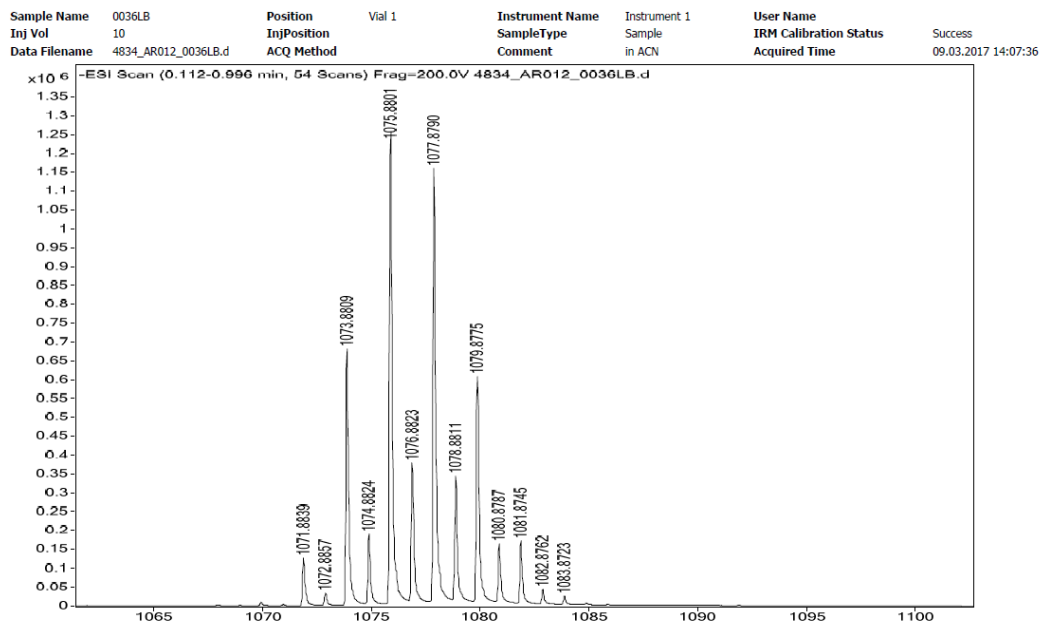


Figure S42. ESI- mass spectrum of (NBu₄)[Cl₃(O)Re{O₂P(^{1,2,3}Tz^{1-Ph})₃}Re(O)Cl₂] (**8**).

6.2.9 Spectroscopic data of (NBu_4) $[\text{ReOCl}_3\{\text{O}_2\text{P}(\text{Ph})_2\}_2]$ (9)

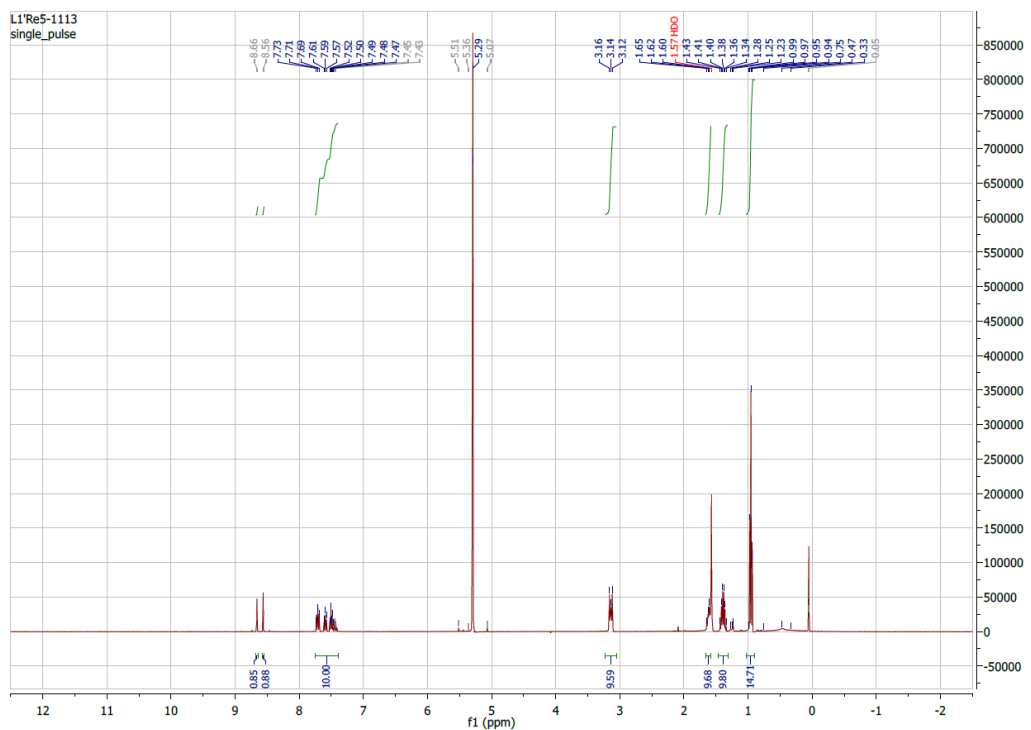


Figure S43. ^1H NMR spectrum of (NBu_4) $[\text{ReOCl}_3\{\text{O}_2\text{P}(\text{Ph})_2\}_2]$ (9) in CDCl_3 .

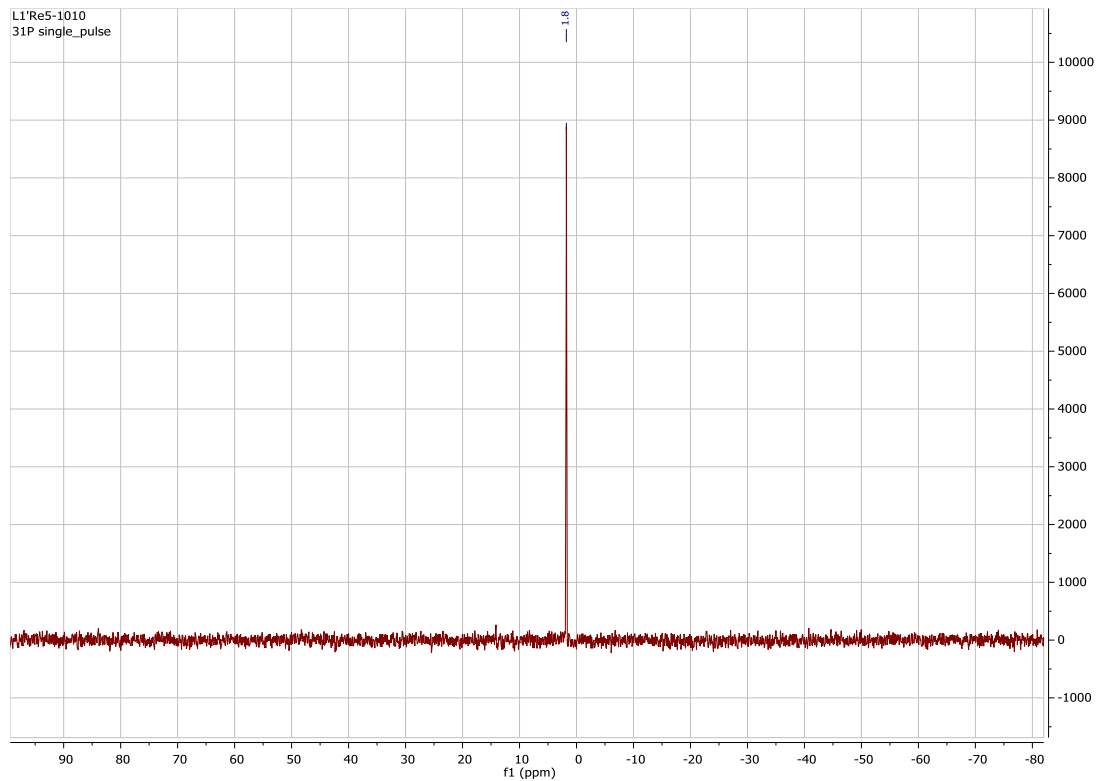


Figure S44. ^{31}P NMR spectrum of (NBu_4) $[\text{ReOCl}_3\{\text{O}_2\text{P}(\text{Ph})_2\}_2]$ (9) in CDCl_3 .

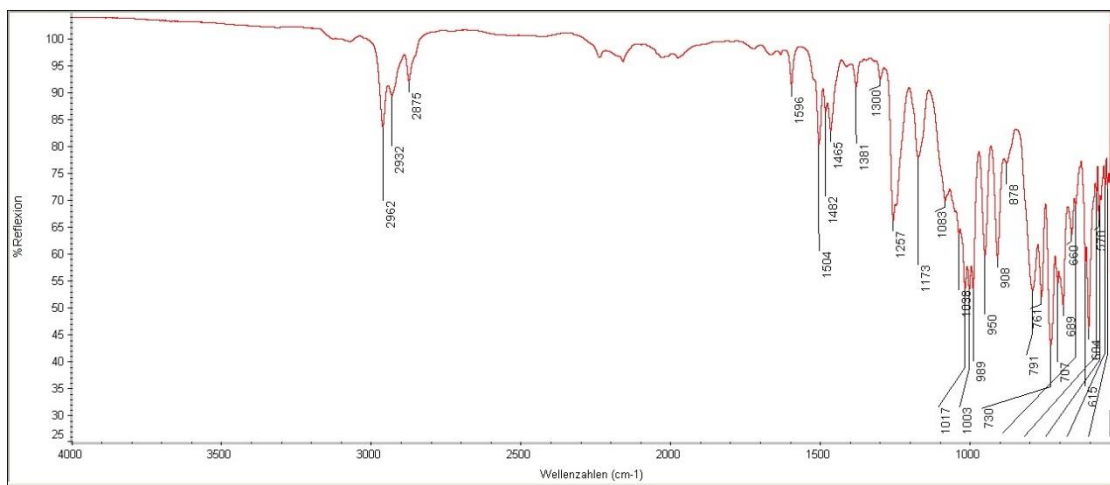


Figure S45. IR spectrum of $(\text{NBu}_4)[\text{ReOCl}_3\{\text{O}_2\text{P}(1,2,3\text{-Tz}^{1-\text{Ph}})_2\}]$ (**9**).

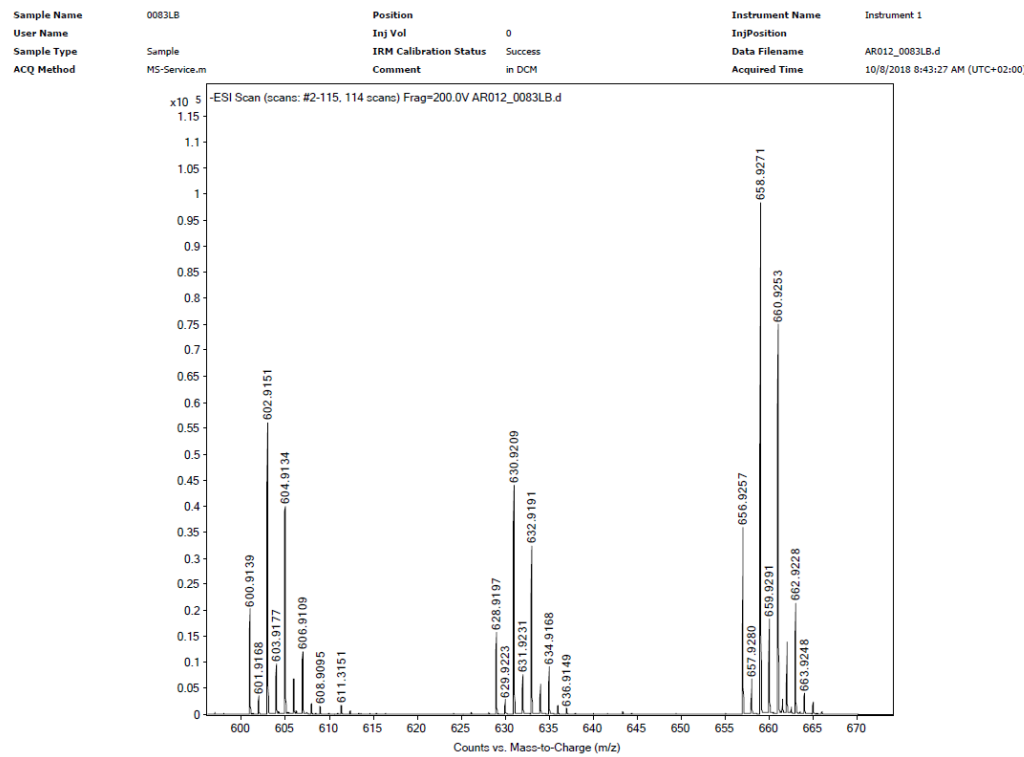


Figure S46. ESI- mass spectrum of $(\text{NBu}_4)[\text{ReOCl}_3\{\text{O}_2\text{P}(1,2,3\text{-Tz}^{1-\text{Ph}})_2\}]$ (**9**).

6.2.10 Spectroscopic data of $(\text{NBu}_4)[\text{Cl}_3(\text{O})\text{Re}\{\text{O}_2\text{P}^{(1,2,3)\text{Tz}^{\text{1-benz}}}\}_3\}\text{Re}(\text{O})\text{Cl}_2$ (10)

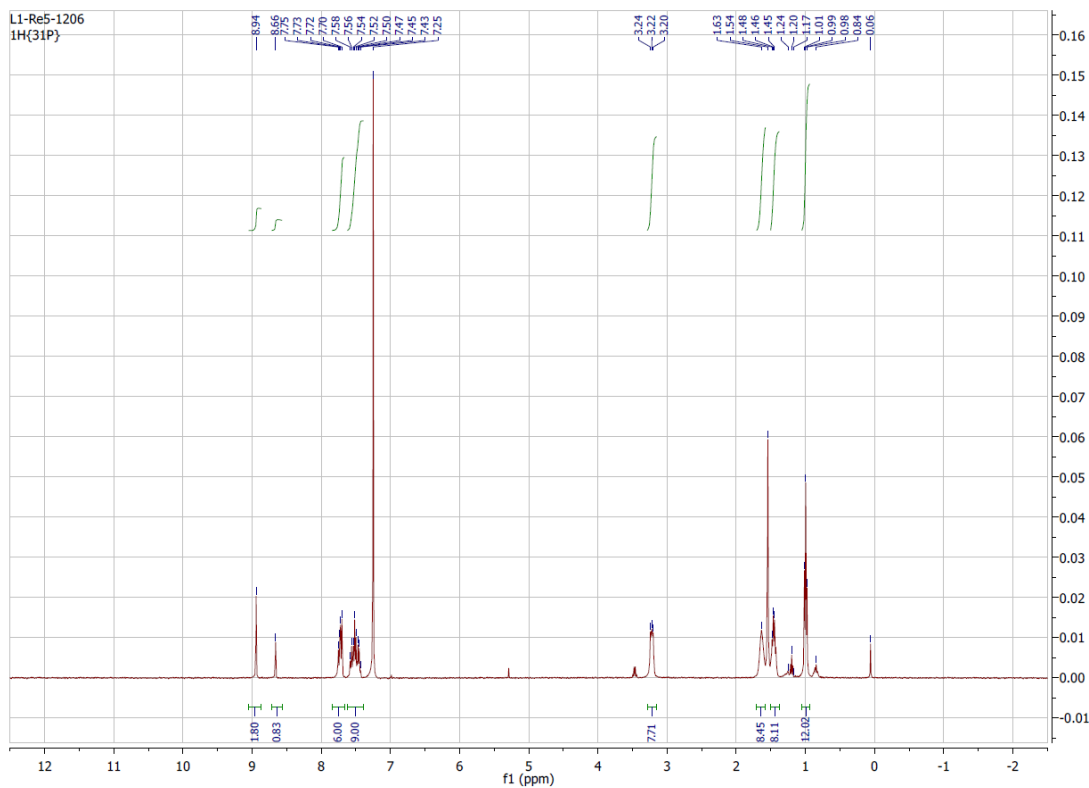


Figure S47. ^1H NMR spectrum of $(\text{NBu}_4)[\text{Cl}_3(\text{O})\text{Re}\{\text{O}_2\text{P}^{(1,2,3)\text{Tz}^{\text{1-benz}}}\}_3\}\text{Re}(\text{O})\text{Cl}_2$ (10) in CDCl_3 .

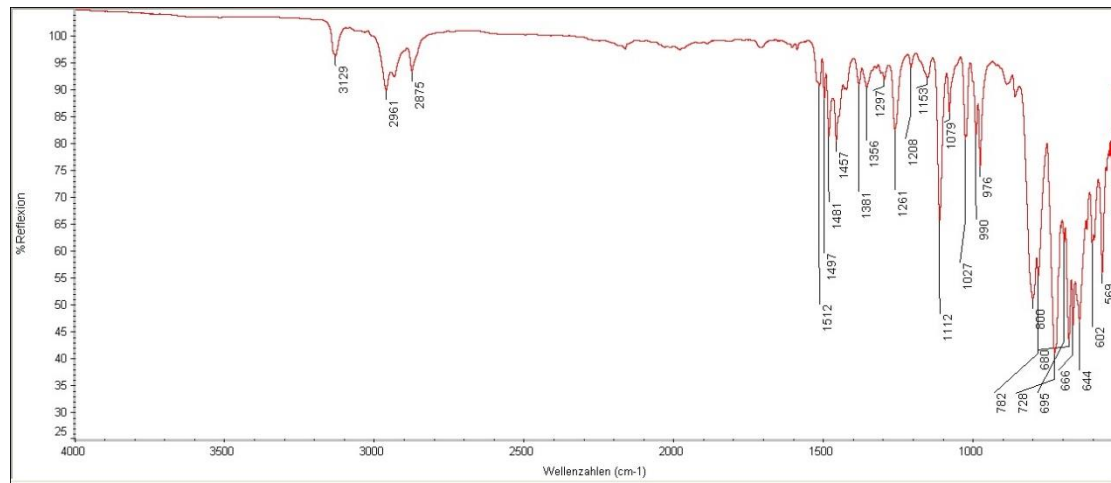


Figure S48. IR spectrum of $(\text{NBu}_4)[\text{Cl}_3(\text{O})\text{Re}\{\text{O}_2\text{P}^{(1,2,3)\text{Tz}^{\text{1-benz}}}\}_3\}\text{Re}(\text{O})\text{Cl}_2$ (10) in CDCl_3 .

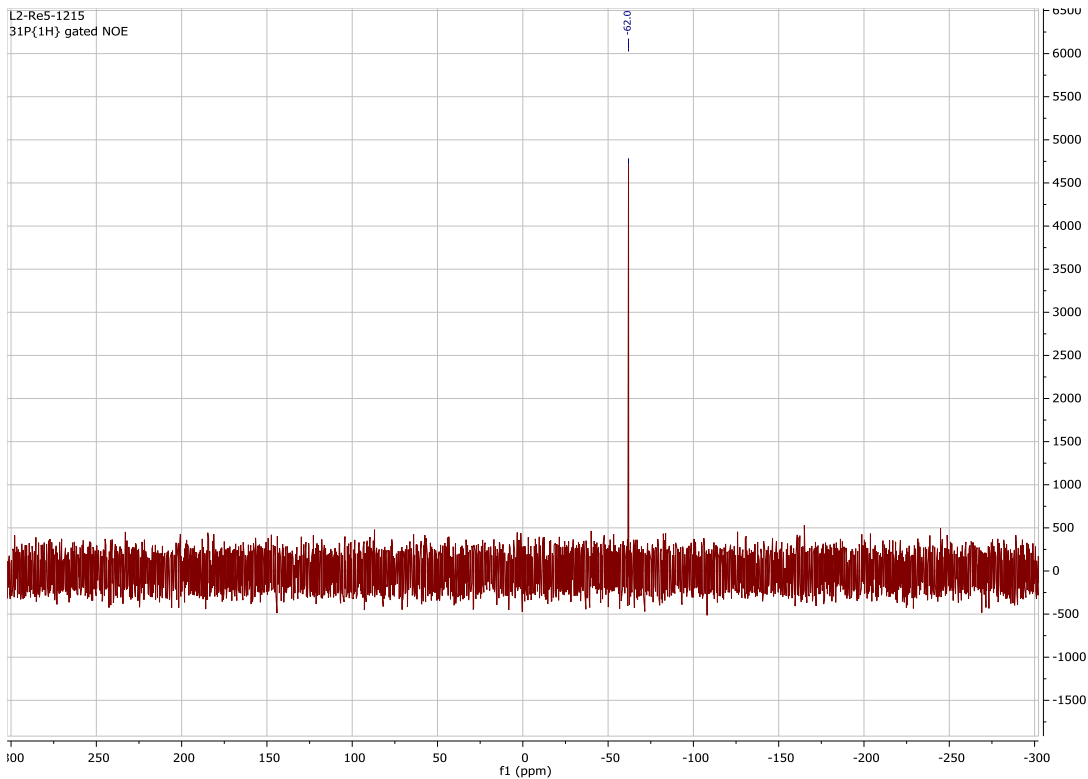


Figure S49. ^{31}P NMR spectrum of $(\text{NBu}_4)[\text{Cl}_3(\text{O})\text{Re}\{\text{O}_2\text{P}(^{1,2,3}\text{Tz}^{1-\text{benz}})_3\}\text{Re}(\text{O})\text{Cl}_2]$ (**10**) in CDCl_3 .

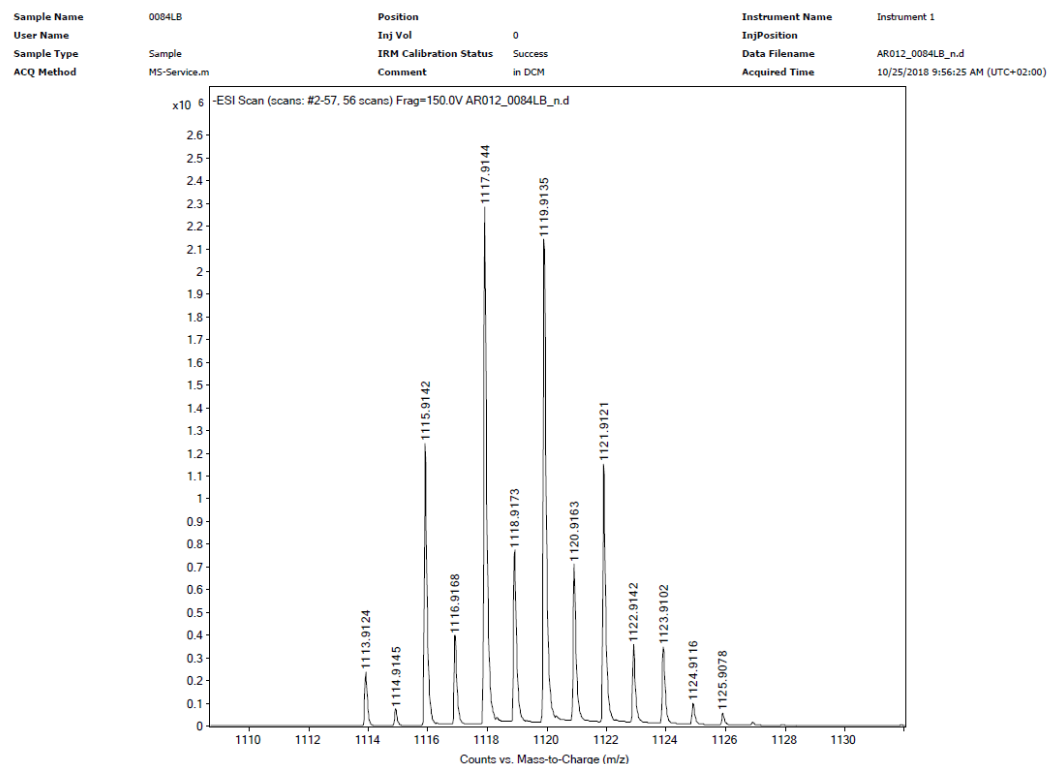


Figure S50. ESI- mass spectrum of $(\text{NBu}_4)[\text{Cl}_3(\text{O})\text{Re}\{\text{O}_2\text{P}(^{1,2,3}\text{Tz}^{1-\text{benz}})_3\}\text{Re}(\text{O})\text{Cl}_2]$ (**10**).

6.2.11 Spectroscopic data of $(\text{NBu}_4)[\text{Cl}_3(\text{O})\text{Re}\{\text{O}_2\text{P}^{(1,2,3}\text{Tz}^{1-\text{benz})_2\}\text{Re}(\text{O})\text{Cl}_3]$ (11)

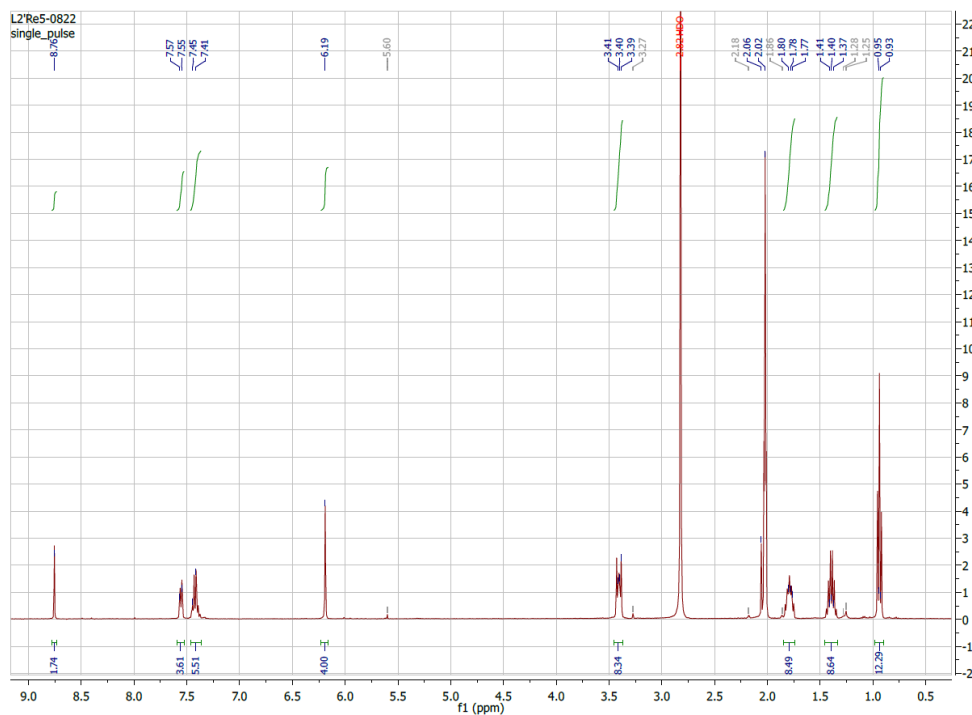


Figure S51. ^1H NMR spectrum of $(\text{NBu}_4)[\text{Cl}_3(\text{O})\text{Re}\{\text{O}_2\text{P}^{(1,2,3}\text{Tz}^{1-\text{benz})_2\}\text{Re}(\text{O})\text{Cl}_3]$ (11) in CDCl_3 .

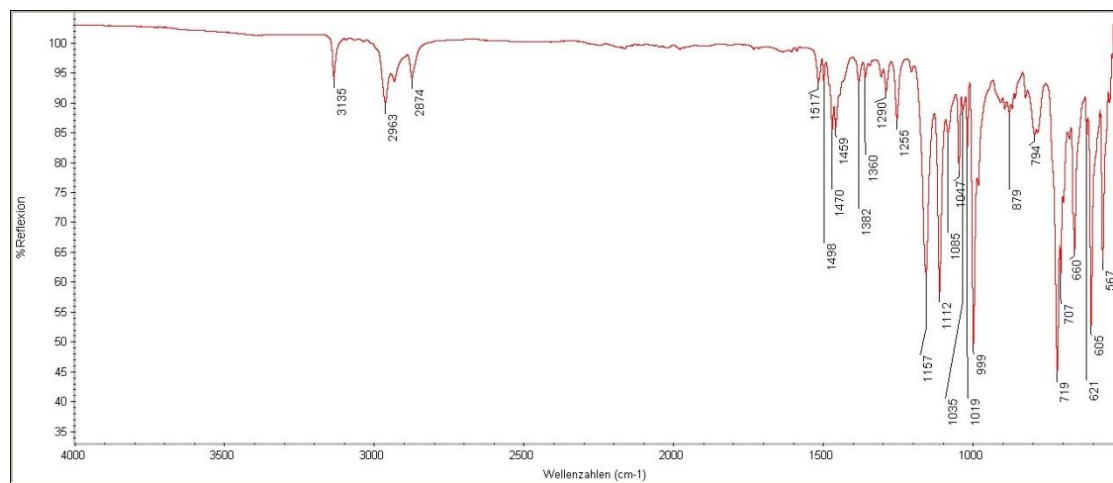


Figure S52. IR spectrum of $(\text{NBu}_4)[\text{Cl}_3(\text{O})\text{Re}\{\text{O}_2\text{P}^{(1,2,3}\text{Tz}^{1-\text{benz})_2\}\text{Re}(\text{O})\text{Cl}_3]$ (11).

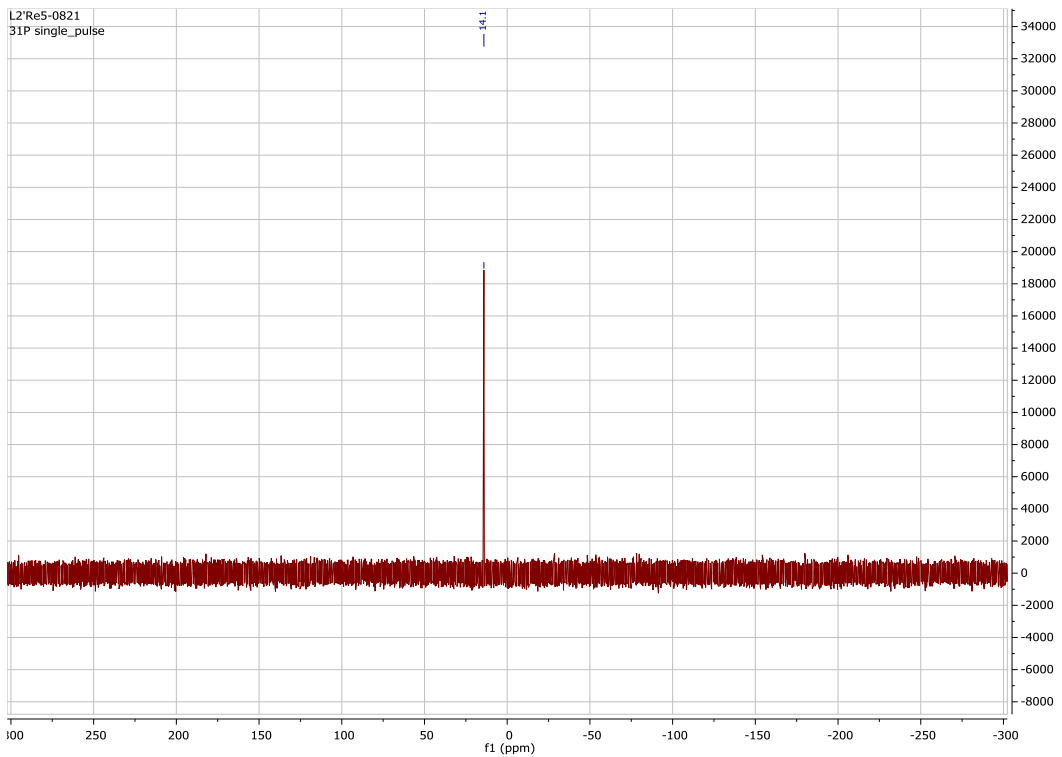


Figure S53. ^{31}P NMR spectrum of $(\text{NBu}_4)[\text{Cl}_3(\text{O})\text{Re}\{\text{O}_2\text{P}(^{1,2,3}\text{Tz}^{1-\text{benz}})_2\}\text{Re}(\text{O})\text{Cl}_3]$ (**11**) in CDCl_3 .

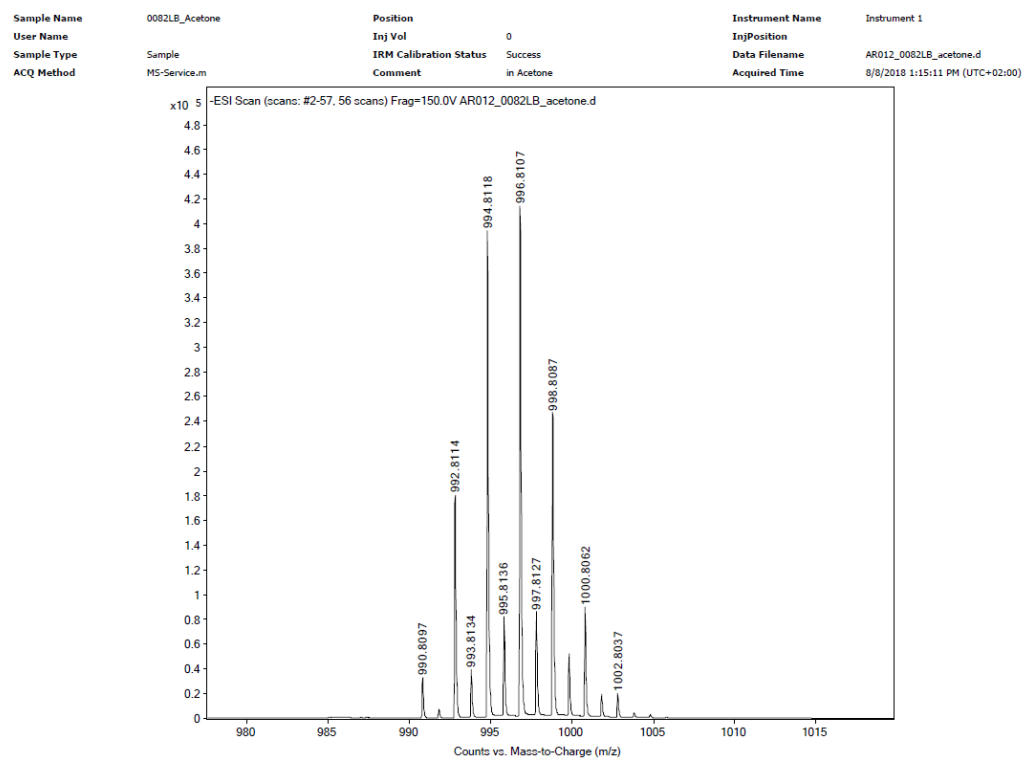


Figure S54. ESI- mass spectrum of $(\text{NBu}_4)[\text{Cl}_3(\text{O})\text{Re}\{\text{O}_2\text{P}(^{1,2,3}\text{Tz}^{1-\text{benz}})_2\}\text{Re}(\text{O})\text{Cl}_3]$ (**11**).

6.2.13 Spectroscopic data of $[\text{Cu}(\kappa^3\text{N-L}^2)_2](\text{NO}_3)_2$ (**12**)

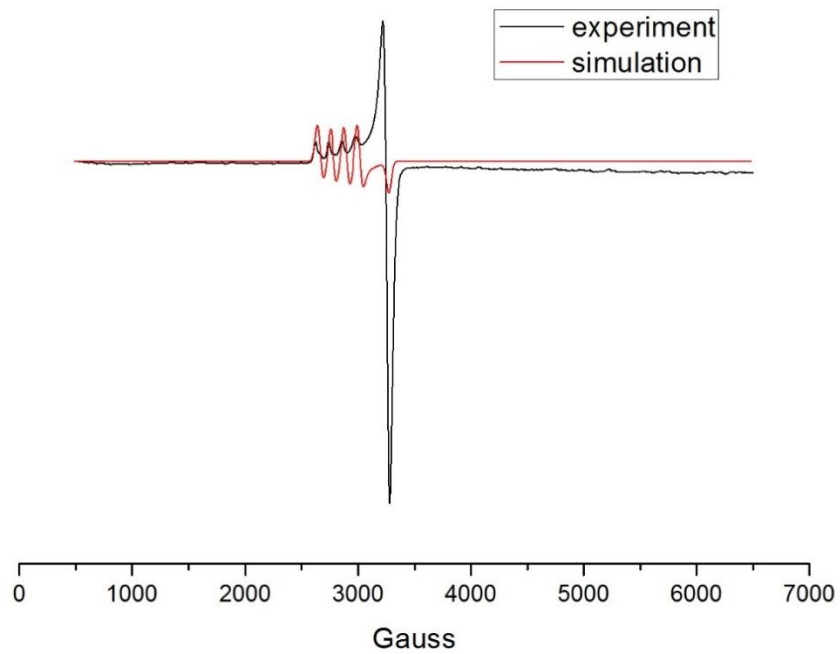


Figure S55. EPR spectrum of $[\text{Cu}(\kappa^3\text{N-L}^2)_2](\text{NO}_3)_2$ (**12**) (77k, methanol).

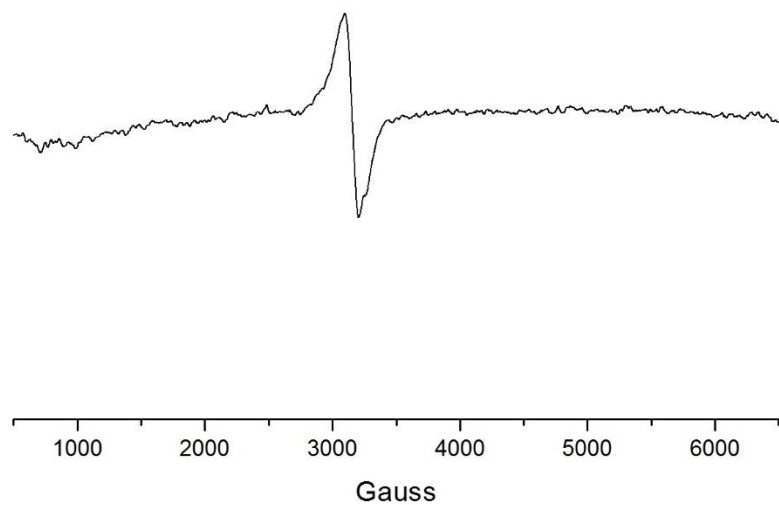


Figure S56. EPR spectrum of $[\text{Cu}(\kappa^3\text{N-L}^2)_2](\text{NO}_3)_2$ (**12**) (298k, CH_2Cl_2).

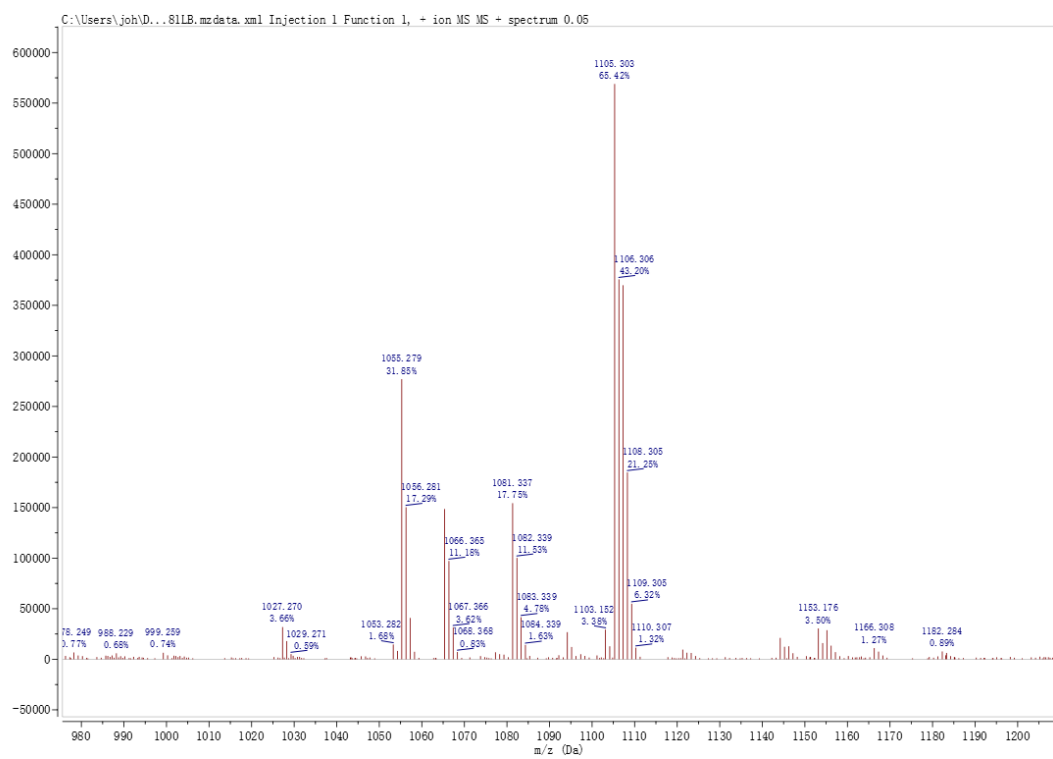


Figure S57. ESI+ mass spectrum of $[\text{Cu}(\kappa^3\text{N-L}^2)_2](\text{NO}_3)_2$ (**13**).

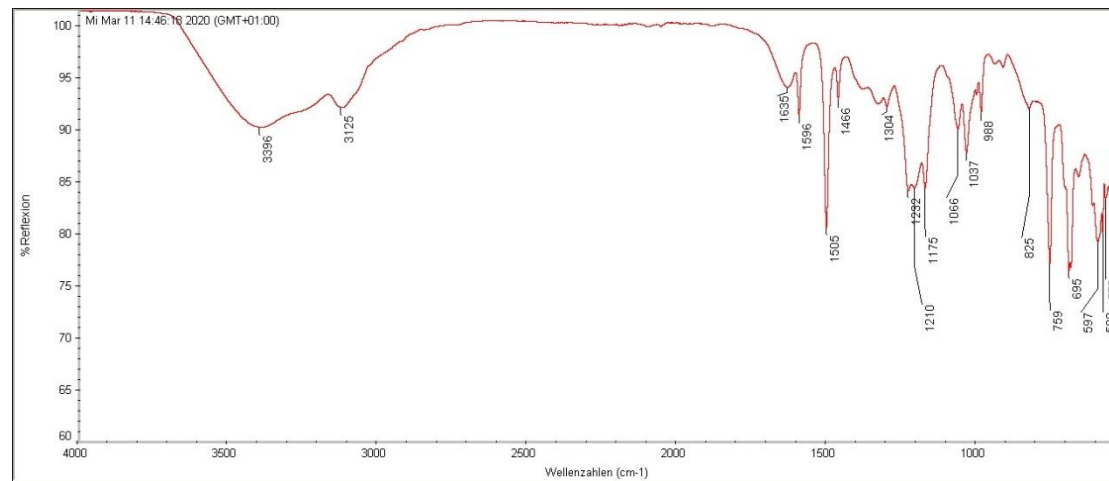


Figure S58. IR spectrum of $[\text{Cu}(\kappa^3\text{N-L}^2)_2](\text{NO}_3)_2$ (**13**).

6.2.12 Spectroscopic data of $[\text{Ni}(\kappa^3\text{N-L}^2)_2](\text{NO}_3)_2$ (13)

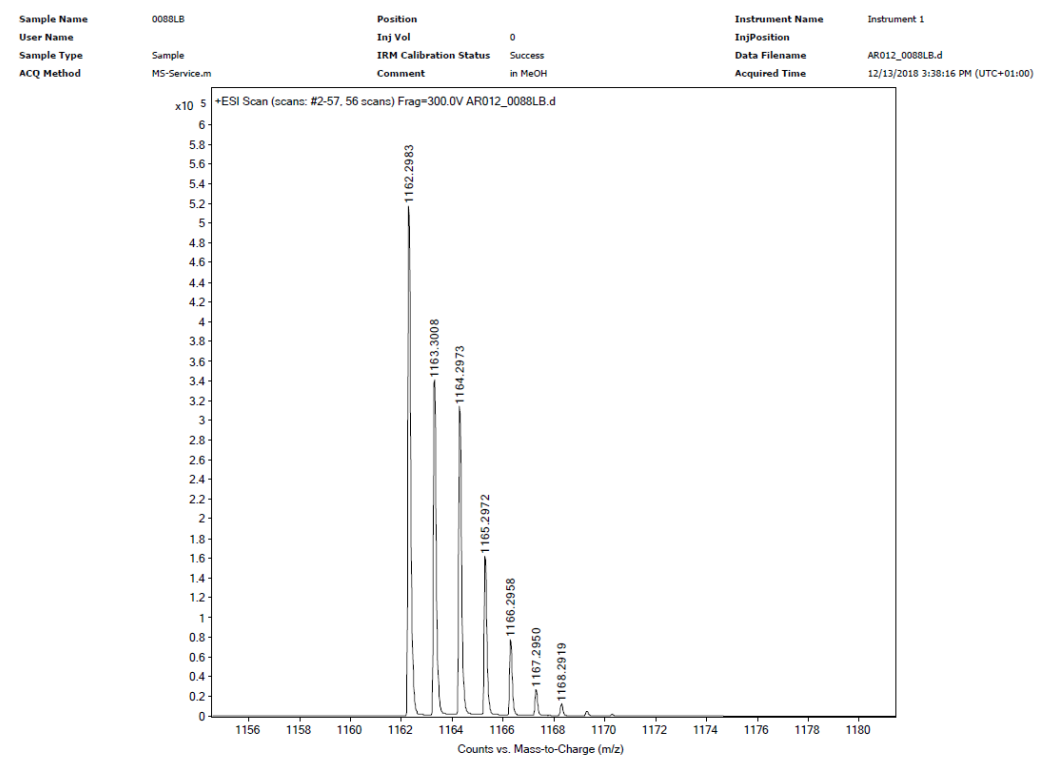


Figure S59. ESI⁺ mass spectrum of $[\text{Ni}(\kappa^3\text{N-L}^2)_2](\text{NO}_3)_2$ (13).

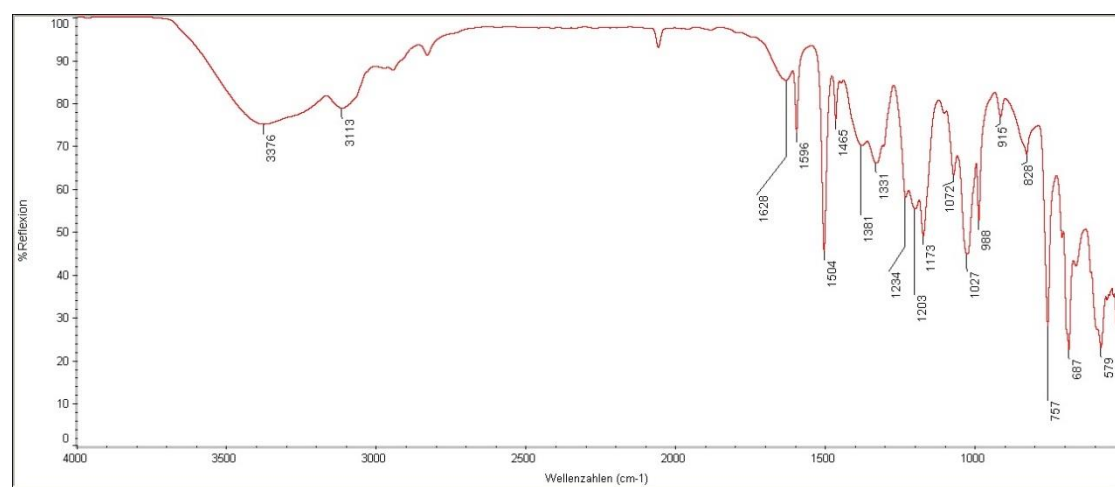


Figure S60. IR spectrum of $[\text{Ni}(\kappa^3\text{N-L}^2)_2](\text{NO}_3)_2$ (13).

Eidesstattliche Erklärung Statutory Declaration

- Ich versichere an Eides Statt, dass ich die vorliegende Arbeit selbstständig ohne fremde Hilfe und nur mit den angegebenen Hilfsmitteln verfasst habe.
- I hereby declare that I have written the present thesis independently, without enlisting any external assistance, and only using the specified aids.

28.10.2020

Datum	Originalunterschrift
Date	Original Signature